978c

THE ULTRAVIOLET SPECTRUM OF THIOFORMALDEHYDE

THE ULTRAVIOLET ABSORPTION SPECTRUM OF THIOFORMALDEHYDE

By

CAROL RUTH DRURY-LESSARD, M.Sc.

A Thesis

Submitted to the School of Graduate Studies

in Partial Fulfilment of the Requirements

for the Degree

Doctor of Philosophy

McMaster University

May, 1980

DOCTOR OF PHILOSOPHY (1980) McMASTER UNIVERSITY

(Chemistry) HAMILTON, ONTARIO

TITLE: The Ultraviolet Absorption Spectrum of Thioformaldehyde

Author: Carol Ruth Drury-Lessard, B.Sc. (Brock University)

M.Sc. (Brock University)

Supervisor: Dr. D. C. Moule

Number of Pages: 108

Abstract

This work extends the knowledge about the excited electronic states of thioformaldehyde. Survey work is reported over the wavelength region from 230 nm to 180 nm and four electronic transitions are identified. These are assigned as the $^1A_1(\pi,\pi^*)$, $^1B_2(n,3s)$, $^1A_1(n,3p_y)$ and $^1B_2(n,3p_z)$ systems.

A vibrational and rotational analysis of the first two systems has been undertaken. The results of these analyses indicate that the molecule remains planar or nearly so in both the $^1A_1(\pi,\pi^*)$ and the $^1B_2(n,3s)$ transitions. This behaviour is contrasted to that of similar molecules which are known to be non-planar in these electronic states and reasons are offered for this observation. The substituted geometry for thioformaldehyde in the $^1B_2(n,3s)$ state has been calculated and provides insight into the changes which occur in the molecule on electronic excitation.

Acknowledgements

I wish to thank Dr. D. C. Moule for suggesting the problem and for guiding me through the intricacies of high-resolution ultraviolet spectroscopy. I also wish to thank Dr. R. H. Judge for his assistance with the chemical and physical aspects of the problem.

A special thank-you goes to my typist, Janet Hastie, for the many hours of work she has expended on this manuscript.

I would also like to thank the other members of staff, both at McMaster University and at Brock University, for their help and encouragement.

I would like to thank Dr. D. A. Ramsay for the use of his equipment for the final stage of this project. I would also like to thank Dr. G. W. King for the sample of deuterated trimethylene sulphide which he provided.

I am very grateful for the financial support of the National Research Council and McMaster University and for the moral support of my lab colleagues Dave Paape, Jeff Robins, Tamara Wijeratne and Ian Littlewood.

Table of Contents

List of Tables

List of Figures

Chapter I

1.1 Introduction

In recent years, interest in the spectroscopic characteristics of thioformaldehyde (H_2CS) has greatly increased; this is a result of the identification of absorption due to thioformaldehyde from the direction of the galactic centre radio source Sagittarius B2 in 1971.[1,2] However, the information available on this molecule has only slowly increased and this is primarily due to the nature of the species. H_2CS is usually created by the pyrolytic cracking of larger sulphur-containing hydrocarbons, and other compounds are inevitably generated by this process. These may interfere through chemical or physical interactions so that the spectrum of thioformaldehyde can often not be clearly seen.

To date, studies have been conducted on thioformaldehyde throughout the spectral range from the microwave to the ultraviolet, and the results of these experiments are summarized in the next section. The present work extends the survey into the vacuum ultraviolet region where several electronic transitions are identified. From the vibrational and rotational analyses of these systems, additional information is derived about the behaviour of thioformaldehyde in its excited electronic states.

1.2 Experimental Background

The monomeric H_2CS was first detected in mass spectrometric studies of the pyrolysis of thiocyclobutane by Jones and Lossing.[3] Then, in 1969, Callear and coworkers[4] reported the observation of a band at 211.7 nm as a result of the flash photolysis of a series of sulphur-containing compounds and they assigned it to a common species, H_2CS. They described the band as being red-shaded and having a "coarse fine-structure", but they were unable to obtain sufficient dispersion to undertake an analysis of the sub-band structure.

The microwave spectra of the four isotopic species $H_2{}^{12}C^{32}S$, $H_2{}^{13}C^{32}S$, $H_2{}^{12}C^{34}S$ and $D_2{}^{12}C^{32}S$ and the millimeter wave spectrum of $H_2{}^{12}C^{32}S$ were reported by Johnson and coworkers[5] in the next few years. A detailed centrifugal distortion analysis was carried out on the species $H_2{}^{12}C^{32}S$. Rotational constants were obtained for these four isotopic species and used to derive a completely substituted structure. These authors[5] also determined that the half-life of thioformaldehyde was about 6 minutes at a pressure of 0.01 to 0.05 torr.

Also in 1971, Johns and Olson[6] observed the infrared spectrum of thioformaldehyde in the C-H stretching region. They assigned the two fundamental modes ν_1 and ν_5 and tentatively identified a third band as $2\nu_6$ (antisymmetric HCH bend). In order to establish the wavenumber assignments of the lower fundamental vibrations, Jacox and Milligan[7] used the matrix isolation technique, working with argon and nitrogen matrices at 14 K. Their data for $H_2{}^{12}CS$, $H_2{}^{13}CS$, $HD^{12}CS$ and $D_2{}^{12}CS$ determine the assignment of ν_4 (out-of-plane deformation)

and ν_3 (C=S stretch) as well as confirming the assignments of Johns and Olson.

The photoelectron spectrum was first observed by Kroto and Suffolk,[8] produced by the pyrolysis products of CH_3SH. A second synthesis was developed by Solouki et al.[9] and they identified five ionization energies below 20 eV corresponding successively to the loss of n, π, nσ, $\sigma_{CH}(b_2)$ and $\sigma_{(CH)}(a_1)$ electrons.

Extensive work by Judge, King and Moule[10] provided additional information about both the ground state and the first excited electronic states. In the region from 900 to 400 nm they identified two electronic transitions, the $^1A_2$ and $^3A_2(n,\pi^*)$ systems. The assignment of all the excited state vibrational frequencies and rotational constants was provided by their work.

A summary of these results has been compiled in Tables 1 to 3.

The notation recommended by the Joint Commission on Spectroscopy of the IAU and IUPAC[11] is such that the C=S bond is oriented along the molecular z-axis and the x-axis is out of the plane of the molecule, since thioformaldehyde is planar in its ground state. In this configuration the molecule has the following elements of symmetry:

1. E, the identity element
2. $C_2(z)$, a two-fold axis of rotation coincident with the molecular z-axis
3. $\sigma_v(xz)$, a reflection plane coincident with the xz plane of the molecule

Table 1

Ground State Rotational Constants[a] (in cm^{-1}) and Substituted Structure[b]

	H_2CS	D_2CS
A	9.72941(17)	4.88206(23)
B	0.59039202(73)	0.4971852(95)
C	0.55545022(91)	0.4501419(97)
$10^5\ \tau_{aaaa}$	-329.081(66)	-71.19(73)
$10^5\ \tau_{bbbb}$	-0.2957(18)	-0.227(25)
$10^5\ \tau_{cccc}$	-0.2312(18)	-0.121(26)
$10^5\ \tau_1$	-7.7439(68)	-4.25(25)
$10^5\ \tau_2$	-0.6151(15)	-0.449(59)
$10^5\ \tau_3$[c]	89.1(1.3)	29.2(5.7)
r_{CS}	1.6108(9) Å	
r_{CH}	1.0925(9) Å	
α_{HCH}	116.87(5)°	
θ(out-of-plane)	0.0°	

(a) reference 10c

(b) reference 5b

(c) The value of τ_3 is constrained by the planarity condition.

(d) The numbers in brackets are the standard deviations on the last two (one) digits.

Table 2

Fundamental Frequencies (in cm^{-1}) of Thioformaldehyde

		H_2CS	D_2CS
a_1	ν_1(CH)	2971[a]	(2146)[b,c]
	ν_2(HCH)	(>1550)[a]	(1203)[b,c]
	ν_3(CS)	1063[b]	941[b]
b_1	ν_4(out-of-plane)	993[b]	783[b]
b_2	ν_5(CH)	3025[a]	(2138)[d]
	ν_6(HCH)	1438[a]	(1017)[d]

(a) reference 6--ν_2 estimated by analogy to H_2CO, CO and CS.

(b) reference 7

(c) calculated using Wilson's F-G matrix formalism

(d) calculated as $\frac{1}{\sqrt{2}} \nu_{H_2CS}$

4. $\sigma_v(yz)$, a reflection plane coincident with the yz plane of the molecule.

These elements constitute the C_{2v} symmetry point group. The complete character table for this group is given in Table 4.

Table 3

Experimental Ionization Energies for Thioformaldehyde[a] (in eV)

State	Energy
$\tilde{X}^2B_2(n)$	9.38
$\tilde{A}^2B_1(\pi)$	11.76
$\tilde{B}^2A_1(n\sigma)$	13.85
$\tilde{C}^2B_2(\sigma_{CH})$	15.20

(a) reference 9a.

Table 4

Character Table for the C_{2v} Point Group

	E	$C_2(z)$	$\sigma_v(xz)$	$\sigma_v'(yz)$	
A_1	1	1	1	1	T_z
A_2	1	1	-1	-1	R_z
B_1	1	-1	1	-1	T_x, R_y
B_2	1	-1	-1	1	T_y, T_x

Chapter II

2.1 Theoretical Background

The quantum-mechanical expression which describes the nuclear and electronic motion of a molecule is called the Schrödinger equation. The time-independent, non-relativistic form is written simply as

$$\mathcal{H}_T \Psi_T = E_T \Psi_T \tag{1}$$

where $\mathcal{H}_T$ is the Hamiltonian operator and E_T and Ψ_T are the energy eigenvalues and eigenfunctions which describe the stationary states of the molecule.

The detailed expression can be extremely complex,[12,13,14] but fortunately the large difference in mass between the nuclei and the electrons permits us to consider the motions of the two particles separately. In that case, the overall rovibronic (rotational-vibrational-electronic) wavefunction Ψ_{evr} can be written as a product of two wavefunctions:

$$\Psi_{evr} = \Psi_e \cdot \Psi_{nuc} \tag{2}$$

The factorization of the wavefunction into components due to electronic and nuclear motion is called the Born-Oppenheimer approximation.[15]

In the zeroeth order Born-Oppenheimer approximation, equation (1) may be rewritten as:

$$\begin{aligned} \mathcal{H}_e(r,Q_0)\Psi_e(r,Q_0) &= E_e(Q_0)\Psi_e(r,Q_0) \\ [\mathcal{H}_{nuc}(Q) + E_e(Q)]\Psi_{nuc}(Q) &= E\Psi_{nuc}(Q) \end{aligned} \tag{3}$$

where r and Q_0 are the electronic and equilibrium nuclear co-ordinates respectively and Q represents the nuclear displacement co-ordinate. The Hamiltonians for the electronic and nuclear motion are given by:

$$\mathcal{H}_e(r,Q_0) = -\sum_i \frac{h^2}{2m_e}\nabla_i^2 - \sum_{i\mu}\sum \frac{z_\mu e}{r_{i\mu}} + \sum_{i>j}\sum \frac{e^2}{r_{ij}} \tag{4a}$$

$$\mathcal{H}_{nuc}(Q) = -\sum_\mu \frac{h^2}{2M_\mu}\nabla_\mu^2 + \sum_{\mu>\nu}\sum \frac{z_\mu z_\nu}{r_{\mu\nu}} \tag{4b}$$

The terms on the right-hand side of equation (4a) refer respectively to the kinetic energy of the individual electrons, attractive forces of the i-th electron for the μ-th nucleus, and the electron-electron repulsion. Similarly, the nuclear Hamiltonian contains a nuclear kinetic energy term and a nucleus-nucleus repulsion term. The solutions of equation (4) yield the electronic and nuclear energy levels and wavefunctions.

2.2 Transition Probability

According to the Bohr theory, a transition between two stationary states with energies E_n and E_m in the molecule may occur with the quantized absorption or emission of radiation of wavenumber ν given by:

$$\nu = \pm\left\{\frac{E_m}{hc} - \frac{E_n}{hc}\right\} \qquad , E_m > E_n \tag{5}$$

The transition probability that an oscillating electromagnetic field induces such a transition in a molecule from state n to state m was first determined by Einstein to be:

$$B_{nm} = \frac{2\pi}{3\hbar^2 c}\left|M_n^m\right|^2 \tag{6}$$

where B_{nm} is the Einstein absorption probability coefficient, M_n^m $(= \langle\Psi_m|\vec{\mu}|\Psi_n\rangle)$ is the transition probability from state n to state m, and $\vec{\mu}$ is the electric dipole operator.

2.3 Selection Rules

In order that an electric dipole transition occur between states m and n, the transition moment must be non-zero,

<u>i.e.</u>, $\langle\Psi_m|\vec{\mu}|\Psi_n\rangle \neq 0$ (7)

In the format provided by group theory, the above integral will be non-zero only if the direct product of the irreducible representations of Ψ_m, $\vec{\mu}$ and Ψ_n contain the totally symmetric representation.

$$\Gamma(\Psi_m) \otimes \Gamma(\vec{\mu}) \otimes \Gamma(\Psi_n) = A_1 \tag{8}$$

The application of this selection rule to specific electronic and rotational transitions in thioformaldehyde will be examined more fully in later sections where the analysis of each is discussed in detail.

2.4 Oscillator Strength

Frequently instead of the transition probability we refer to the so-called oscillator strength f^{nm} which is defined as:

$$f^{nm} = \frac{m_e hc\nu_{nm}}{\pi e^2} B_{nm} \tag{9}$$

This is a useful quantity since f^{nm} can also be related directly to experimental measurements.[16]

$$f^{nm} = 4.32 \times 10^{-9} \int \varepsilon d\nu \tag{10}$$

where ε is the molar extinction coefficient and the integration is over the wavenumber range of the absorption. For transitions which

are electronically allowed (i.e., meet the requirements of equation (8) for Ψ_e), f is of the order of 0.01 to 0.4; other transitions have much smaller values.

2.5 The Ground Electronic State of Thioformaldehyde

Standard analytical methods may be used to generate a set of valence shell occupied and unoccupied molecular orbitals for thioformaldehyde from individual atomic orbitals. We will concern ourselves only with those orbitals which are relevant to the work of this thesis, namely the highest occupied and lowest unoccupied orbitals. These valence orbitals are described as follows, in order of increasing energy:

$a_1 n\sigma$(CS)--either a weak σ(C=S) orbital or a non-bonding n(CS) orbital

$b_1 \pi$(CS) --a bonding π(C-S) orbital

$b_2 n$(S) --a non-bonding n(S) orbital

$b_1 \pi^*$(CS)--an anti-bonding π^*(C-S) orbital

$a_1 \sigma^*$(CH)--an anti-bonding σ^*(CH) orbital

The ground state electronic configuration is then

$$\ldots(7a_1)^2(2b_1)^2(3b_2)^2(3b_1)^0(8a_1)^0 \quad {}^1A_1$$

Schematic representations of these orbitals and the electronic transitions of lowest energy are shown in Figure 1.

In addition to the valence shell orbitals, there are a large number of higher energy orbitals referred to as Rydberg orbitals.

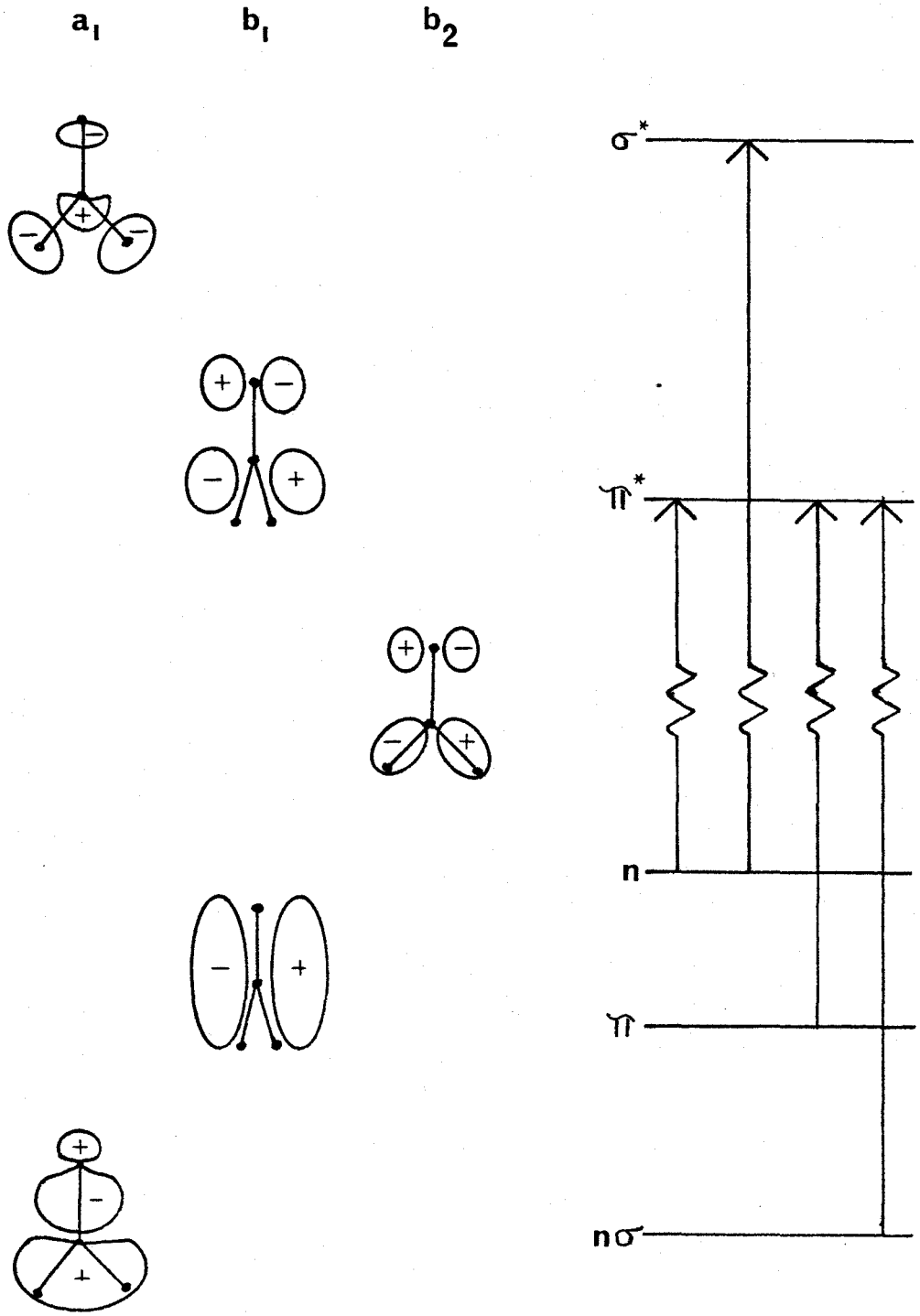

Figure 1

Valence Orbitals and Transitions

These have a principal quantum number n greater than that of the ground state orbitals and as n increases, they become more like atomic orbitals. They give rise to a series of Rydberg states which converge on a limit corresponding to the complete removal of the electron.

To a good approximation, the energies of the Rydberg states can be represented by the formula

$$E_R = \text{I.P.} - \frac{R}{(n - \delta)^2}$$

where I.P. is the ionization potential

R is the mass-dependent Rydberg constant ($R_\infty = 109737.3\ cm^{-1}$)

n is the principal quantum number

δ is the quantum defect

Values of δ for first row elements have been determined from experimental data as follows:[13]

$\delta < 0.1$	for nd electrons
$0.3 < \delta < 0.5$	for np electrons
$0.9 < \delta < 1.2$	for ns electrons

Although Rydberg orbitals are generally considered not to mix with valence-shell orbitals, for small values of n the two types of transitions have energies of the same order of magnitude and it is sometimes questionable initially as to what the proper electronic assignment should be. By reference to the work of Mulliken,[17] we have assumed that the Rydberg s orbital is a mix of the carbon 3s and

sulphur 4s orbitals. Then the LCAO (linear combination of atomic orbitals) approach indicates that the first s Rydberg should have the value 3.

A number of qualitative predictions about the molecular configurations of thioformaldehyde in its various excited states can be deduced from the correlation diagrams developed by A. D. Walsh[18] in accordance with the following rules:

1. Molecular orbitals of the two geometrical extrema are joined if they exhibit identical behaviour with respect to a symmetry element common to both configurations. In correlating orbitals, the conditions of the non-crossing rule must be obeyed.
2. Whether the energy of the M.O. increases or decreases on changing geometry is determined by the decrease or increase of s orbital contributions from the constituent atomic orbitals.

These rules are represented in Figure 2 for any H_2XY molecule. As can be seen from the diagram, all molecular orbitals up to and including the non-bonding orbital show a slight increase in energy with an increase in the out-of-plane angle. However, the π^* M.O., which consists of contributions from the p-A.O.'s exclusively, experiences a marked decrease in energy on correlation to the a' molecular orbital of the non-planar configuration. Accordingly, the molecule is expected to be planar in its ground state and non-planar in its first excited states.

Extensive SCF (self-consistent field) and CI (configuration interaction) calculations have been carried out by Bruna et al.[19]

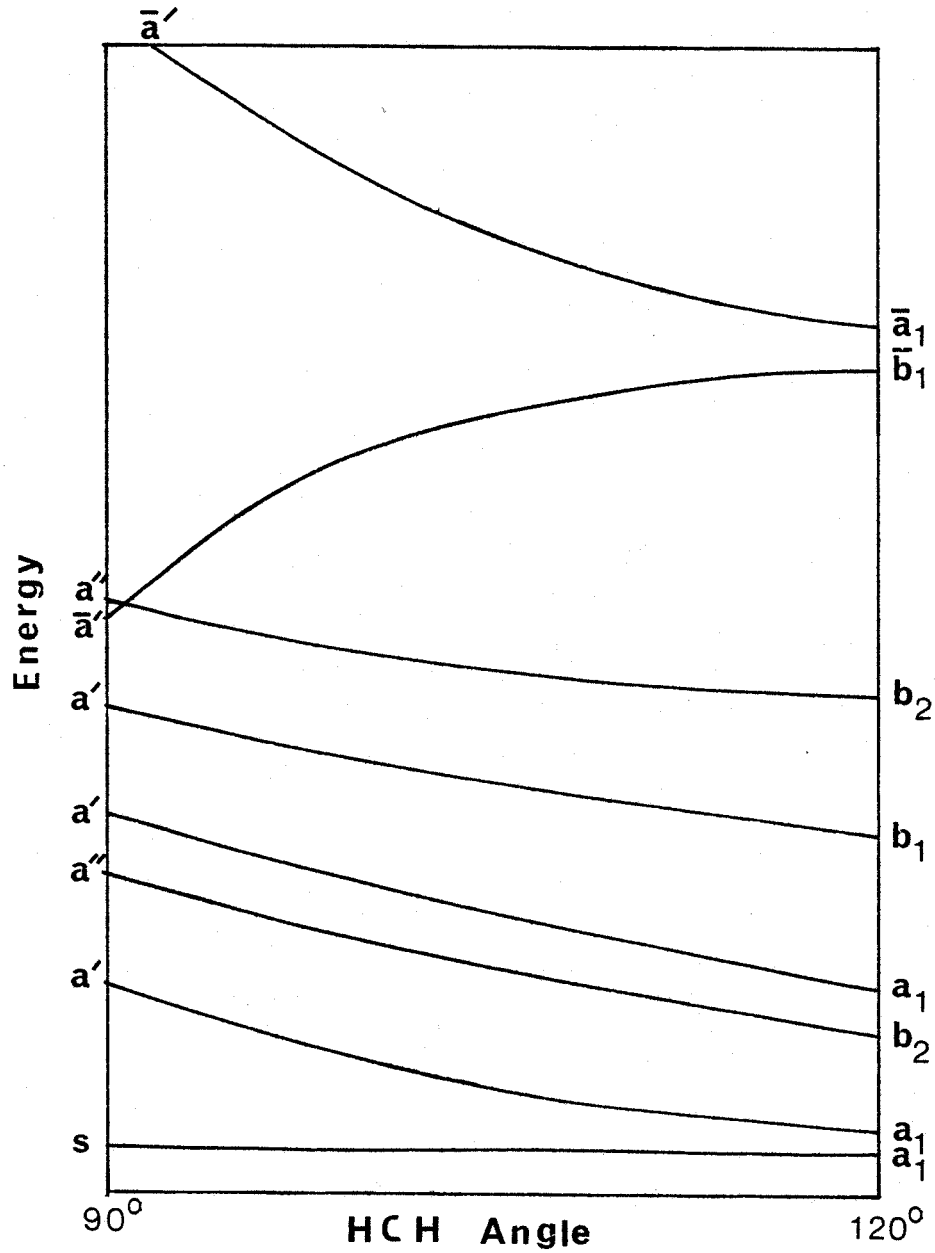

Figure 2

Walsh Diagram

on this system. Their conclusions substantiate the above hypothesis, both as to the ordering of the M.O.'s by energy and as to the nature of the first excited states. They find that the placement of an electron in the π^* orbital leads to a slightly non-planar (θ = 16 to 19°) geometry.

Although the above qualitative calculations can be very useful in the first steps of an analysis, when high-resolution data is available more sophisticated methods of analysis are required. The development of such techniques will be discussed in a later section.

2.6 The Electronic Transitions of Thioformaldehyde

Once the orbital energies are known, it is a simple matter on paper to arbitrarily promote electrons from occupied ground state orbitals to unoccupied valence or Rydberg orbitals. However, the symmetry requirements of equation (8) for the electronic wavefunction limit the transitions which are allowed to occur. The transition moment M may be directed along any one of the three principal axes of the molecule (a, b or c) and thus be of symmetry species A_1, B_1 or B_2 respectively. Since the direct product must be totally symmetric, we can construct the following table to determine the allowed interactions and the symmetry species of the resulting transitions:

Ψ_n \ Ψ_m	A_1	A_2	B_1	B_2
A_1	M_z			
A_2	f	M_z		
B_1	M_x	M_y	M_z	
B_2	M_y	M_x	f	M_z

f = forbidden

Since the ground state configuration is of A_1 symmetry, three types of electronic transitions may arise. The lowest-lying transitions of each type are predicted to be:

$^1A_1$	$^1B_1$	$^1B_2$
$\pi \longrightarrow \pi^*$	$\pi \longrightarrow 3s$	$n \longrightarrow 3s$
$n \longrightarrow 3p_y$	$n\sigma \longrightarrow \pi^*$	$n \longrightarrow 3p_z$
		$n \longrightarrow \sigma^*$

In fact, the transitions of lowest energy which have been observed are the $^{1,3}A_2(n,\pi^*)$ electron promotions.[10] These are not electronically allowed and consequently their oscillator strengths are of the order of 10^{-5}.

2.7 Rotational Analysis

In order to describe the properties of the nuclear angular momentum (and consequently the rotation of the molecule), it is necessary to begin with the appropriate commutation relations among the variables of interest. There are two sets of co-ordinates

involved, the space-fixed and the molecule-fixed axes shown in Figure 3. In terms of the space-fixed co-ordinates X, Y, Z, the classical expression for the angular momentum of a point mass is

$$P = R \times p$$

where R is the position vector of the point in space co-ordinates and p = mv is the linear momentum of the point mass of velocity v and mass m. Using matrix notation for convenience we have:

$$P = \begin{vmatrix} i & j & k \\ X & Y & Z \\ P_X & P_Y & P_Z \end{vmatrix} \tag{11}$$

and $P^2 = P_X^2 + P_Y^2 + P_Z^2$.

The quantum mechanical commutation relations of interest can now be obtained by replacing the dynamic variables in (11) with operators and using the commutation relations for linear momentum. The results of these manipulations are:

$$\begin{aligned} [\mathcal{P}_X,\mathcal{P}_Y] &= \mathcal{P}_X\mathcal{P}_Y - \mathcal{P}_Y\mathcal{P}_X = \frac{\hbar}{i}\mathcal{P}_Z \\ [\mathcal{P}_Y,\mathcal{P}_Z] &= \mathcal{P}_Y\mathcal{P}_Z - \mathcal{P}_Z\mathcal{P}_Y = \frac{\hbar}{i}\mathcal{P}_X \\ [\mathcal{P}_Z,\mathcal{P}_X] &= \mathcal{P}_Z\mathcal{P}_X - \mathcal{P}_X\mathcal{P}_Z = \frac{\hbar}{i}\mathcal{P}_Y \\ [\mathcal{P}^2,\mathcal{P}_X] &= [\mathcal{P}^2,\mathcal{P}_Y] = [\mathcal{P}^2,\mathcal{P}_Z] = 0 \end{aligned} \tag{12}$$

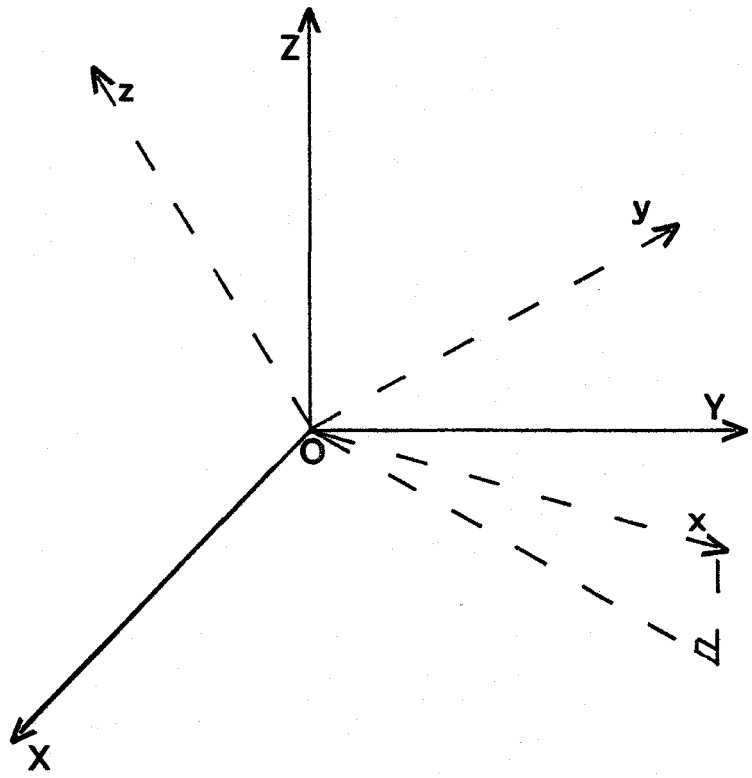

Figure 3

Molecular Co-ordinates

X, Y, Z = space-fixed co-ordinates

x, y, z = molecule-fixed co-ordinates

The transformation to molecule-fixed co-ordinates changes only the sign of the right-hand side of equations (12).[14] Also, the two systems have the following relationship:

$$[\mathcal{P}_F, \mathcal{P}_g] = 0 \qquad F = X,Y,Z; \quad g = x,y,z$$

This means that $\mathcal{P}^2$, $\mathcal{P}_Z$ and $\mathcal{P}_z$ form a set of commuting operators (or matrices). (The choice of Z,z is conventional, although Y,y or X,x could be used as well.) Then these matrices have only diagonal elements:

$$\langle JKM|\mathcal{P}^2|JKM\rangle = k_J$$
$$\langle JKM|\mathcal{P}_Z|JKM\rangle = k_M$$
$$\langle JKM|\mathcal{P}_z|JKM\rangle = k_K$$

where J,M,K are labels for the eigenfunctions associated with $\mathcal{P}^2$, $\mathcal{P}_Z$ and $\mathcal{P}_z$, respectively and k_J, k_M, k_K are the corresponding eigenvalues.

Further manipulation of these basic relations finally yields the matrix elements of the rotational angular momentum $\mathcal{P}$ in diagonal representations in the molecule-fixed frame of reference, as given below:

Element	Value
$\langle JKM \| \mathcal{P}^2 \| JKM \rangle$	$\hbar^2 J(J+1)$
$\langle JKM \| \mathcal{P}_z \| JKM \rangle$	$\hbar K$
$\langle JKM \| \mathcal{P}_x \| JK{+}1M \rangle$	$\frac{1}{2}\hbar(J(J+1) - K(K+1))^{\frac{1}{2}}$
$= \langle JK{+}1M \| \mathcal{P}_x \| JKM \rangle$	
$\langle JKM \| \mathcal{P}_y \| JK{+}1M \rangle$	$\frac{-i\hbar}{2}(J(J+1) - K(K+1))^{\frac{1}{2}}$
$= -\langle JK{+}1M \| \mathcal{P}_y \| JKM \rangle$	

All other elements of interest are zero in value. The quantum number M is relevant only to space-fixed axes, so we may suppress that label in the following discussion.

The classical rigid-rotor Hamiltonian, in operator form, is:

$$\mathcal{H} = \frac{\mathcal{P}_x^2}{2I_{xx}} + \frac{\mathcal{P}_y^2}{2I_{yy}} + \frac{\mathcal{P}_z^2}{2I_{zz}} \tag{13}$$

For the particular case of thioformaldehyde, we can correlate $x \longrightarrow c$, $y \longrightarrow b$ and $z \longrightarrow a$. We also define for convenience:

$$A = \frac{\hbar}{4\pi c I_A}, \qquad B = \frac{\hbar}{4\pi c I_B}, \qquad C = \frac{\hbar}{4\pi c I_C}$$

Then the Hamiltonian can be rewritten as:

$$\mathcal{H} = \frac{2\pi c}{\hbar}(AP_a^2 + BP_b^2 + CP_c^2) \tag{14}$$

The matrix elements for P_x^2, P_y^2 and P_z^2 may now be generated. P_z is diagonal, so only terms of the form $\langle JK|P_z^2|JK\rangle$ appear. P_x and P_y step up or down one, so their squares may have two forms, $\langle JK|P_x^2|JK\rangle$ and $\langle JK|P_x^2|JK\pm 2\rangle$. The resulting matrix elements are listed below.

$$\langle JK|P_z^2|JK\rangle = \hbar^2 K^2$$

$$\langle JK|P_x^2|JK\rangle = \frac{\hbar^2}{2}\,[J(J+1) - K^2]$$

$$\langle JK|P_x^2|JK\pm 2\rangle = \frac{\hbar}{4}\,\{[J(J+1) - K(K+1)][J(J+1) - K(K\pm 1)(K\pm 2)]\}^{\frac{1}{2}}$$

$$\langle JK|P_y^2|JK\rangle = \langle JK|P_x^2|JK\rangle$$

$$\langle JK|P_y^2|JK\pm 2\rangle = -\langle JK|P_x^2|JK\pm 2\rangle$$

For the prolate symmetric top (B = C), the familiar energy relationship is then obtained by direct substitution

$$F(J,K) = (A - B)K^2 + BJ(J+1) \tag{15}$$

For $K \neq 0$, the energy levels represented by F(J,K) are doubly degenerate.

For the asymmetric top ($A \neq B \neq C$) the energy matrix is no longer diagonal in K and it must be diagonalized to obtain the energies. In the past this procedure was greatly facilitated by a change of variable proposed by Ray.[20] An asymmetry parameter κ was defined as:

$$\kappa = \frac{2B - A - C}{A - C} \tag{16}$$

so that $-1 \leq \kappa \leq 1$. The chief merit of using κ is apparent from the relationship:

$$E^J_\tau(\kappa) = -E^J_{-\tau}(-\kappa)$$

where τ (which replaces K) runs from $-J$ to J. The limit $\kappa = -1$ ($B = C$) corresponds to the prolate symmetric top, $\kappa = +1$ ($A = B$) to the oblate symmetric top.

Explicit expressions for $E(\kappa)$ have been given by King, Hainer and Cross.[21] However, with modern computational methods, the matrix can be diagonalized directly after application of the Wang transformation $X^{-1}EX$ which factors $E(\kappa)$ into the four submatrices, E^+, E^-, O^+, O^-. E and O refer to the evenness or oddness of the K values and + and - refer to the evenness or oddness of a parameter γ.

A diagram correlating the asymmetric top energy levels to the prolate and oblate symmetric top limits is shown in Figure 4. Each level of the asymmetric top is designated by the three quantum numbers J, K_{-1} (= K_a) and K_{+1} (= K_c) since K_{+1} and K_{-1} are individually valid only when the levels are degenerate ($\kappa = -1$ or $\kappa = +1$).

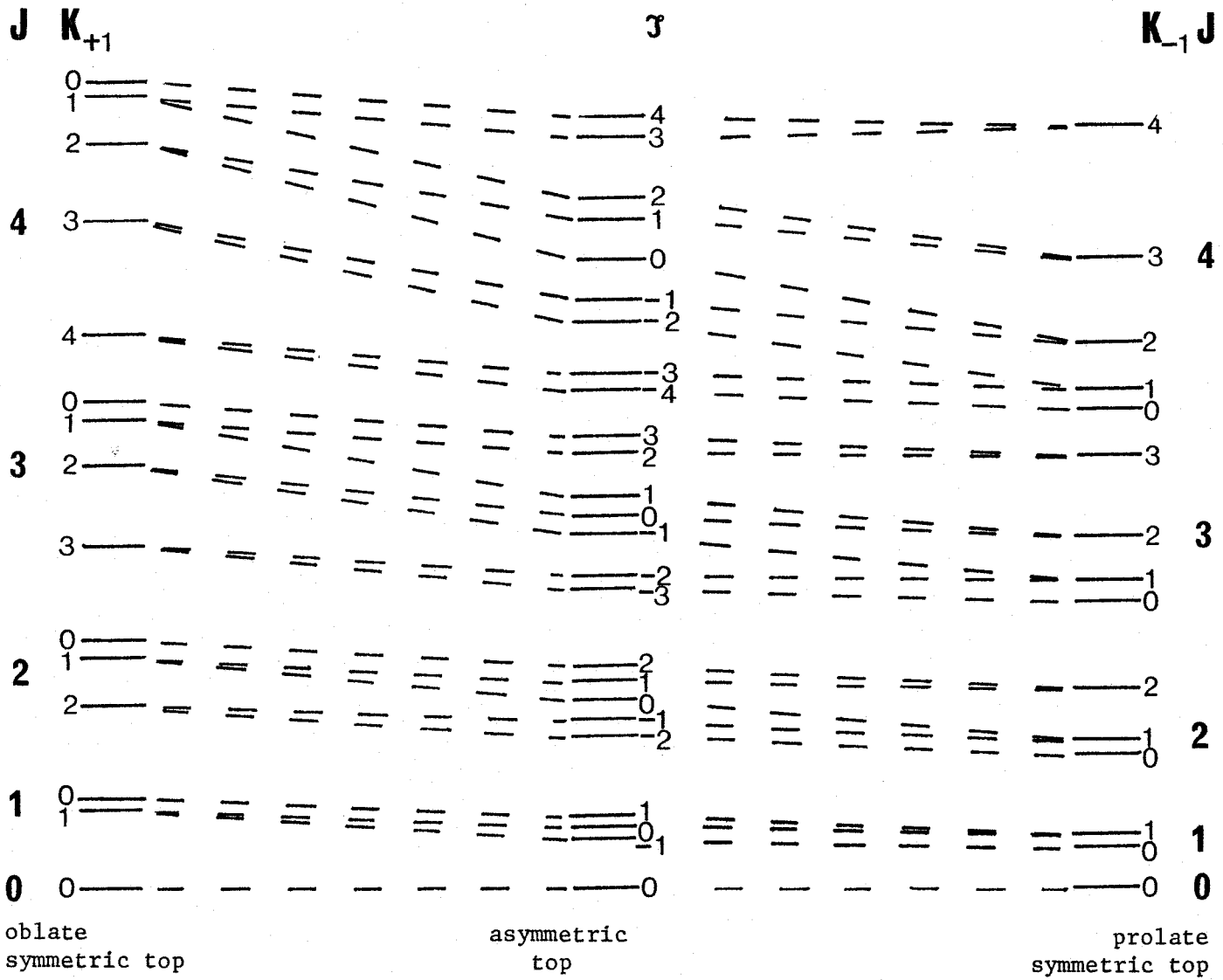

Figure 4
Correlation of Energy Levels

2.8 Symmetry Properties

Before we can consider the rotational transitions which are allowed by equation (8), we must define the symmetry properties of the rotational eigenfunction. Because of the symmetry of the momental ellipsoid, orientations which differ only by rotation of 180° about one of the principal axes must have the same probability.[22] This implies that Ψ_r must either stay unchanged or change only in its sign in order that Ψ_r^2 is the same after such a rotation. Thus the rotational levels of an asymmetric top may be distinguished by their behaviour (+ or -) with respect to the three operators $C_2(a)$, $C_2(b)$ and $C_2(c)$. Since one of these operations is equivalent to the other two carried out in succession, it is sufficient to designate the behaviour of each level with respect to two of the axes, usually chosen as $C_2(a)$ and $C_2(c)$. It has been shown by Dennison[23] that the sequence with respect to $C_2(c)$ is +--++--, starting with the level J_{+J}. With respect to $C_2(a)$, the sequence is also +--++--, but the designation begins with the level J_{-J}. There are thus four different types of levels, briefly described as ++, +-, -+ and --, where the first sign refers to behaviour with respect to $C_2(c)$, the second to behaviour with respect to $C_2(a)$.[22]

If an asymmetric top molecule has a pair of identical nuclei, the total eigenfunction must be either symmetric or antisymmetric with respect to an exchange of these nuclei. For thioformaldehyde, this exchange takes place by rotation about the $C_2(a)$ axis. Hence those rotational levels that are positive with respect to this

rotation are symmetric in the nuclei, those that are negative with respect to a $C_2(a)$ rotation are antisymmetric in the nuclei. Because of the spin of the identical nuclei, the symmetric and antisymmetric levels have different statistical weights. For H_2CS, which follows Fermi statistics ($I_H = \frac{1}{2}$), the ratio is

$$s/a = \frac{I}{I + 1} = \frac{1}{3}$$

For D_2CS, which follows Bose statistics ($I_D = 1$)

$$s/a = \frac{I + 1}{I} = \frac{2}{1}$$

2.9 Rotational Selection Rules

Since thioformaldehyde has an axis of symmetry, only those rotational levels can combine for which the eigenfunctions have the same symmetry with respect to a rotation of 180° about the principal axis which coincides with the direction of the transition moment. They then have opposite symmetry with respect to rotations about the other two axes. The following selection rules summarize this relationship.

1. If the transition moment is along the a axis

   ++ ⟷ −+ ; +− ⟷ −−

2. If the transition moment is along the b axis

   ++ ⟷ −− ; +− ⟷ −+

3. If the transition moment is along the c-axis

$$++ \longleftrightarrow +- \; ; \quad -+ \longleftrightarrow --$$

A careful correlation between the asymmetric top levels and those of the corresponding prolate and oblate tops results in the following alternative statement of the selection rules for thioformaldehyde.

1.	a-axis	$\Delta K_a = 0, \pm 2, \ldots$;	$\Delta K_c = \pm 1, \pm 3, \ldots$
2.	b-axis	$\Delta K_a = \pm 1, \pm 3, \ldots$;	$\Delta K_c = \pm 1, \pm 3, \ldots$
3.	c-axis	$\Delta K_a = \pm 1, \pm 3, \ldots$;	$\Delta K_c = 0, \pm 2, \ldots$

It must be realized that these rules are further restricted in that $K_a + K_c = J$ or $J + 1$; in addition, $\Delta J = 0, \pm 1$ and $J = 0 \not\longleftrightarrow J = 0$.

2.10 Centrifugal Distortion

The development of the energy expression from the rotational Hamiltonian of equation (13) was based on a rigid-rotor molecular model. In fact, the molecule is not a rigid rotor; there are centrifugal forces acting on the nuclei which increasingly distort the molecule in the higher rotational levels. Then the rotational Hamiltonian may be written as

$$\mathcal{H}_r = \mathcal{H}_0 + \mathcal{H}_1$$

where $\mathcal{H}_0$ represents the zeroeth-order (i.e., rigid rotor) approximation and $\mathcal{H}_1$ represents the centrifugal distortion term. We can write

$$H_0 + H_1 = A_0 P_a^2 + B_0 P_b^2 + C_0 P_c^2 + \tfrac{1}{4}\sum_{gg'jj'} \tau_{gg'jj'} P_g P_{g'} P_j P_{j'}$$

$$g,g',j,j' = a,b,c$$

where A_0, B_0 and C_0 represent the distortion-free-constants. Alternatively, if we use the experimentally measured values, A, B and C, we can express the Hamiltonian as[24]

$$H = AP_a^2 + BP_b^2 + CP_c^2 + \tfrac{1}{4}\sum_{gg'} \tau'_{ggg'g'} P_g^2 P_{g'}^2$$

The relationships among these two sets of constants and a third set developed by Nielsen[25] are given in Table 5. This last form is useful in that D_K, D_{JK} and D_J represent the symmetric top distortion constants. The additional perturbations due to asymmetry are expressed by δ_J, R_5 and R_6 and these can be evaluated only by very precise calculations.

Table 5

Relationships Between Observed Rotational Constants and Distortion-free Constants

$$A = A_0 + \frac{\hbar}{4}(3\tau_{bcbc} - 2\tau_{abab} - 2\tau_{caca})$$

$$B = B_0 + \frac{\hbar}{4}(3\tau_{caca} - 2\tau_{abab} - 2\tau_{bcbc})$$

$$C = C_0 + \frac{\hbar}{4}(3\tau_{abab} - 2\tau_{bcbc} - 2\tau_{caca})$$

$$\tau'_{gggg} = \hbar^4\tau_{gggg} \qquad , g = a, b, c$$

$$\tau'_{ggg'g'} = \hbar^4(\tau_{ggg'g'} + 2\tau_{gg'gg'}) \qquad , g \neq g'$$

$$D_J = -\frac{\hbar^4}{32}(3\tau_{cccc} + 3\tau_{bbbb} + 2\tau_{ccbb} + 4\tau_{bcbc})$$

$$D_K = D_J - \frac{\hbar^4}{4}(\tau_{aaaa} - \tau_{aacc} - \tau_{bbaa} - 2\tau_{caca} - 2\tau_{baba})$$

$$D_{JK} = -D_J - D_K - \frac{\hbar^4}{4}\tau_{aaaa}$$

$$R_5 = \frac{-\hbar^4}{32}(\tau_{bbbb} - \tau_{cccc} - 2(\tau_{aabb} + 2\tau_{abab}) + 2(\tau_{aacc} + 2\tau_{acac}))$$

$$R_6 = \frac{\hbar^4}{64}(\tau_{bbbb} + \tau_{cccc} - 2(\tau_{bbcc} + 2\tau_{bcbc}))$$

$$\delta = -\frac{\hbar^4}{16}(\tau_{bbbb} - \tau_{cccc})$$

Chapter III

Experimental Work

Thioformaldehyde is an unstable molecule, with a half-life of about six minutes at a total pressure of 10^{-2} torr.[5] There are several synthetic procedures which lead to its creation; the major drawback to most of these is that the percentage of H_2CS is low relative to the percentage of other products of the reaction. The most satisfactory (i.e., highest yield) technique used in these experiments was the pyrolytic cracking of trimethylene sulfide (TMS),[10a] as shown below:

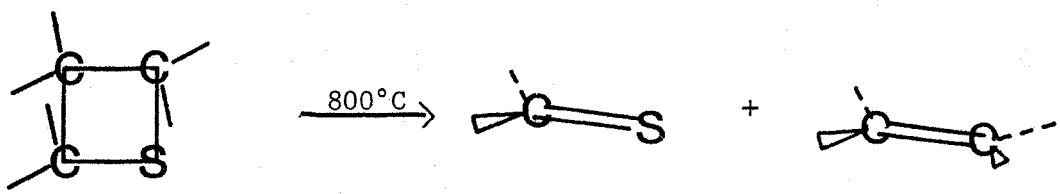

Whenever the absorption spectra of the two primary product molecules did not overlap, the amount of thioformaldehyde produced was adequate for photographic studies. For the photographs of the region below 180 nm, however, an alternate synthesis was required because the spectrum of ethylene begins to interfere seriously with that of thioformaldehyde. The route which we used involved the cracking of 1,2,4-trithiolane:

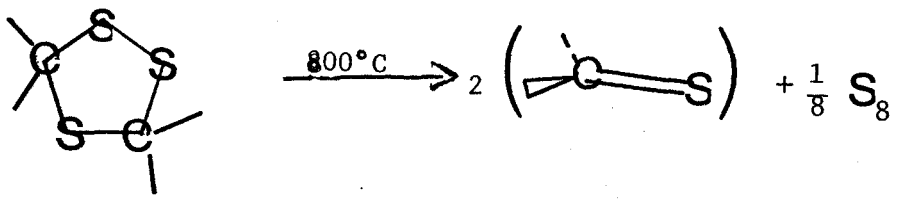

The starting material had to be heated to 50°C initially in order to supply a sufficient vapour pressure, and it rapidly decomposed at that temperature. In addition, 1,2,4-trithiolane must be synthesized[48] and it is produced in combination with 1,2,4,6-tetrathiepane. As a result, this technique for producing thioformaldehyde is of limited use.

The pyrolysis apparatus consisted of two quartz tubes, dimpled to provide increased surface area, connected directly to the absorption cell. The tubes were inserted into clamshell furnaces with the heating controlled by Variacs. The temperatures were measured directly to ±50°C by a thermocouple inserted into the central portion of the furnaces.

It was noted that two temperature-dependent absorption spectra could be observed. If the furnaces were run below 800°C, absorption due to unreacted TMS could be identified as a progression with a frequency of about 100 cm^{-1} above 220 nm and a pair of broad bands at 200 nm. On the other hand, if the pyrolysis temperature rose above 950°C, the rate of decomposition increased significantly and a very intense series of bands with a frequency of about 400 cm^{-1} due to CS_2 absorption was observed in the region below 210 nm. The potential

interference of these systems with the absorption due to H_2CS is shown in Figure 5. A balance could be found between the two extremes, depending on the region under examination, but constant monitoring of temperature and flow rate was required.

A quartz cell, 0.5 m in length, and glass cells, 1.5 and 3 m in length, with a total pressure of less than 2 torr provided the necessary pressure-path conditions. The use of a 6 m aluminum White cell was attempted, but the large volume and the adsorption properties of aluminum created insurmountable problems and no acceptable results were obtained.

An internal pressure of more than 2 torr resulted in the formation of the polymeric substance $(H_2CS)_3$ which not only coated the cell windows, but also produced a fine suspension of particles in the light beam. Constant application of heat to the windows permitted exposures of up to one hour; at that time the windows had to be removed and thoroughly cleaned. A constant flow of helium in front of the windows was introduced in an attempt to keep them clean; unfortunately, the slightest leak in the cylinder connection resulted in the appearance of the very strong absorption bands due to SO_2 below 230 nm. Since a pure low-pressure flow of helium could not be maintained, this idea was not carried further.

The light source was a conventional 450 watt xenon arc for exposures above 200 nm and a hydrogen microwave discharge lamp for the vacuum ultraviolet region. Calibration lines were provided by a Pfund arc for the first order of the holographic grating and an Fe-Ne hollow

Figure 5

Absorption Spectra on the Cary-14 Spectrometer

A. Trimethylene Sulphide

B. Thioformaldehyde

C. Carbon Disulphide

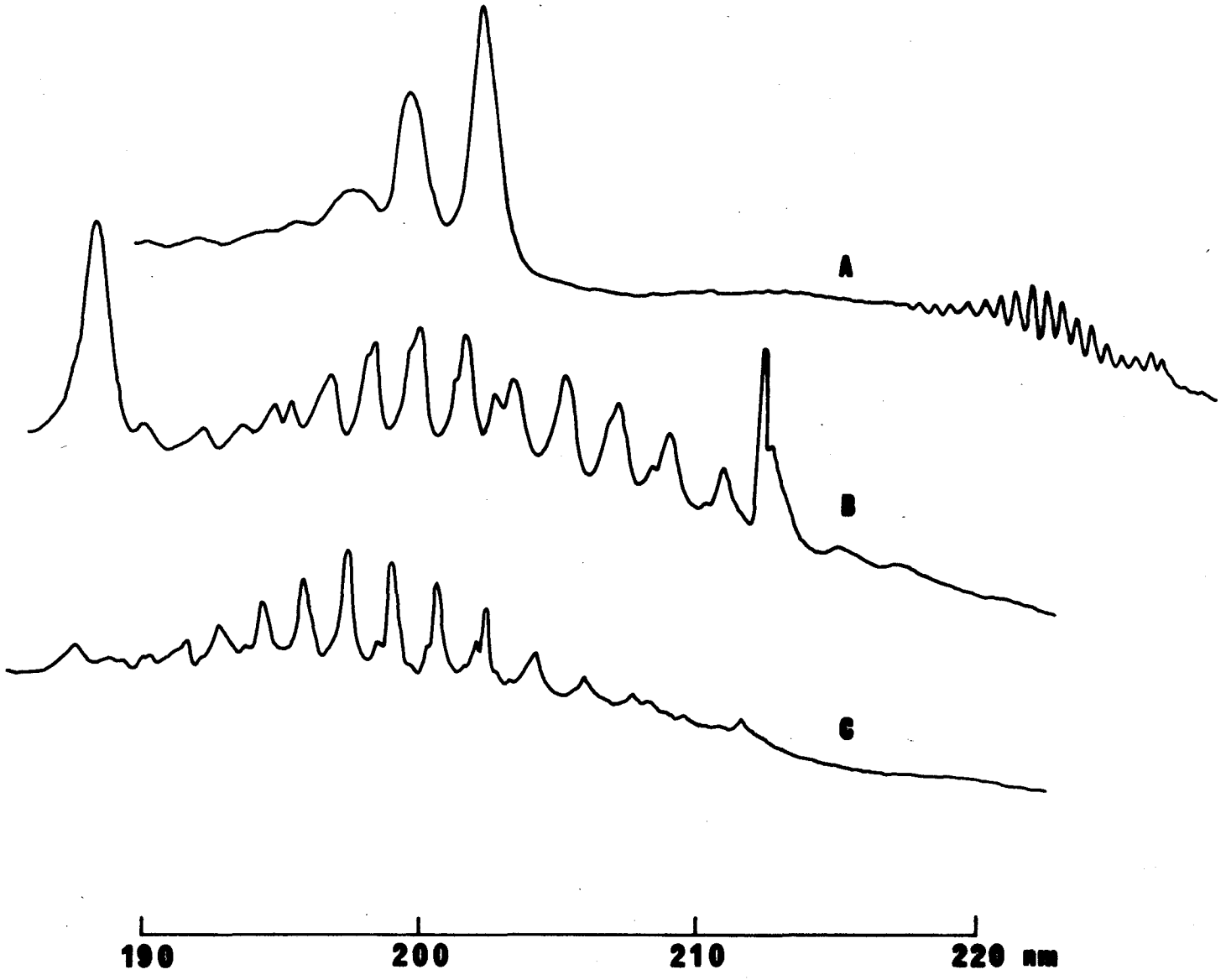
A
B
C
190
200
210
220 nm

cathode lamp for higher orders of the echelle grating. The instruments were a Cary-14 recording spectrophotometer and two Ebert spectrographs, a two-meter system evacuated for work below 200 nm and a twenty-foot system for the high resolution work. The two-meter instrument was operated in the first order with an 1180 line/mm replica grating or a 3650 line/mm holographic grating; the reciprocal dispersions at 210 nm were 4.19 and 1.35 nm/cm, respectively. The twenty-foot instrument also accommodated the holographic grating, with a resulting plate factor of 0.42 nm/cm. This grating was interchangeable with a 300 grooves/mm echelle grating operated in the twenty-seventh and twenty-eighth orders with a reciprocal dispersion of 0.08 to 0.10 nm/cm.

The use of the echelle grating required preselection of the wavelength region to prevent order overlap and this proved to be a difficult task to carry out. The final alignment for the 3 m cell, shown in Figure 6, was set up as follows.

Light from the xenon arc was gathered by a fused silica lens, L_1 (focal length ≈ 28 cm in the visible region, ≈ 25 cm at 210 nm). The lens was moved along the beam axis so that the light source was at the focal point for the wavelength region being examined. Thus the transmitted beam was nearly plane parallel as it traversed the cell. This beam was focussed by a concave mirror M_1 (f ≈ 13 cm) onto the slit of the order sorter. The diverging beam partly filled the front surface of a 30° suprasil Littrow prism P_1 and was reflected back to a second concave mirror M_2 (f ≈ 23 cm) which focussed the light onto the slit of the spectrograph. The prism was mounted on a table which could be

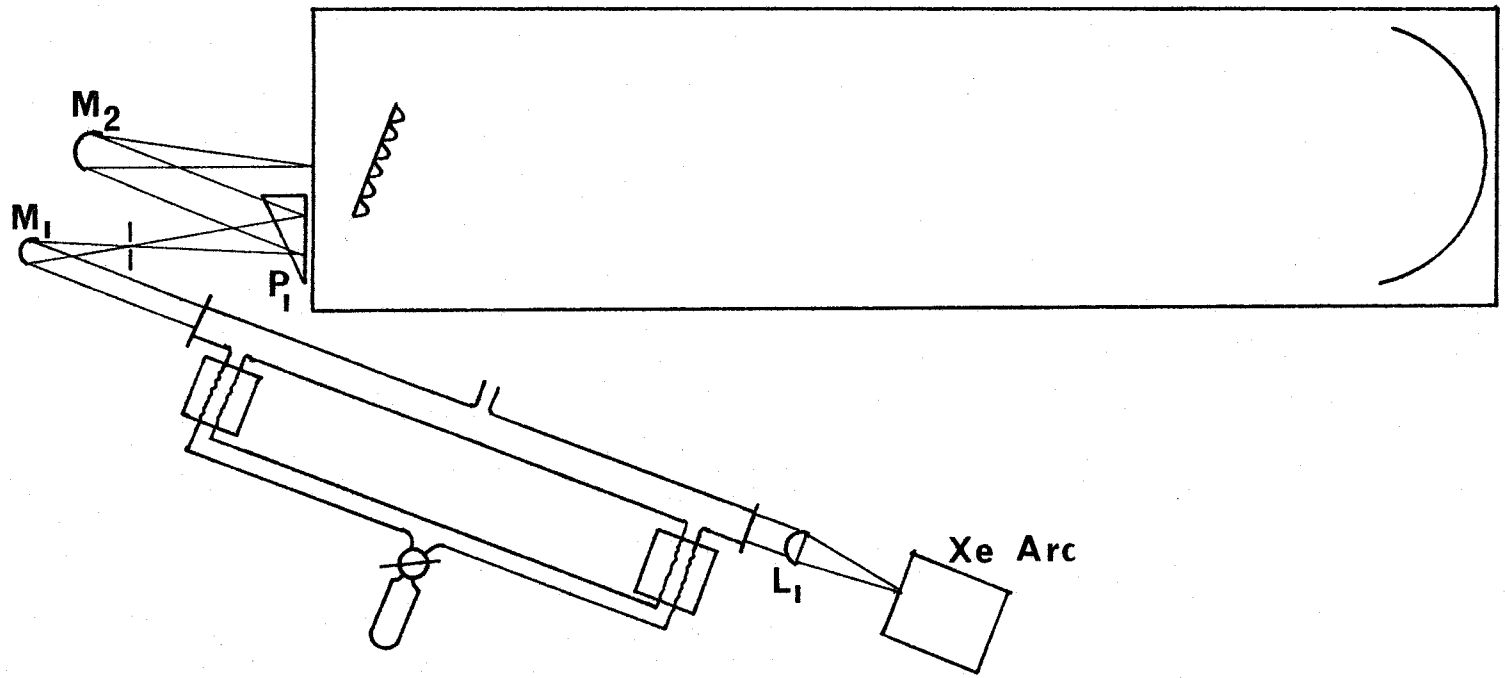

Figure 6

Ebert Spectrograph with Order Sorter and Pyrolysis Apparatus

delicately rotated with a calibrated micrometer screw. Although aberrations were introduced because the light was not plane parallel when reaching the prism, this sacrifice was necessary in order to get sufficient transmission at 220 nm for photographic exposures.

Figure 7a compares the transmission properties of vitreous fused silica, suprasil and borosilicate glass in this region;[49] Figure 7b shows the decline in radiant output of xenon arcs.[49] These factors also show to reduce the intensity of light reaching the detector, and very careful external and internal alignments were necessary for high resolution work.

A check on the resolution being obtained and the identification of the order could be done after an initial calibration with the very strong sharp absorption spectrum of SO_2 over this region. The calculated resolution for the echelle grating in the twenty-eighth order is

$$R = m \times N$$
$$= 28 \times 300 \times 256$$
$$= 2.1 \times 10^6$$

where m = order of the spectrum
N = total number of lines on the grating

The observed resolution was about 1×10^6 for the rotationally resolved bands of H_2CS.

The spectra were recorded on Kodak SWR film and Ilford Q plates with exposures ranging from 20 minutes for the medium resolution work to two hours under conditions of high resolution with long pressure-pathlength.

Figure 7.

(a) Percentage Transmission of Various Materials as a Function of Wavelength.

A. Ultraviolet Grade Fused Silica

B. Infrared Grade Fused Silica

C. Optical and Schlieren Grade Fused Silica

D. Borosilicate Crown Glass

(b) Spectral Irradiance of Xenon Arcs as a Function of Wavelength.

A. 1000 Watt Xenon Lamp

B. 150 Watt Xenon Lamp

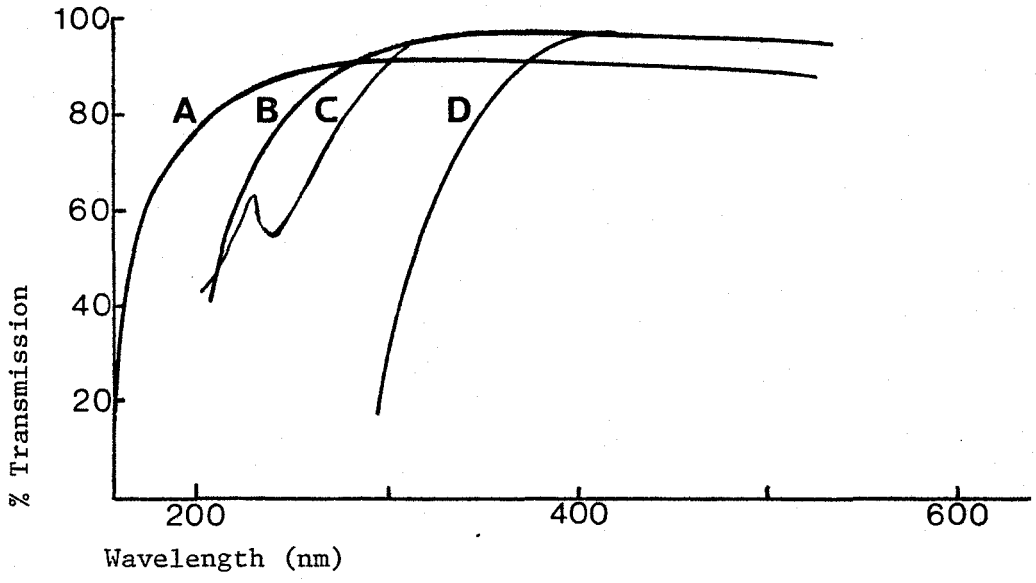
100
80
60
40
20
% Transmission
A
B
C
D
200
400
600
Wavelength (nm)

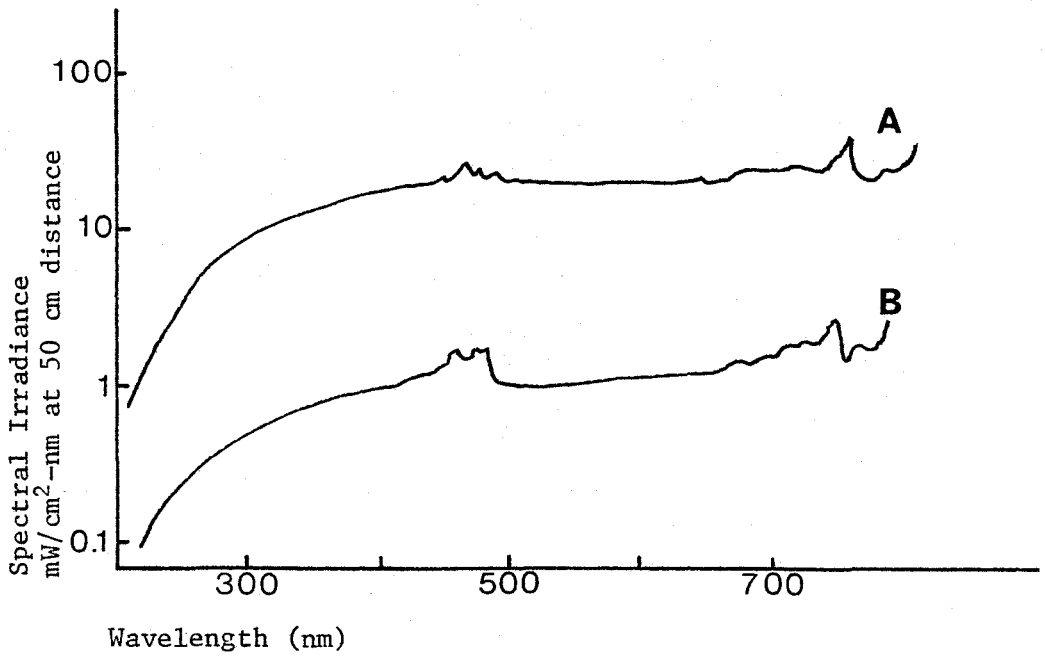
100
10
1
0.1
Spectral Irradiance
mW/cm2-nm at 50 cm distance
A
B
300
500
700
Wavelength (nm)

In the low-resolution spectrum of H_2CS we identified a single transition at 212 nm with sharp rotational structure, a series of broad equidistant bands from 220 nm to 190 nm, and an intense band at 187 nm. Photographic work with a 50 cm cell on the two-meter vacuum spectrograph confirmed these assignments; an additional band at 181 nm was also tentatively identified.

When the spectrum of the deuterated species was analyzed, we noted that the band at 212 nm had shifted to 211 nm, and two bands with similar rotational structure appeared weakly at 208 and 203.5 nm.

With a path length of 1.5 and finally 3 m, the series of equidistant bands could be extended to the red by several intervals until at 221.3 nm for H_2CS and 221.1 nm for D_2CS, the bands developed clear rotational structure.

It has proven difficult to extend the medium resolution work to the red of the band at 221.3 nm. The required increase in pressure-path conditions appears to result in the formation of compounds which are totally absorbing in this region. Consequently, it is not certain if other bands of thioformaldehyde exist to higher wavelength of the one at 221.3 nm.

The most accurate set of measurements for the rotational lines of the origin band of the system at 212 nm was obtained from a series of three Ilford Q plates taken over a range of pressures on a twenty-foot vacuum spectrograph at the National Research Council in Ottawa. All lines were measured on a Leeds and Northrup comparator. It was possible to assign over twenty iron hollow cathode lines on each plate

and these were fitted by a least squares' procedure to a cubic equation with a standard deviation of not more than 0.011 cm^{-1}. This relationship was then used to assign the wavenumbers of almost 300 rotational lines for the normal species and 400 for the deuterated compound. Correlation between plates was excellent and the average of two measured values was used for many lines. In cases where a line appeared to be sharp at only one pressure, the less exact measurement was discarded. In this way, an overall precision of ±0.05 cm^{-1} for H_2CS and ±0.03 cm^{-1} for D_2CS was obtained for the lines used in the computer analysis.

The second system, at 221.3 nm, was much more difficult to measure due to the low intensity of the bands superimposed on a rising background continuum. The lines could not be distinguished under the magnification needed for accurate measurements; the only alternative was to obtain a microdensitometer trace of the band features and fit this to a theoretical band pattern. In this case, wavenumber assignments were made by a simple linear interpolation between successive iron lines and errors were of the order of 0.3 cm^{-1}. Since the individual lines were somewhat broad, they likely encompassed several rotational transitions and no precise analysis could be carried out.

The low-resolution Cary-14 scans were used to calculate oscillator strengths for the two transitions. The areas under the absorption curves were integrated, and absorption due to CS_2 subtracted to give an estimated value of greater than one for the system

originating at 221.3 nm and a value of about 0.1 for the transition at 212 nm. These numbers reflect the ratio of the intensity of the two systems but may be overestimates of the true oscillator strengths since background absorption from other species could not be eliminated entirely.

Chapter IV

Analysis of the $^1B_2(n,3s)$ System

The experimental results indicated the presence of two electronic transitions in thioformaldehyde in the region of 250 to 200 nm. The band at 212.0 nm stood out quite prominently in the spectrum and had been previously identified under low resolution by Callear and Dickson.[4] The second system was more difficult to identify because of overlapping absorption from impurities present in the system. We therefore begin by discussing the well-resolved system which appeared at higher energy.

From the low-resolution scan on the Cary-14, it was evident that the band was rotationally sharp and was not a member of the somewhat diffuse series lying beneath it. The oscillator strength was high, since pressure-path conditions of 10^{-4} m atm were sufficient to bring up the features. In fact, the experimental value for the oscillator strength was ≈ 0.1 and therefore the band must be the result of an electronically allowed transition.

From the original scan of the deuterated compound it was possible to tentatively identify two peaks to lower wavelength which could be vibrational quanta attached to the band at 211.0 nm. These peaks are indicated in Figure 8. The increased resolution of the 2 m vacuum Ebert spectrograph provided verification of these assignments

Figure 8

The Vibrational Spectrum of the $^1B_2(n,3s)$ System of D_2CS

A. Cary-14 trace.

Inset. 2-m Ebert photograph showing the characteristic rotational structure of these bands.

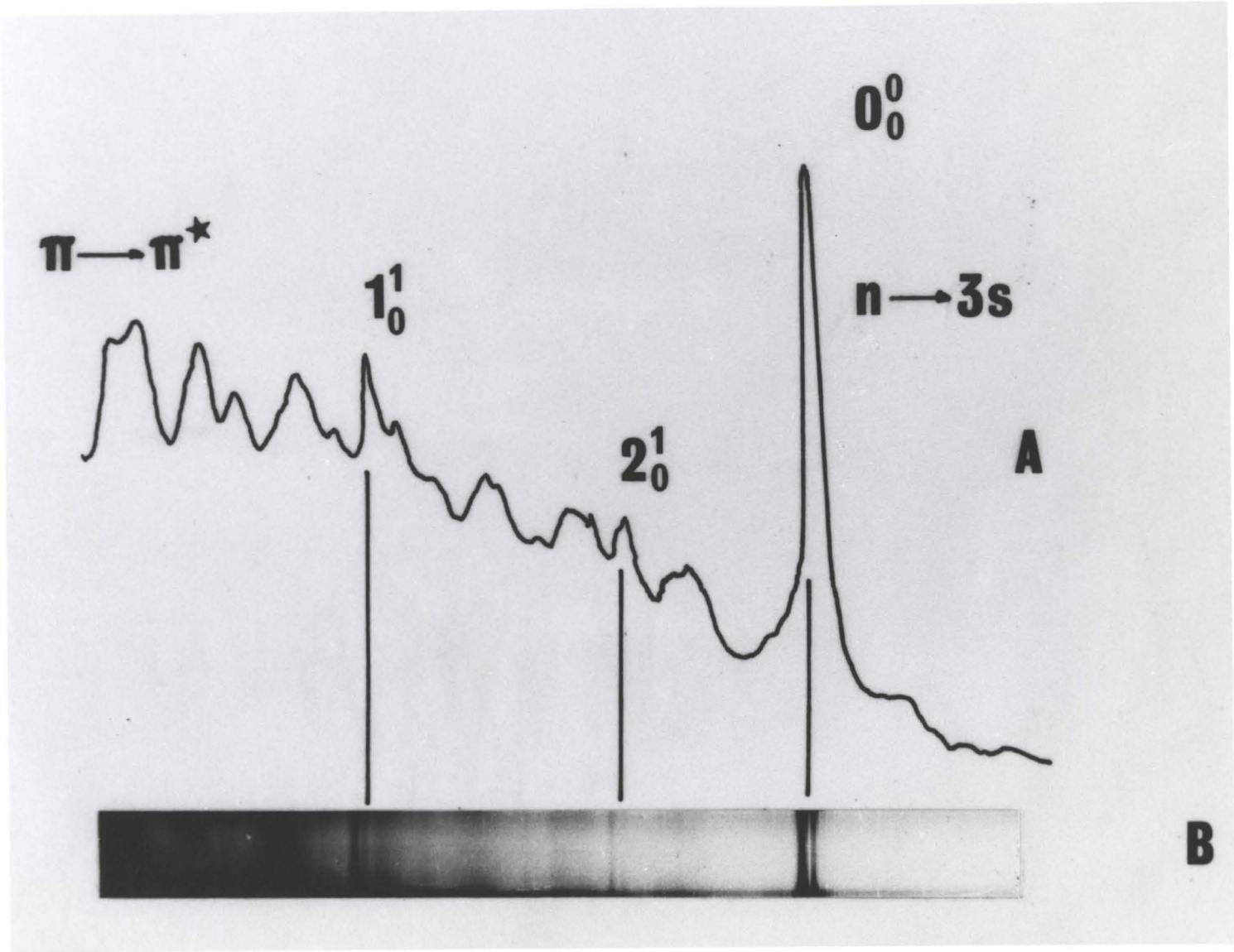
0_0^0
$\pi \rightarrow \pi^*$
1_0^1
$n \rightarrow 3s$
2_0^1
A
B

as all three bands appeared to have the same well-defined rotational structure, unlike the other bands in the region.

The first band, at 211.1 nm, was the most intense, while the peaks at 207.9 nm and 203.5 nm were relatively weak. No other structure appeared with increased pressure-path conditions; we therefore assigned the strongest line to the 0-0 vibronic transition and the two satellites to vibrational quantum additions. According to the Franck-Condon principle,[26,27] this intensity pattern was indicative of a transition in which there was little or no geometry change on excitation. This in turn suggested that non-bonding, weakly bonding or Rydberg orbitals were involved in the transition.

Further evidence as to the likely assignment of this transition came from a comparison between the transition energies of thioformaldehyde and formaldehyde, as shown in Table 6. These indicated that electron promotions required less energy when a sulphur atom had been substituted for an oxygen atom in the molecule. Thus we could reasonably correlate the energy for this transition, 5.84 eV, with the value of 7.09 eV for formaldehyde and assign the sharp band at 212.0 nm to the 0-0 band of the $^1B_2(n,3s) \longleftarrow \tilde{X}^1A_1$ transition in thioformaldehyde.

The <u>ab initio</u> calculations of Bruna <u>et al.</u>[19] placed this transition at 5.83 eV, in excellent agreement with our observed value. Such an assignment had the advantage of involving a non-bonding and a Rydberg orbital and increased the likelihood of there being very little change in geometry on excitation.

Table 6

Transition Energies (eV) for Thioformaldehyde and Formaldehyde

State	Excitation	$\Delta E_{calc}^{(a)}(H_2CS)$	$\Delta E_{obs}(H_2CS)$	$\Delta E_{obs}(H_2CO)$	$\Delta E_{calc}^{(g)}(H_2CO)$
$\tilde{X}^1A_1$	ground state	0.0	0.0	0.0	0.0
$\tilde{a}^3A_2$	$n \longrightarrow \pi^*$	1.84	1.80[b]	3.12[e]	3.41
$\tilde{A}^1A_2$	$n \longrightarrow \pi^*$	2.17	2.03[c]	3.50[e]	3.81
$\tilde{B}^1A_1$	$\pi \longrightarrow \pi^*$	7.92	5.60[d]	--	11.41
$\tilde{C}^1B_2$	$n \longrightarrow 3s$	5.83	5.84[d]	7.09[f]	7.38
$\tilde{D}^1A_1$	$n \longrightarrow 3p_y$	6.62	6.60[d]	7.97[f]	8.11
$\tilde{E}^1B_2$	$n \longrightarrow 3p_z$	--	6.82[d]	8.11[f]	8.39
$\tilde{F}^1A_2$	$n \longrightarrow 3p_x$	7.88	--	8.47[f]	9.07

(a) calculated vertical excitation energies, reference 19.

(b) observed 0_0^0 energy, reference 10b.

(c) observed 0_0^0 energy, reference 10d.

(d) observed 0_0^0 energies, this work.

(e) observed 0_0^0 energies, reference 13.

(f) observed 0_0^0 energies, reference 28.

(g) calculated vertical excitation energies, reference 29.

The wavenumbers of the two vibrational bands in the D_2CS spectrum were 746 ± 40 cm^{-1} and 1783 ± 40 cm^{-1}. The latter could be readily identified from a comparison with the ground state frequencies listed in Table 7. The value for ν_1''(CD) had been calculated to be 2146 cm^{-1} on the basis of isotopic substitution in the F and G matrices.[7] The excited state value of 1783 cm^{-1} then represented a 17% decrease in frequency, which correlated exactly with the observed change in ν_1 for formaldehyde on n $\longrightarrow$ 3s excitation.[28a] These values are listed in Table 8 for comparison.

The assignment of the band at +746 cm^{-1} at first seemed as clearcut. The ground state value for ν_3''(CS) had also been calculated from the F and G matrices and was given as 941 cm^{-1}. A decrease on excitation of 20% was in line with that for ν_1(CD). However, the vibrational analysis of the n $\longrightarrow$ 3s transition in formaldehyde indicated that there was no activity in the CO vibrational mode but that there was a 50% drop in the frequency of the HCH symmetric vibration due to a large change in the HCH angle. The band could be identified in the spectra of both H_2CO and D_2CO and the isotopic shift verified this assignment.

We were unable to obtain this confirmation for the sulphur compounds as the band could not be identified in the spectrum of the normal compound and was assumed to be rotationally diffuse. However, the origin isotope shift for the two compounds could be used to elucidate the problem.

Table 7

Observed Frequencies and Assignments for the Vibrational Transitions in the Electronic States of Thioformaldehyde (in cm^{-1})

		ν_1(CH)	ν_2(HCH)	ν_3(CS)	ν_4(out-of-plane)
$\tilde{X}$	H_2CS	2971[a]	>1550[a]	1063[b]	993[b]
	D_2CS	(2146)[b]	(1203)[b]	941[b]	783[b]
$\tilde{a}$	H_2CS[c]	--	1320	859	711[d]
	D_2CS[c]	--	1012	798	516[d]
$\tilde{A}$	H_2CS[e]	3034	1316	820	371[f]
	D_2CS[e]	2139	1013	771	275[f]
$\tilde{B}$	H_2CS	--	--	476[g]	
	D_2CS	--	--	436[g]	
$\tilde{C}$	H_2CS	--	--		
	D_2CS	1783[g]	746[g]		

(a) reference 6--ν_2 estimated by analogy to H_2CO, CO and CS.

(b) reference 7--numbers in brackets calculated from the symmetrized G matrix.

(c) reference 10d.

(d) $\sigma 4_0^2 - \sigma 0_0^0$, reference 10d.

(e) reference 10b.

(f) $\sigma 4_0^1 - \sigma 0_0^0$, reference 10b.

(g) this work.

Table 8

A Comparison of Vibrational Frequencies (cm^{-1})

		H_2CO	D_2CO	D_2CS
$\tilde{X}^1A_1$	$\nu_s(CX)$	2766.4[a]	2055.8[a]	(2146)[c]
	$\nu_s(CY)$	1746.1	1700.0	941
	$\nu_s(XCX)$	1500.6	1105.7	(1203)
	$\nu_{as}(CX)$	2843.4	2159.7	(2138)
	$\nu_{as}(XCX)$	1251.2	990.4	(1017)
$^1A_2(n,\pi^*)$	$\nu_s(CX)$	2847[a]	2079[a]	2139[d]
	$\nu_s(CY)$	1173	1176	771.3
	$\nu_s(XCX)$	887	(625)	1013
	$\nu_{as}(CX)$	2968	2233	2324.85
	$\nu_{as}(XCX)$	904	705	599
$^1B_2(n,3s)$	$\nu_s(CX)$	2275[b]	1701[b]	1783[e]
	$\nu_s(CY)$	--	--	--
	$\nu_s(XCX)$	822	501	746
	$\nu_{as}(CX)$	--	--	--
	$\nu_{as}(XCX)$	--	--	--

X = H, D

Y = O, S

(a) data for $^1A_1$ and $^1A_2$ states of formaldehyde from reference 30.

(b) data for the $^1B_2$ state of formaldehyde from reference 28a.

(c) data for the $^1A_1$ state of thioformaldehyde from reference 7.

(d) data for the $^1A_2$ state of thioformaldehyde from reference 10b.

(e) data for the $^1B_2$ state of thioformaldehyde from this work.

The observed origin isotope shift is the result of changes in the zero-point energy of the upper state relative to that of the ground state. This difference is expressed as

$$\nu_0(D_2CS) - \nu_0(H_2CS)$$
$$= \left(\sum_{i=1}^{6} \frac{\nu_i'}{2} - \sum_{i=1}^{6} \frac{\nu_i''}{2}\right)_{D_2CS} - \left(\sum_{i=1}^{6} \frac{\nu_i'}{2} - \sum_{i=1}^{6} \frac{\nu_i''}{2}\right)_{H_2CS}$$

and therefore the effect measures the total change in vibrational frequency of all six modes on electronic excitation.

The observed shifts for several electronic transitions in similar molecules are listed in Table 9. From the relationship given above, we would expect that large decreases in frequencies involving the isotopic atoms would result in large 0-0 shifts. However, it is also true that corresponding increases in these frequencies will yield small shifts or even reverse the direction of the shift. Table 9 indicates that the shift of 214 cm^{-1} for the 0-0 band in the $n \longrightarrow 3s$ transition in thioformaldehyde is quite large relative to that for other transitions in thioformaldehyde. A similar trend has been observed for formaldehyde; the shift of 311 cm^{-1} is nearly three times that for the $n \longrightarrow \pi^*$ system. In the $n \longrightarrow 3s$ system, the large shift has been partially accounted for by large decreases in both ν_1(CH) and ν_3(HCH) as indicated in Table 8, but there is also evidence of a large change in either ν_4(out-of-plane) or ν_6(HCH).[28a] By contrast, in the $n \longrightarrow \pi^*$ system, ν_1(CH) and ν_5(CH) have increased slightly on excitation.

Table 9

Observed Isotope Shifts of the Origin Bands of Formaldehyde, Thioformaldehyde and Thiocarbonyl Dichloride (in cm^{-1})

Transition	H_2CO [a]	H_2CS [a]	Cl_2CS [b]
$\tilde{a}^3A_2(n,\pi^*) \longleftarrow \tilde{X}^1A_1$	118.57 [c]	106.16 [f]	--
$\tilde{A}^1A_2(n,\pi^*) \longleftarrow \tilde{X}^1A_1$	112.96 [d]	89.03 [g]	0.43 [i]
$\tilde{B}^1A_1(\pi,\pi^*) \longleftarrow \tilde{X}^1A_1$	--	29 [h]	0.27 [j]
$\tilde{C}^1B_2(n,3s) \longleftarrow \tilde{X}^1A_1$	311 [e]	214 [h]	--
$\tilde{D}^1A_1(n,3p_y) \longleftarrow \tilde{X}^1A_1$	197 [e]	77 [h]	--
$\tilde{E}^1B_2(n,3p_z) \longleftarrow \tilde{X}^1A_1$	192 [e]	--	--

(a) $\sigma 0_0^0$ (D_2CX-H_2CX).

(b) $\sigma 0_0^0$ ($^{35}Cl^{37}ClCS-^{35}Cl_2CS$).

(c) H_2CO, reference 31.

D_2CO, reference 32.

(d) reference 30.

(e) reference 28.

(f) reference 10d.

(g) reference 10b.

(h) this work.

(i) reference 33.

(j) reference 34.

Although this is counterbalanced by large drops in ν_3(HCH) and ν_6(HCH), the net result is a 198 cm^{-1} decrease in the value of the shift. In other words, changes in the CH stretching modes have a significant influence on the origin isotope shift. Thus, in order to account for the large origin isotope shift in the n $\longrightarrow$ 3s system, there must be a large decrease in both ν(CH) and ν(HCH). In the spectrum of thioformaldehyde-d_2 then, the assignment of the band at +746 cm^{-1} to ν_2'(DCD) was essential in order to explain the observed large isotope shift.

In order to obtain further information about the molecule in this excited state, we then carried out a line-by-line rotational analysis as discussed below.

The overall symmetry of this transition is B_2, which indicates that the direction of the transition moment is along the b axis and the rotational transitions follow the selection rules for a type B band:

$$\Delta K_a = \pm 1, \pm 3, \ldots$$

$$\Delta K_c = \pm 1, \pm 3.$$

or $\quad ++ \longleftrightarrow --$

$\quad +- \longleftrightarrow -+$

H_2CS is a near prolate symmetric top in the ground electronic state (κ = -0.992) and is not expected to be greatly different in this state. We therefore refer to the symmetric top quantum number K_a (= K_{-1}) for convenience. Transitions with a constant value of K_a in both the ground and excited states (e.g., K_a'' = 3, K_a' = 2, J" = 3, 4, 5, ...)

form a group that is referred to as a subband. Each subband within the spectrum is designated by both a superscript P or R depending on whether $\Delta K = K_a' - K_a'' = -1$ or $+1$ respectively, and a subscript designating the value of K_a in the ground state. Since ΔJ may take the values -1, 0 or +1, each subband will consist of a P, Q and R branch. Therefore the total subband notation takes the form ${}^{\Delta K_a}\Delta J_{K_a''}(J'')$. When this designation is used, it always describes two possible transitions if $K_a > 0$. This degeneracy is artificial for an asymmetric top and for low values of K and high values of J the separation of the two lines can be observed. For these lines, the value of K_c'' must be included to unambiguously identify the transition.

The high resolution photographs of the 0-0 band for both H_2CS and D_2CS are shown in Figure 9. Certain features stood out in the structure of lines and these were used for initial assignments of J and K quantum numbers.

We have stated that each K subband is composed of a P, Q and R branch, but theoretical intensity calculations indicate that the ${}^{P}R$ and ${}^{R}P$ branches for $K_a'' \geq 3$ will be quite weak and will not be readily observed. The most intense branches are the ${}^{P}P$ and ${}^{R}R$ wings and in fact the P subband region was the most clearly defined region. The ${}^{P}Q$ branches were not resolved and gave the appearance of a single broad band due to their close spacing, but individual ${}^{P}P$ lines were sharp and easily identified. A consideration of the selection rules told us that the first member of a branch must have the assignment $J'' = K_a''$ and from this we established the value of K_a'' within one number by measuring back

Figure 9a

The Rotational Spectrum of the $^1B_2(n,3s)$ System of H_2CS.

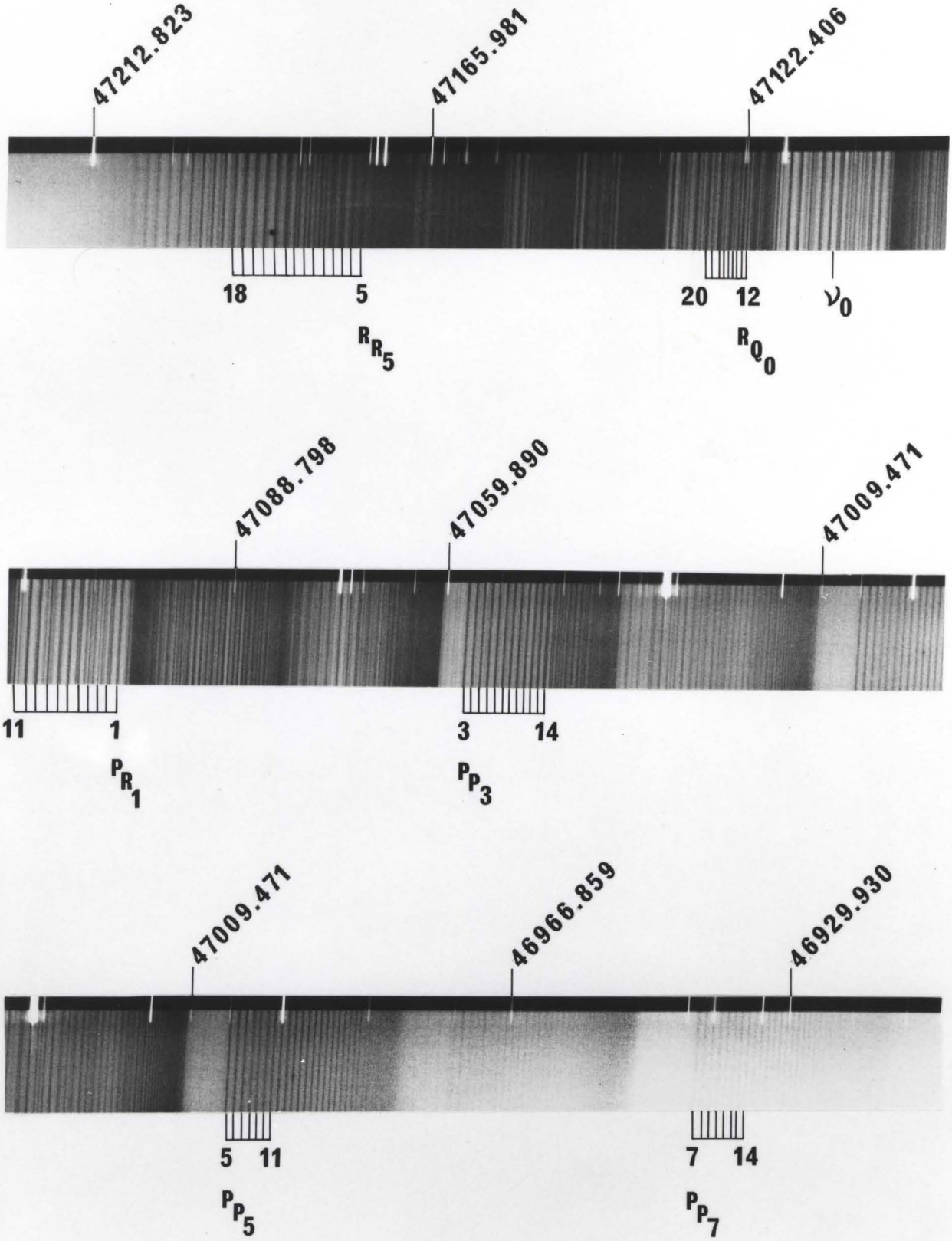
47212.823
47165.981
47122.406
18
5
20
12
ν_0
R_{R_5}
R_{Q_0}
47088.798
47059.890
47009.471
11
1
3
14
P_{R_1}
P_{P_3}
47009.471
46966.859
46929.930
5
11
7
14
P_{P_5}
P_{P_7}

Figure 9b

The Rotational Spectrum of the $^1B_2(n,3s)$ System of D_2CS

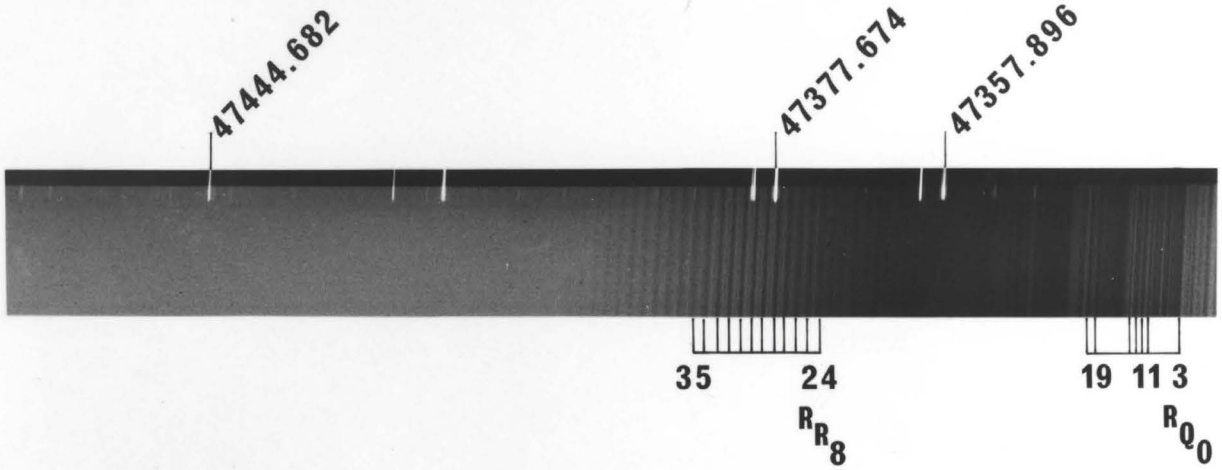
47444.682
47377.674
47357.896
35
24
R_{R_8}
19
11
3
R_{Q_0}

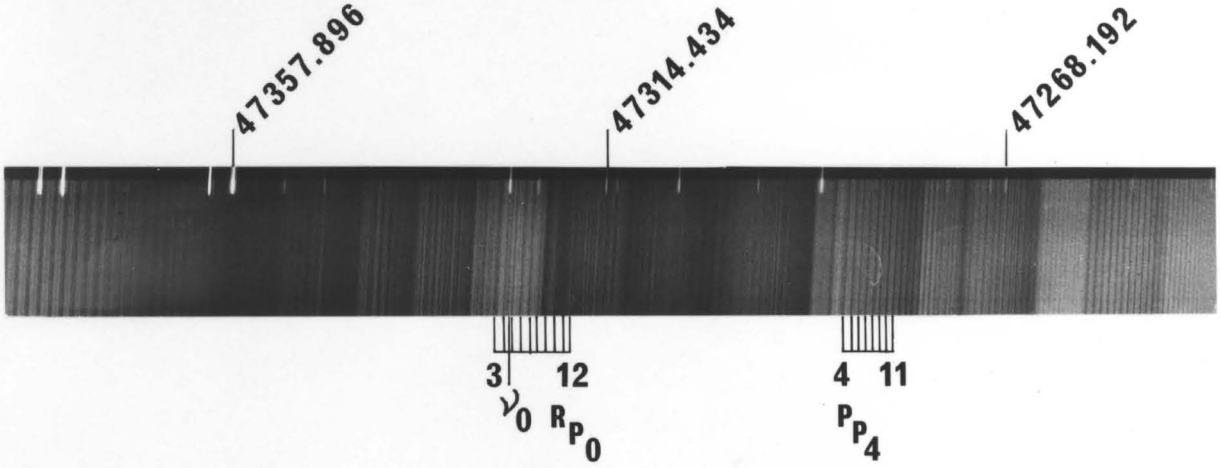
47357.896
47314.434
47268.192
3
12
ν_0
R_{P_0}
4
11
P_{P_4}

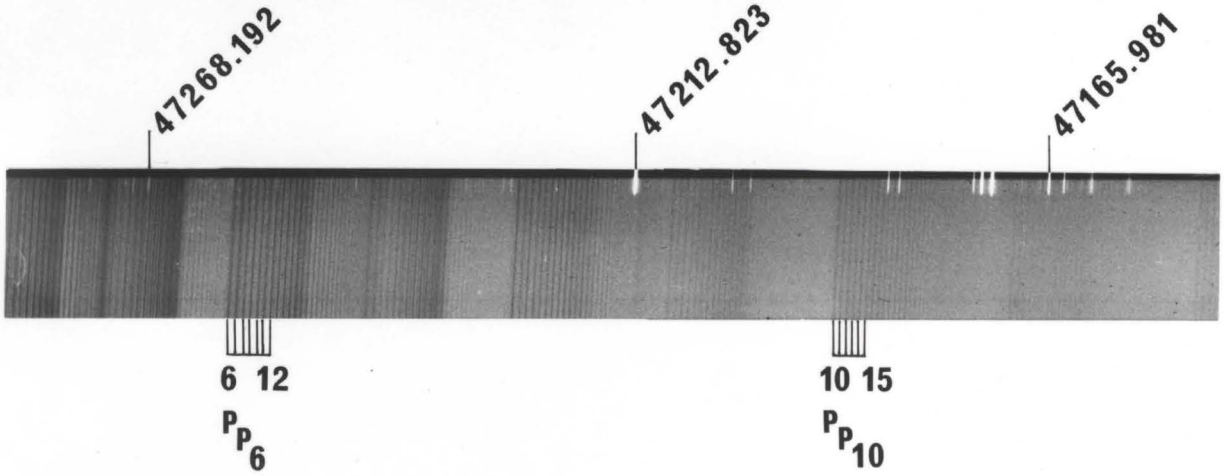
47268.192
47212.823
47165.981
6
12
P_{P_6}
10
15
$P_{P_{10}}$

to the ^{P}Q band. The statistical weight factor of 1:3 for the intensity ratio of even K" to odd K" in the normal compound was quite evident in the spectrum and provided the definitive assignment for the K_a'' values.

For high K values, the molecule closely approximates a symmetric top and the assignment of J and K was straightforward. However, resolution of the asymmetry doubling could first be identified within the $^{P}P_3$ branch of the H_2CS spectrum. A splitting of 0.176 cm^{-1} was measured between the lines $^{P}P_{3,12}(14)$ and $^{P}P_{3,11}(14)$. Further assignments could be made to form the basis for the complete rotational analysis for an asymmetric top molecule. This calculation was carried out as a line by line fitting of the data to the energy equation using a computer programme described by Johns and Olson.[6]

The programme first generated the non-rigid asymmetric rotor ground state energies by direct diagonalization of the four Wang submatrices. The calculation proceeded by computing a trial set of energies from an initial set of parameters. The parameters to be varied in the fit were each in turn changed by a small amount and new energies computed. The differences between the new energies and the corresponding trial energies were then divided by the change made in the parameter. This set of coefficients (the Jacobian) together with the differences between the observed energies and the trial set formed a system of linearized equations of condition. These were solved, in the least squares sense, by standard methods and an improved set of parameters obtained. The whole process was repeated until the predicted corrections to the parameters were all less than their standard

deviations. Finally, the computer was instructed to perform a back calculation to predict the positions of unassigned lines.

In order for this procedure to be useful, it was necessary to have a fairly accurate initial set of trial parameters and a definite assignment for all lines used in the fitting procedure. Initial values for A', B' and C' were obtained in the following manner. The molecule was assumed to be a rigid, symmetric top. Then the subband origins (J" = 0) were described by the following energy expression:

$$\nu_0^{sub} = \nu_0' + (A' - \bar{B}') \pm 2(A' - \bar{B}')K_a'' + [(A' - \bar{B}') - (A'' - \bar{B}'')]K_a''^2 , \quad \bar{B} = \frac{B + C}{2}$$

where the + sign referred to the R subbands and the - sign to the P subbands. In fact, it was noted that the R subbands rapidly converged and then turned back at about J = 8 for the normal species. This alone indicated that $\Delta(A - \bar{B})$ was negative. The value of this parameter was obtained by forming the second differences $\delta_2^K = 2[A' - \bar{B}' - (A'' - \bar{B}'')]$ between successive band heads of the P wing.

Within one subband the values of K_a'' and K_a' do not change. Successive lines in a P subband were therefore described by the energy equation

$$\nu_P = \nu_0^{sub} + (\bar{B}' - \bar{B}'')J''^2 - (\bar{B}' + \bar{B}'')J''$$

Thus $\Delta\bar{B} = \bar{B}' - \bar{B}''$ could be obtained by forming second differences $\delta_2^J = 2(\bar{B}' - \bar{B}'')$ between successive lines within a subband. Since values for A'' and $\bar{B}''$ are known, A' and $\bar{B}'$ were easily calculated. Subbands for which $K_a'' > 3$ only were used so that the symmetric approximation was justifiable.

To determine B' and C' separately we invoked the planarity constraint (i.e., assumed that the inertial defect $\Delta = 0$). Then

$$B = -(A - \bar{B}) + \sqrt{A^2 + \bar{B}^2}$$

$$C = (A + \bar{B}) - \sqrt{A^2 + \bar{B}^2}$$

The distortion constants D_K, D_{JK}, D_J, δ_J and R_5 were set at their ground state values and the band origin was established by inspection.

Assignments for some of the R subbands were confirmed by a manual calculation using the appropriate differences and sums from the known ^PP assignments.

i.e., $^R R_{K_a''}(J) = {}^P P_{K_a''}(J + 2) + F''_{J+2} - F''_J$

The correlation coefficient of the calculation was 1.30 for the normal compound and 1.41 for the deuterated species, indicating an excellent fit and the absence of any rotational perturbations.

A total of 357 assignments for H_2CS and 476 for D_2CS were used in the final fitting. These are listed in Appendix 1. The final set of

rotational constants for each species is tabulated in Table 10.

These experimental rotational constants are inversely proportional to the effective moments of inertia, I°, of the molecule, where I° is defined by the equation

$$\frac{1}{I^\circ} = \left(\frac{1}{\sum m_i r_i^2}\right)_{Av}$$

and to a first approximation the r_i are the instantaneous positions of the atoms.

By definition, if a molecule is planar then the equilibrium moments of inertia fulfill the relation

$$I_C^e = I_A^e + I_B^e$$

This is not true of the effective moments of inertia so that

$$\Delta = I_C^\circ - (I_A^\circ + I_B^\circ) \neq 0$$

Δ is referred to as the inertial defect.

The values of Δ for this state are 0.089 and 0.109 amu $\mathring{A}^2$ for the normal and the deuterated molecules respectively. The ground state values for the planar molecule are 0.063 and 0.083 amu $\mathring{A}^2$, while the slightly non-planar $^1A_2(n,\pi^*)$ state has inertial defects of 0.038 and 0.017 amu $\mathring{A}^2$ respectively[10c] for the 0-0 band. This information suggests that the molecule is planar or slightly non-planar, but more

Table 10

Excited State Rotational Constants for the n $\longrightarrow$ 3s Transition (in cm^{-1})

	H_2CS	D_2CS
A	8.55748(73)	4.34969(17)
B	0.603329(10)	0.510491(45)
C	0.56192(11)	0.455527(44)
D_K	$1.2585(11) \times 10^{-3}$	$2.121(11) \times 10^{-4}$
D_{JK}	$1.55(15) \times 10^{-5}$	$1.868(28) \times 10^{-5}$
D_J	$1.340(84) \times 10^{-6}$	$4.22(39) \times 10^{-7}$
ν_o	47110.8209(86)	47325.5631(42)

The numbers in brackets are the standard deviations on the last two digits.

definite conclusions can be drawn from the complete geometrical analysis.

There are two approximate methods in general use to calculate structures, referred to as the r_o and r_s calculations. The first of these is usually a straightforward process and is a reasonable indicator of the true r_e structure. In order to provide four rotational constants for a fit, the assumption must be made that the r_o geometry does not change on isotopic substitution. For our calculations the rotational constants of the deuterated species were thus incorporated into a least squares' fitting procedure. The programme required initial estimates for the geometrical parameters and varied them continuously until the calculated rotational constants were in good agreement with the experimental values. In fact, it was found impossible to obtain convergence in the programme and reasonable values for α and θ if all four parameters were allowed to vary. Since we already had an indication that the value of θ was near zero, it was fixed at zero; a good fit for the other three parameters could then be found. Changes in the value of θ of up to 5° did not alter the final geometry within the error of the technique. The geometry thus calculated is given in Table 11.

Costain[35] has pointed out that the effective geometry is different for each isotopic molecule since the vibrational frequencies are different. Consequently, the r_o structure as determined by this method would suffer an additional discrepancy with the r_e values. Some parameters may vary by as much as 0.01 Å when a different set of isotopic constants is used for the calculation.

Table 11

r_o and r_s Structures for the $^1B_2$ State

	r_o	r_s
r_{CS} (Å)	1.6073 ± 0.0027	1.6047 ± 0.0016
r_{CH} (Å)	1.1124 ± 0.0042	1.1119 ± 0.0056
α_{HCH} (degrees)	123.74 ± 0.80	122.68 ± 0.10

A more satisfactory method of structure calculation has been developed by Kraitchman[36] and elaborated by Costain. Isotopic substitution is performed sequentially on each of the atoms of the reference molecule (usually the normal isotopic species). The rotational constants for all of the isotopic species are then used in an equation to specify the position of each isotopic atom with respect to the centre of mass of the reference molecule. If equilibrium moments of inertia could be used, the equilibrium structure would be obtained, but the effective moments of inertia will yield a substituted or r_s structure. The co-ordinates determined from this method are closer to the equilibrium values than are the r_o estimates. Costain concludes that the relation among the three is given by

$$r_s \simeq (r_o + r_e)/2$$

Since our only isotopic data involved the substitution of two atoms simultaneously, we developed a variation of Kraitchman's equation as shown below.

The planar dyadic P is defined with respect to the centre of mass as

$$P = \sum_i m_i r_i r_i - \left(\sum_i m_i r_i\right)\left(\sum_i m_i r_i\right) \Big/ \sum_i m_i \qquad (1)$$

Typical elements have the form

$$P_x = \sum_i m_i x_i^2 \tag{2}$$

$$P_{xy} = \sum m_i x_i y_i \tag{3}$$

These are related to the moments of inertia by relations of the form

$$P_\alpha = \tfrac{1}{2}(I_\beta + I_\gamma - I_\alpha) \quad , \qquad \alpha, \beta, \gamma = x, y, z \quad \alpha \neq \beta \neq \gamma \tag{4}$$

If the origin of the molecule-fixed co-ordinate system is chosen so as to coincide with the centre of mass of the normal species, then only the first term in equations (2) and (3) remains and the others add to zero. The same co-ordinate system is then used to calculate P' for the deuterated molecule such that

$$P'_x = P_x + \frac{2\Delta mM}{2\Delta m+M} x_H^2 = P_x + \mu x_H^2$$

$$P'_y = P_y + 2\Delta m y_H^2$$

$$P'_z = P_z + \mu z_H^2$$

$$P'_{xy} = P'_{yz} = 0$$

$$P'_{xz} = \mu x_H z_H$$

The secular equation then has the form

$$\begin{vmatrix} P_x + \mu x_H^2 - P' & 0 & \mu x_H z_H \\ 0 & P_y + 2\Delta m y_H^2 - P' & 0 \\ \mu x_H z_H & 0 & P_z + \mu z_H^2 - P' \end{vmatrix} = 0 \qquad (5)$$

and this can be expanded to give a cubic equation in P'.

If the assignment is reversed so that the molecule-fixed axes coincide with the centre of mass of the deuterated molecule, the net result must be the same. The determinant has the form

$$\begin{vmatrix} P_x' - P' & 0 & 0 \\ 0 & P_y' - P' & 0 \\ 0 & 0 & P_z' - P' \end{vmatrix} = 0 \qquad (6)$$

From these two equations, the coefficients of like powers in P' can be equated to give the following non-linear simultaneous equations:

$$\mu(x^2 + z^2) + \mu_y y^2 + P_x + P_y + P_z - P_x' - P_y' - P_z' = 0 \qquad (7)$$

$$\begin{aligned} &\mu x^2(P_y + P_z) + \mu_y y^2(P_x + P_z) + \mu z^2(P_x + P_y) \\ &+\mu_y y^2 \mu z^2 + \mu_y y^2 \mu x^2 + P_y P_z + P_x P_z + P_x P_y \\ &- P_x' P_y' - P_x' P_z' - P_y' P_z' = 0 \end{aligned} \qquad (8)$$

$$\begin{aligned} &\mu x^2 P_y P_z + \mu_y y^2 P_x P_z + \mu z^2 P_x P_y + \mu_y y^2 \mu x^2 P_z \\ &+ \mu_y y^2 \mu z^2 P_x + P_x P_y P_z - P_x' P_y' P_z' = 0 \end{aligned} \qquad (9)$$

Only one solution of these equations resulted in a reasonable set of $|x|$, $|y|$ and $|z|$ values for the hydrogen atoms. Values of +15.43 and -1.028 $\mathring{A}^2$ for y^2 were rejected in favour of the value $y^2 = 0.95201\ \mathring{A}^2$. Resubstitution into equations (2) and (3) or the moment of inertia relationship yielded the co-ordinates for the carbon and sulphur atoms. Different choices gave slightly different structures and these discrepancies are reflected in the uncertainties quoted for each parameter in Table 11.

Analysis of the $^1A_1(\pi,\pi^*)$ System

The second electronic system at 221.3 nm consisted of a long progression of diffuse vibrational bands with one or two sharp members at the red end of the series, as shown in Figure 10. The oscillator strength, integrated approximately from the Cary-14 trace, was greater than one; this transition was therefore an electronically allowed valence transition. The wavenumber assignments of the bands, listed in Table 12, indicate that there is only a single vibrational mode active in the spectrum, with a value of 476 ± 2 cm^{-1} for the first quantum addition in the hydrogen compound and 436 ± 10 cm^{-1} for the deuterated species. The intensity maximum occurred at $v \simeq 11$, indicating on Franck-Condon grounds that a large change along a single normal co-ordinate had occurred. This would generally be accompanied by a large drop in the vibrational frequency related to the structural change. Either ν_3(CS stretch) or ν_4(out-of-plane deformation) were likely assignments for this activity. Since ν_4 is an asymmetric

Figure 10

The $^1A_1(\pi,\pi^*)$ System of Thioformaldehyde

A. Cary-14 trace

Inset. 20-foot Ebert photograph of the rotational structure of the 0-0 band.

B. H_2CS

C. D_2CS

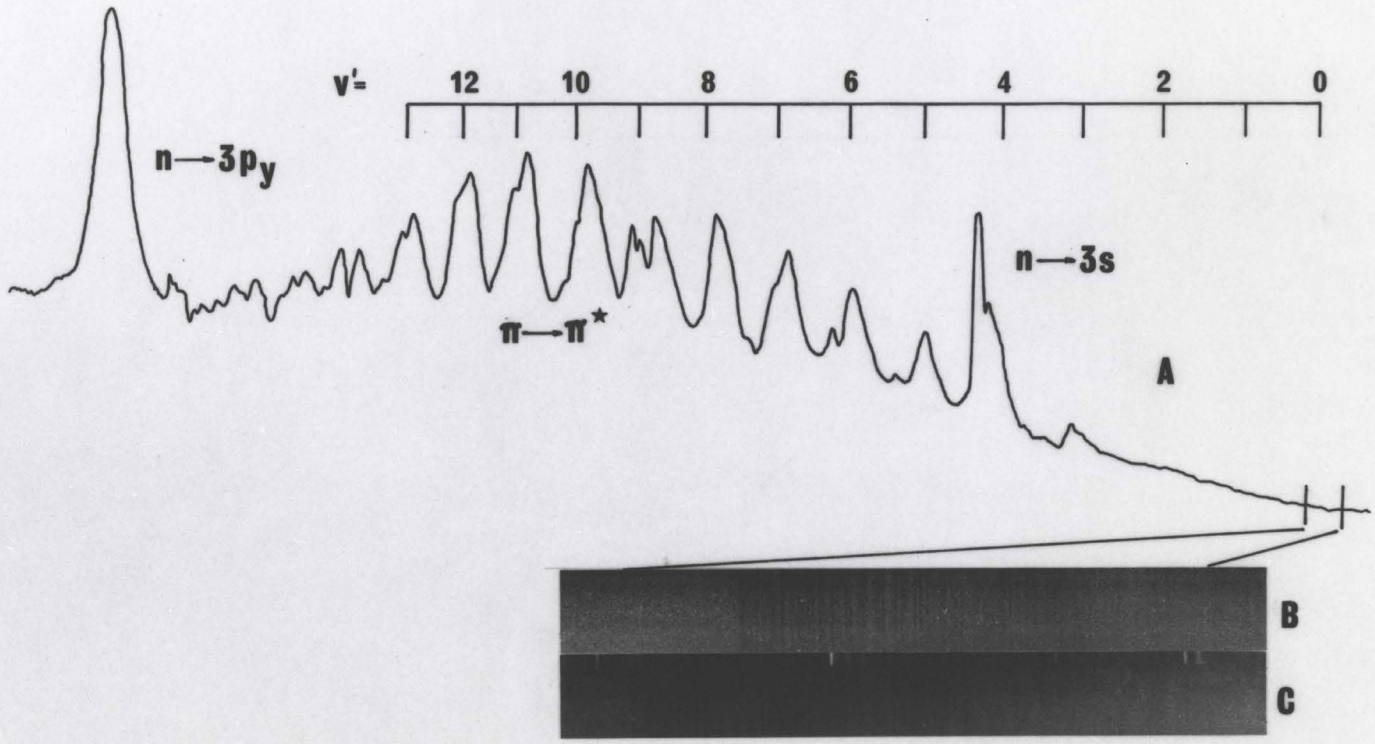
v'=
12
10
8
6
4
2
0
n→3p$_y$
π→π*
n→3s
A
B
C

Table 12

Observed Frequencies and Assignments for the Vibrational Transitions in the $\tilde{B}^1A_1(\pi,\pi^*) \longleftarrow \tilde{X}^1A_1$ System (in cm^{-1})

	H_2CS		D_2CS	
Assignment	Wavenumber	Absorbance[e]	Wavenumber	Absorbance[e]
v' = 0	45197[a]	--	45226	--
1	45673	--	45662	--
2	46142	0.08	--	--
3	46601	0.14	46625	--
4	--[b]	--	--	--
5	47486[c]	0.45	--	--
6	47921	0.60	47885	0.55
7	48374	0.74	48271	0.70
8	48817	0.88	48651	0.81
9	49276	0.82	49038	0.84
10	49729[d]	1.00	49453	0.90
11	50228	1.00	49840	1.00
12	50622	0.90	50200	0.89
13	51034	0.50	50541	0.57
14	51454	0.20	51018	0.31

(a) v' = 0 to v' = 3 were measured on the high frequency edge of the bands recorded with the 20-foot spectrograph and the holographic grating. The estimated error is ±2 cm^{-1}.

(b) obscured by $n \longrightarrow 3s$ absorption.

(c) v' = 5 to v' = 9 measured at the centre of the diffuse bands recorded with the 2-meter spectrograph and an 1180 lines/mm grating. The estimated error is ±25 cm^{-1}.

(d) v' = 10 to v' = 14 measured from the peaks recorded on the Cary-14 spectrophotometer. The estimated error is ±50 cm^{-1}.

(e) maximum peak heights from the Cary-14 trace, scaled to v' = 11, A = 1.00.

vibration and the transition is electronically allowed, only even quanta of ν_4 would have appreciable intensity and thus ν_4' would be less than or equal to 475 cm^{-1} depending on the inversion splitting. A comparison with ν_4' for other states, listed in Table 7, indicated that the shift on deuterium substitution should be at least 100 cm^{-1}. This fact eliminated this assignment in favour of one which did not involve the hydrogen atoms. Thus ν_3(CS) was assigned as the vibrational mode active in this state.

The combination of high oscillator strength and strong C-S activity suggested that this transition should be given the assignment $^1A_1(\pi,\pi^*) \longleftarrow \tilde{X}^1A_1$. On the one hand, the vertical energy of 6.2 eV observed for this transition was lower than the calculated value of 7.92 eV.[19] However, the authors suggested that their value is dependent on the choice of basis set and may be lower. They do not locate any other intervalence transitions in this region. On the other hand, this assignment was compatible with the assignment of $\pi \longrightarrow \pi^*$ transitions observed in the thiocarbonyl compounds F_2CS[37] and Cl_2CS[38] at 4.9 and 4.46 eV respectively.

The origin band showed evidence of rotational structure but it did not have sufficient definition to warrant a line-by-line analysis. We therefore turned to a band contour analysis, using a computer programme originally written by Parkin[39] and modified by Balfour.[40] This programme computes the rotational band contour for an asymmetric rotor with allowance for differing asymmetry in the two states. The main feature of the modified programme is that instead of calculating

all the transitions which go to make up a band, the exact transition energy is calculated for J = 0, 1, 2 and specified spot values over the range of interest; the other values are filled in by interpolation. The resulting spectrum is plotted by specifying the linewidth, temperature and wavenumber interval required.

A number of band contours were generated for type A, B and C bands for various values of the rotational constants. The range for A was kept low since it would be unaffected by changes in the CS bond length. Both B and C were expected to drop significantly so they were allowed much greater variation. The inertial defect was maintained near its ground state value (Δ = 0.068 amu $\mathring{A}^2$) so that the molecule was constrained in the planar configuration. A selection of these contours are shown in Figure 11; the corresponding rotational constants for each are listed in Table 13.

The main feature of this band was its very sharp, sudden cutoff in intensity at the high energy end. The band had an irregular structure which consisted of about seventy lines gradually decreasing in intensity and increasing in separation to lower wavenumbers. From an examination of the computed spectra, we could immediately conclude that only a type A band could reproduce the sharp drop in intensity at the high wavenumber end. The continuous decrease in intensity was also only associated with the type A bands, although this was less certain as no regular pattern could be identified.

Differentiation among contours of type A was not straightforward. Changes in the value of A affected the band structure at the high

Figure 11

Trial Band Contours for the $^1A_1(\pi,\pi^*)$ System of Thioformaldehyde

(Rotational constants listed in Table 13, p. 72.)

(a) Type A Bands

(b) Type B Bands

(c) Type C Bands

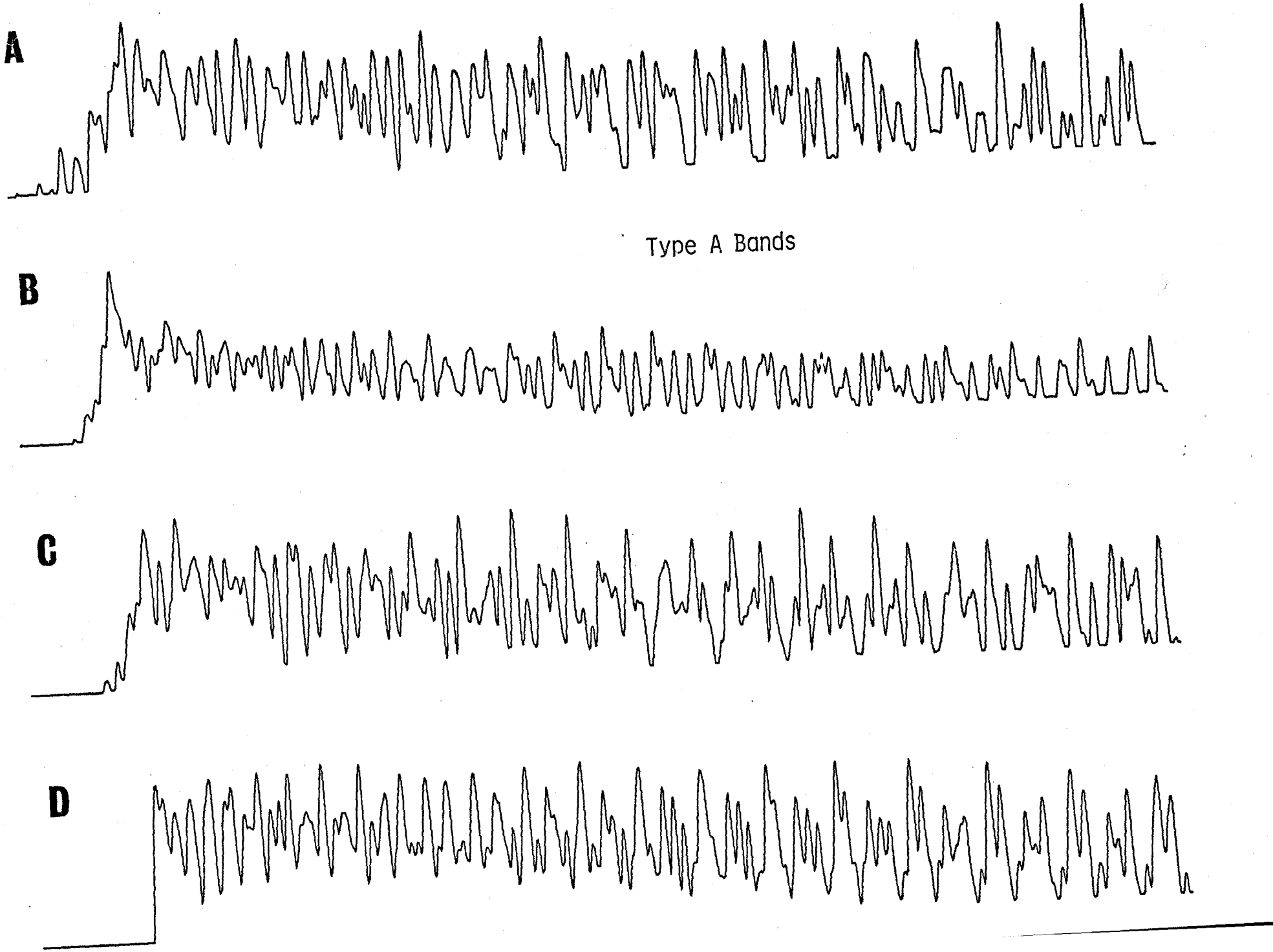
A
Type A Bands
B
C
D

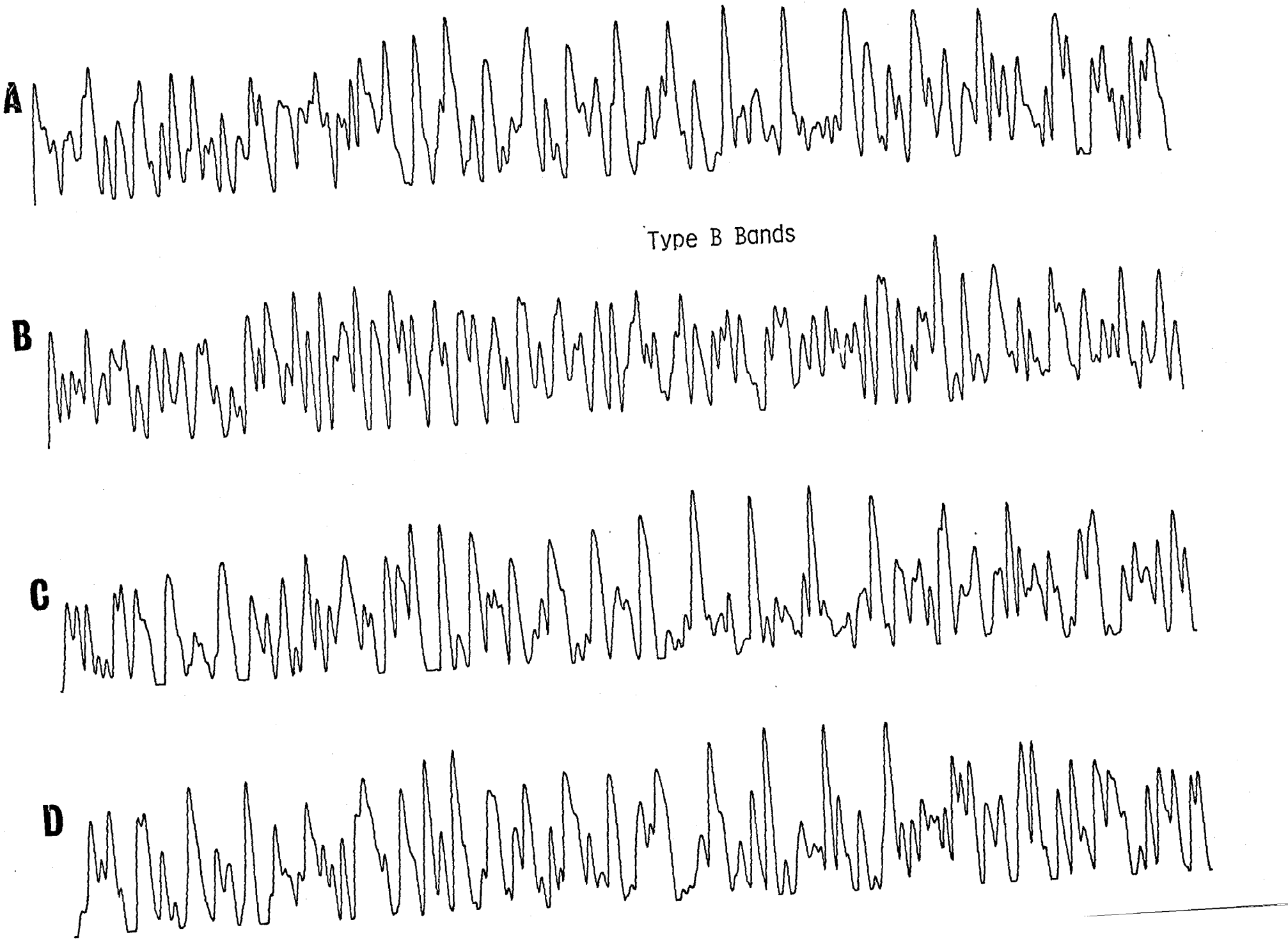
A
Type B Bands
B
C
D

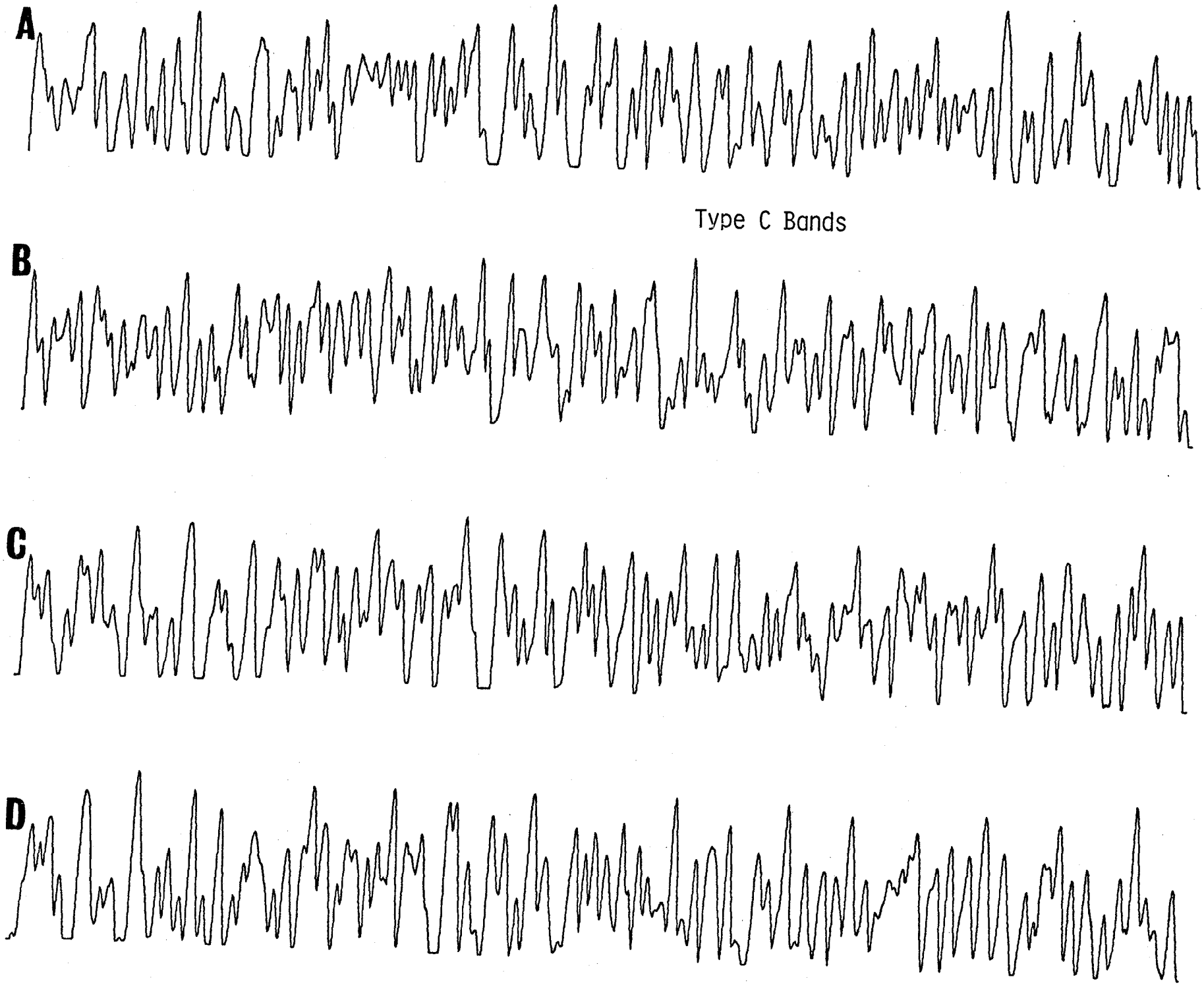
A
Type C Bands
B
C
D

Table 13

Trial Sets of Rotational Constants (cm^{-1})

	A	B	C
Contour A	9.82	0.45	0.4297
Contour B	9.72	0.50	0.4748
Contour C	9.72	0.45	0.4294
Contour D	9.55	0.45	0.4292

wavenumber end. The reason for this was that with $\Delta K_a = 0$ and $\delta_2^K = 2[(A' - \bar{B}') - [A'' - \bar{B}'')]$ being near zero, the branches with successive K values were nearly coincident and a change of 0.1 cm^{-1} drastically altered the overlap. If A' was greater than or equal to A", a number of weaker lines were observed beyond the cutoff point, whereas when A' was less than A", the intensity dropped immediately to zero. Our spectrum contained several weak lines to high wavenumber of the sharp drop in intensity; this established A' as being 9.7 or greater.

Changes in B and C were inter-related and together had a significant effect on the spacing of prominent lines toward the red end of the spectrum. Each of these lines was the superposition of a number of lines with the same J" value but different K" values and the separation was roughly represented by $\delta_2^J = 2(\bar{B}' - \bar{B}'')$, where $\bar{B} = \frac{B + C}{2}$. In order to reproduce this spacing, both B and C were reduced by nearly 25%. Further small adjustments in these constants were required to alter the intensity pattern somewhat until a best fit was achieved. The resultant computer contour and the experimentally derived contour are shown in Figure 12.

At this point, a simple computer programme was used to generate values of A, B and C for a wide range of structures. Since data for the deuterated species were not available, an infinite number of sets of the four geometrical parameters could be found to fit three rotational constants. The assumption that θ(out-of-plane) was small reduced the variable parameters to three and the geometry thus calculated is given in Table 14 along with the values of A, B and C. As expected, the only

Figure 12

Band Contour and Observed Spectrum for the $^1A_1(\pi,\pi^*)$ System of Thioformaldehyde

A. Observed Spectrum--the disjointed lines descending from the body of the spectrum are due to calibration lines in emission from the iron arc.

B. Calculated Type A Band Contour.

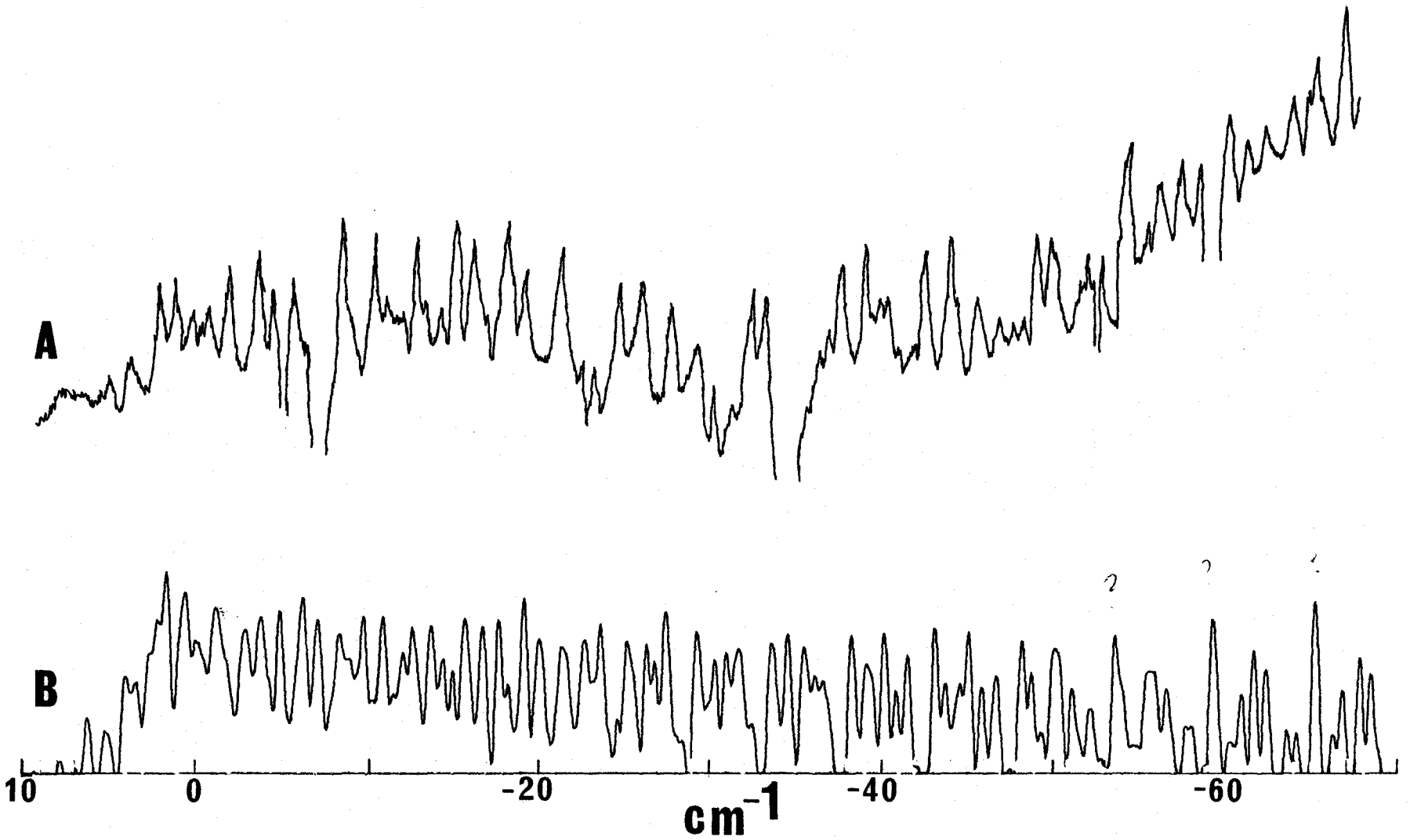
A
B
10
0
-20
-40
-60
cm-1

Table 14

Excited State Rotational Constants and Geometry for the $\tilde{B}^1A_1(\pi,\pi^*) \longleftarrow \tilde{X}^1A_1$ Transition

A (cm^{-1})	9.73 ± 0.05
B (cm^{-1})	0.450 ± 0.01
C (cm^{-1})	0.429 ± 0.01
r_{CS} (Å)	1.86 ± 0.03
r_{CH} (Å)	1.10 ± 0.01
α_{HCH} (degrees)	114 ± 2
θ (out-of-plane)	0°[a]

(a) preset value

gross change was in the CS bond length, which had increased by 15% from the ground state.

The question still unanswered was whether this band was in fact the 0-0 band for the transition. In an attempt to determine this, we again turned to the data on origin isotope shifts listed in Table 9. The isotope shift for the $\pi \longrightarrow \pi^*$ transition of 29 cm^{-1} is remarkably low relative to that for the $n \longrightarrow 3s$ system of 214 cm^{-1} or the $n \longrightarrow \pi^*$ system of 112.6 cm^{-1}. Since the corresponding transition for H_2CO has not been observed, we can refer only to Cl_2CS. This molecule does exhibit the same trend with a decrease in isotope shift from the $n \longrightarrow \pi^*$ (0.49 cm^{-1}) to the $\pi \longrightarrow \pi^*$ (0.21 cm^{-1}) system of over 50%.

The observed shift for thioformaldehyde can be easily accounted for by the drop in CS frequency:

$$\tfrac{1}{2}(436 - 941) - \tfrac{1}{2}(476 - 1063) = 41 \text{ cm}^{-1}$$

This implies that decreases in some vibrational modes must be counterbalanced by increases in other modes, a situation observed in the spectrum of formaldehyde in the (n,π^*) state, as previously mentioned. Alternatively, if we extrapolate to the red by one quantum of ν_3', the isotope splitting then becomes $(29 + 40) = 69$ cm^{-1} and the band which we have analyzed would bear the assignment 3_0^1 rather than 0_0^0. An assignment of 3_0^2 could also be accepted, with an origin isotope shift close to that for the $n \longrightarrow \pi^*$ transition. At the present time, we do not have sufficient information to make a decision on this point.

Other Electronic Transitions

Two diffuse bands were identified in the vacuum ultraviolet region of the spectrum of thioformaldehyde, at 187 and 181 nm respectively. The assignment of these bands was easily accomplished by reference to the data of Table 6. The transition at 187 nm was assigned to the promotion of the n electron to the $3p_y$ Rydberg orbital, while the higher energy system was given the designation $n \longrightarrow 3p_z$. The agreement with the theoretical calculation and the correlations with formaldehyde assignments were excellent. No vibrational activity could be identified in relation to either system under our experimental conditions.

The first ionization potential for thioformaldehyde is 9.38 eV.[9a] The Rydberg equations for the three observed transitions are:

$$E_{3s} = 75{,}657 - \frac{109737.3}{(3 - \delta_s)^2}$$

$$E_{3p_y} = 75{,}657 - \frac{109737.3}{(3 - \delta_{p_y})^2}$$

$$E_{3p_z} = 75{,}657 - \frac{109737.3}{(3 - \delta_{p_z})^2}$$

and therefore the quantum defects are:

$$\delta_s = 1.04$$

$$\delta_{p_y} = 0.79$$

$$\delta_{p_z} = 0.69$$

These are within the range found experimentally for similar molecules.[16,28] In particular, they correlate well with the observed values for formaldehyde:

$\delta_s = 1.04$

$\delta_{p_y} = 0.84$

$\delta_{p_z} = 0.77$

If we had assinged the principal quantum number as n = 4, the values for the quantum defects would show a very poor correlation to formaldehyde. The fact that the first Rydberg orbitals have a principal quantum number of 3 in both H_2CO and H_2CS suggests that the character of the orbitals is primarily that of the carbon 3s and 3p orbitals. Bruna et al.[19] have noted that it makes little difference to the calculated orbital energies if the orbital is centred on the carbon, on the sulphur or midway between the two atoms, so that this representation of the first Rydberg orbitals is also acceptable from the theoretical point of view.

Chapter V

Discussion and Conclusions

Four separate electronic transitions have been observed and assigned in the ultraviolet spectrum of thioformaldehyde. These are:

$\tilde{B}^1A_1(\pi,\pi^*) \longleftarrow \tilde{X}^1A_1$	5.60 eV
$\tilde{C}^1B_2(n,3s) \longleftarrow \tilde{X}^1A_1$	5.84 eV
$\tilde{D}^1A_1(n,3p_y) \longleftarrow \tilde{X}^1A_1$	6.60 eV
$\tilde{E}^1B_2(n,3p_z) \longleftarrow \tilde{X}^1A_1$	6.82 eV

The three members of the Rydberg series leading to complete ionization from the n orbital appear to fit reasonably well into the established pattern. It is not surprising that the third p Rydberg, $n \longrightarrow 3p_x$, has not been observed since its overall electronic symmetry is A_2 and hence the transition is electronically forbidden. Its presence or absence cannot be confirmed at this time, although it is expected to appear as a very weak line in the region overlapped by the spectrum of ethylene.

The line-by-line rotational analysis of the $\tilde{C}^1B_2(n,3s) \longleftarrow \tilde{X}^1A_1$ system has yielded a molecular geometry which is significantly different from that of the ground state. Not only is there a large (5.8°) change in the HCH angle, but there is also a negative (-0.006 Å) change in the

CS bond length on electronic excitation. These observations can be more easily accepted when we refer to work done on the $^2B_2(n)$ state of formaldehyde.[28b] A semi-empirical claculation was carried out to find the equilibrium geometry for this state. The results of that three-point interpolation form the first line of Table 15. However, these values did not produce the observed intensity pattern when used in a Franck-Condon calculation. In order to correlate the geometry with the intensity, it was found necessary to take account of the differences in internal mixing in the two combining states. The solution to the problem lay in the recognition that the n orbital was anti-bonding in the CO bond as shown in Figure 1. This meant that removal of an electron from that orbital should lead to structural stability in the $^2B_2(n)$ ionic state and to a reduction in the CO bond length. This change of sign in the internal co-ordinate r_{CO} caused destructive interference with α_{HCH} and r_{CH} in the normal co-ordinate which generated ν_{HCH}. Consequently, it was possible to construct a spectrum in which very little Franck-Condon activity appeared in the ν_{HCH} normal co-ordinate even though the change in HCH angle was given an appreciable size. The final set of parameters for H_2CO are reproduced in Table 15 and compare favourably with the parameters obtained for H_2CS from the detailed rotational analysis.

This geometry is also in accord with the assignment of the vibrational spectrum of D_2CS. The two weak bands were identified as ν_1'(CD) and ν_3'(DCD). The drop in frequency from 2146 to 1783 cm^{-1} and 1203 to 746 cm^{-1} respectively reflect the increases in the CD bond

Table 15

Geometry Changes on Excitation

	ΔR_{CX}(Å)	ΔR_{CH}(Å)	$\Delta\alpha_{HCH}$(degrees)	
$H_2CO^{(a)}$ $^2B_2(n)$	+0.0072	+0.0095	+5.8	CNDO/2
	-0.020	+0.015	+5.0	Franck-Condon
$H_2CS^{(b)}$ $^1B_2(n,3s)$	-0.0061	+0.0194	+5.81	

X = O, S

(a) reference 28b.

(b) this work.

length and DCD angle.

The observed vibrational spectrum of the $\pi \longrightarrow \pi^*$ transition and the rotational analysis of the 0-0 band led us to conclude that thiocarbonyl compounds did not have a non-planar configuration in this excited state.

Barrier heights and out-of-plane angles have been observed for a number of carbonyl and thiocarbonyl compounds. These are summarized in Table 16. Most of these molecules stabilize in a non-planar configuration in both the ($n\pi^*$) and the ($\pi\pi^*$) states. This can be interpreted readily with the aid of the Walsh diagram discussed earlier. In this qualitative picture it is the presence of the electron in the π^* orbital which is held to be responsible for stabilizing the nonplanar configuration. From the table it can be deduced that the stabilization is less effective for the hydrogen compound than for its halogenated analog, but that the orbital from which the electron originates has a much less noticeable effect on the barrier to inversion. Thioformaldehyde in its $^1A_2(n,\pi^*)$ state has been referred to as a "pseudo-planar" molecule because its barrier to inversion of 20 cm^{-1} is only a very small fraction of its zero-point energy. It may be then that in the $^1A_1(\pi,\pi^*)$ state the molecule is also "pseudo-planar". In that case, vibrational activity in the out-of-plane motion would be weak and not readily observed.

The structural change which occurs in the CS bond can likewise be attributed to the partially filled π^* orbital. The extension of the bond length by 0.25 Å and the drop in ν(CS) from 941 to 476 cm^{-1} on

Table 16

Barrier Heights to Inversion in Carbonyl and Thiocarbonyl Compounds (cm^{-1})

Molecule	System	
	$^1A_2(n,\pi^*)$	$^1A_1(\pi,\pi^*)$
H_2CO	356[a]	--
F_2CO	>4000[b]	--
H_2CS	20[c]	--
F_2CS	>3200[d]	3300[e]
Cl_2CS	620[f]	--
ClFCS	1556[g]	>2000[h]

(a) reference 41.

(b) reference 42.

(c) reference 10b.

(d) reference 43.

(e) reference 44.

(f) reference 33.

(g) reference 45.

(h) reference 46.

excitation is commensurate with a change in bond order of the CS group from 2 to 1. In fact, according to Badger's rule,[47] this change in the "force constant" of the bond represented by the large frequency drop should result in an increase of 0.5 Å in the bond length.

Appendix I

Wavenumber Assignments for the Rotational Lines of the $^1B_2(n,3s)$ System

(a) H_2CS

(b) D_2CS

H2CS

UPPER STATE			LOWER STATE			OBSERVATION	CALCULATION	RESID.
J	KA	KC	J	KA	KC			
1	0	1	2	1	2	47099.3720	47099.4452	-0.0732
2	0	2	3	1	3	47098.4490	47098.3904	0.0586
3	0	3	4	1	4	47097.3940	47097.3720	0.0220
4	0	4	5	1	5	47096.4900	47096.3897	0.1003
5	0	5	6	1	6	47095.4640	47095.4428	0.0212
6	0	6	7	1	7	47094.5240	47094.5306	-0.0066
7	0	7	8	1	8	47093.6610	47093.6523	0.0087
8	0	8	9	1	9	47092.8400	47092.8068	0.0332
9	0	9	10	1	10	47092.0060	47091.9929	0.0131
10	0	10	11	1	11	47091.2960	47091.2093	0.0867
11	0	11	12	1	12	47090.4370	47090.4544	-0.0174
12	0	12	13	1	13	47089.7460	47089.7268	0.0192
13	0	13	14	1	14	47089.0040	47089.0245	-0.0205
14	0	14	15	1	15	47088.3560	47088.3459	0.0101
15	0	15	16	1	16	47087.7860	47087.6889	0.0971
16	0	16	17	1	17	47086.9890	47087.0514	-0.0624
17	0	17	18	1	18	47086.3430	47086.4315	-0.0885
18	0	18	19	1	19	47085.7770	47085.8270	-0.0500
19	0	19	20	1	20	47085.1720	47085.2357	-0.0637
20	0	20	21	1	21	47084.7330	47084.6555	0.0775
4	1	3	5	2	4	47076.9310	47076.8528	0.0782
7	1	6	8	2	7	47074.1610	47074.1338	0.0272
8	1	7	9	2	8	47073.3530	47073.3060	0.0470
10	1	9	11	2	10	47071.7840	47071.7666	0.0174
11	1	10	12	2	11	47071.0870	47071.0541	0.0329
12	1	11	13	2	12	47070.2920	47070.3791	-0.0871
13	1	12	14	2	13	47069.7840	47069.7411	0.0429
14	1	13	15	2	14	47069.1400	47069.1396	0.0004
15	1	14	16	2	15	47068.4750	47068.5738	-0.0988
6	1	6	7	2	5	47074.1610	47074.1184	0.0426
8	1	8	9	2	7	47071.7840	47071.7826	0.0014
9	1	9	10	2	8	47070.6030	47070.6049	-0.0019
2	2	0	3	3	1	47057.0020	47056.9777	0.0243
3	2	1	4	3	2	47055.9040	47055.8903	0.0137
4	2	2	5	3	3	47054.8260	47054.8228	0.0032
5	2	3	6	3	4	47053.8010	47053.7758	0.0252
6	2	4	7	3	5	47052.7990	47052.7496	0.0494
7	2	5	8	3	6	47051.7510	47051.7450	0.0060
8	2	6	9	3	7	47050.7690	47050.7627	0.0063
9	2	7	10	3	8	47049.8030	47049.8034	-0.0004
10	2	8	11	3	9	47048.8320	47048.8683	-0.0363
11	2	9	12	3	10	47047.9130	47047.9582	-0.0452
12	2	10	13	3	11	47047.0090	47047.0742	-0.0652
13	2	11	14	3	12	47046.2070	47046.2177	-0.0107

H2CS

UPPER STATE			LOWER STATE			OBSERVATION	CALCULATION	RESID.
J	KA	KC	J	KA	KC			
14	2	12	15	3	13	47045.3930	47045.3897	0.0033
16	2	14	17	3	15	47043.7910	47043.8249	-0.0339
13	2	12	14	3	11	47046.0210	47045.9974	0.0236
14	2	13	15	3	12	47045.1700	47045.0962	0.0738
15	2	14	16	3	13	47044.2620	47044.2084	0.0536
16	2	15	17	3	14	47043.2570	47043.3329	-0.0759
18	2	17	19	3	16	47041.7100	47041.6151	0.0949
3	3	1	4	4	0	47031.7160	47031.7274	-0.0114
4	3	2	5	4	1	47030.6900	47030.6585	0.0315
5	3	3	6	4	2	47029.6080	47029.6089	-0.0009
6	3	4	7	4	3	47028.5470	47028.5785	-0.0315
7	3	5	8	4	4	47027.5890	47027.5673	0.0217
8	3	6	9	4	5	47026.5330	47026.5752	-0.0422
9	3	7	10	4	6	47025.6090	47025.6022	0.0068
10	3	8	11	4	7	47024.7800	47024.6484	0.1316
11	3	9	12	4	8	47023.6430	47023.7135	-0.0705
12	3	10	13	4	9	47022.8170	47022.7976	0.0194
13	3	11	14	4	10	47021.8740	47021.9006	-0.0266
14	3	12	15	4	11	47021.0730	47021.0223	0.0507
15	3	13	16	4	12	47020.1770	47020.1626	0.0144
16	3	14	17	4	13	47019.3610	47019.3214	0.0396
17	3	15	18	4	14	47018.5130	47018.4985	0.0145
18	3	16	19	4	15	47017.7560	47017.6937	0.0623
19	3	17	20	4	16	47016.9660	47016.9067	0.0593
20	3	18	21	4	17	47016.2520	47016.1373	0.1147
4	4	1	5	5	0	47004.0420	47004.1498	-0.1078
5	4	2	6	5	1	47003.0330	47003.0994	-0.0664
6	4	3	7	5	2	47002.0060	47002.0680	-0.0620
7	4	4	8	5	3	47001.0600	47001.0555	0.0045
8	4	5	9	5	4	47000.1460	47000.0619	0.0841
9	4	6	10	5	5	46999.1140	46999.0870	0.0270
10	4	7	11	5	6	46998.1520	46998.1309	0.0211
12	4	9	13	5	8	46996.3380	46996.2744	0.0636
13	4	10	14	5	9	46995.4470	46995.3738	0.0732
14	4	10	15	5	10	46994.5300	46994.4915	0.0385
15	4	12	16	5	11	46993.6590	46993.6272	0.0318
16	4	13	17	5	12	46992.8190	46992.7810	0.0380
17	4	14	18	5	13	46992.0280	46991.9525	0.0755
18	4	15	19	5	14	46991.1730	46991.1418	0.0312
19	4	16	20	5	15	46990.4270	46990.3485	0.0785
20	4	17	21	5	16	46989.6630	46989.5724	0.0906
21	4	18	22	5	17	46988.8870	46988.8134	0.0736
22	4	19	23	5	18	46988.2130	46988.0713	0.1417
23	4	20	24	5	19	46987.4580	46987.3457	0.1123

H2CS

UPPER STATE			LOWER STATE			OBSERVATION	CALCULATION	RESID.
J	KA	KC	J	KA	KC			
24	4	21	25	5	20	46986.7430	46986.6366	0.1064
25	4	22	26	5	21	46986.0570	46985.9435	0.1135
5	5	0	6	6	1	46974.1040	46974.2250	-0.1210
6	5	1	7	6	2	46973.2690	46973.1924	0.0766
7	5	2	8	6	3	46972.1880	46972.1785	0.0095
8	5	3	9	6	4	46971.1520	46971.1833	-0.0313
10	5	5	11	6	6	46969.2770	46969.2482	0.0288
11	5	6	12	6	7	46968.3610	46968.3081	0.0529
12	5	7	13	6	8	46967.4180	46967.3862	0.0318
13	5	8	14	6	9	46966.5060	46966.4823	0.0237
14	5	9	15	6	10	46965.6530	46965.5962	0.0568
15	5	10	16	6	11	46964.7680	46964.7278	0.0402
16	5	11	17	6	12	46963.8930	46963.8769	0.0161
17	5	12	18	6	13	46963.0720	46963.0433	0.0287
18	5	13	19	6	14	46962.2430	46962.2267	0.0163
19	5	14	20	6	15	46961.4830	46961.4270	0.0560
20	5	15	21	6	16	46960.7060	46960.6440	0.0620
21	5	16	22	6	17	46959.9520	46959.8772	0.0748
22	5	17	23	6	18	46959.2150	46959.1266	0.0884
23	5	18	24	6	19	46958.4630	46958.3918	0.0712
6	6	0	7	7	1	46941.9280	46941.9220	0.0060
7	6	1	8	7	2	46940.9700	46940.9065	0.0635
8	6	2	9	7	3	46939.9360	46939.9093	0.0267
9	6	3	10	7	4	46938.9590	46938.9304	0.0286
10	6	4	11	7	5	46937.9680	46937.9695	-0.0015
11	6	5	12	7	6	46937.0150	46937.0267	-0.0117
12	6	6	13	7	7	46936.1730	46936.1017	0.0713
13	6	7	14	7	8	46935.2450	46935.1943	0.0507
14	6	8	15	7	9	46934.3250	46934.3045	0.0205
16	6	10	17	7	11	46932.6400	46932.5765	0.0635
17	6	11	18	7	12	46931.8360	46931.7380	0.0980
18	6	12	19	7	13	46930.9770	46930.9160	0.0610
19	6	13	20	7	14	46930.1830	46930.1105	0.0725
20	6	14	21	7	15	46929.4280	46929.3211	0.1069
21	6	15	22	7	16	46928.6310	46928.5476	0.0834
22	6	16	23	7	17	46927.8950	46927.7896	0.1054
23	6	17	24	7	18	46927.1500	46927.0468	0.1032
24	6	18	25	7	19	46926.4220	46926.3190	0.1030
25	6	19	26	7	20	46925.7730	46925.6058	0.1672
8	8	0	9	9	1	46870.0190	46870.0015	0.0175
9	8	1	10	9	2	46869.1540	46869.0171	0.1369
10	8	2	11	9	3	46868.0790	46868.0502	0.0288
11	8	3	12	9	4	46867.1110	46867.1006	0.0104
12	8	4	13	9	5	46866.1810	46866.1681	0.0129

H2CS

UPPER STATE			LOWER STATE			OBSERVATION	CALCULATION	RESID.
J	KA	KC	J	KA	KC			
13	8	5	14	9	6	46865.2560	46865.2526	0.0034
14	8	6	15	9	7	46864.3480	46864.3539	-0.0059
2	1	2	1	0	1	47121.1720	47121.0820	0.0900
7	1	7	6	0	6	47126.7800	47126.7765	0.0035
8	1	8	7	0	7	47127.8340	47127.9120	-0.0780
9	1	9	8	0	8	47129.1060	47129.0467	0.0593
10	1	10	9	0	9	47130.1800	47130.1811	-0.0011
11	1	11	10	0	10	47131.4030	47131.3154	0.0876
12	1	12	11	0	11	47132.4690	47132.4500	0.0190
14	1	14	13	0	13	47134.7630	47134.7220	0.0410
15	1	15	14	0	14	47135.9020	47135.8604	0.0416
2	2	1	1	1	0	47135.9020	47135.8765	0.0255
3	2	2	2	1	1	47137.0630	47137.0450	0.0180
5	2	4	4	1	3	47139.4270	47139.3868	0.0402
6	2	5	5	1	4	47140.4990	47140.5598	-0.0608
7	2	6	6	1	5	47141.8070	47141.7340	0.0730
9	2	8	8	1	7	47144.0940	47144.0852	0.0088
10	2	9	9	1	8	47145.2740	47145.2619	0.0121
11	2	10	10	1	9	47146.3790	47146.4390	-0.0600
12	2	11	11	1	10	47147.6430	47147.6164	0.0266
13	2	12	12	1	11	47148.7470	47148.7937	-0.0467
14	2	13	13	1	12	47149.9780	47149.9708	0.0072
16	2	15	15	1	14	47152.3250	47152.3231	0.0019
17	2	16	16	1	15	47153.4620	47153.4978	-0.0358
18	2	17	17	1	16	47154.6460	47154.6712	-0.0252
19	2	18	18	1	17	47155.8130	47155.8429	-0.0299
2	2	0	1	1	1	47135.9020	47135.9115	-0.0095
3	2	1	2	1	2	47137.0630	47137.1506	-0.0876
4	2	2	3	1	3	47138.4390	47138.4271	0.0119
5	2	3	4	1	4	47139.6940	47139.7416	-0.0476
6	2	4	5	1	5	47141.1480	47141.0947	0.0533
9	2	7	8	1	8	47145.2740	47145.3946	-0.1206
10	2	8	9	1	9	47146.9410	47146.9117	0.0293
11	2	9	10	1	10	47148.5310	47148.4727	0.0583
12	2	10	11	1	11	47149.9780	47150.0791	-0.1011
13	2	11	12	1	12	47151.7570	47151.7325	0.0245
14	2	12	13	1	13	47153.4620	47153.4343	0.0277
15	2	13	14	1	14	47155.1450	47155.1864	-0.0414
7	3	5	6	2	4	47154.4470	47154.4297	0.0173
8	3	6	7	2	5	47155.8130	47155.7237	0.0894
10	3	8	9	2	7	47158.4940	47158.3612	0.1328
11	3	9	10	2	8	47159.5490	47159.7034	-0.1544
12	3	10	11	2	9	47161.1070	47161.0600	0.0470
14	3	11	13	2	12	47164.0430	47163.9528	0.0902

H2CS

UPPER STATE			LOWER STATE			OBSERVATION	CALCULATION	RESID.
J	KA	KC	J	KA	KC			
16	3	13	15	2	14	47166.8500	47166.8572	-0.0072
8	4	5	7	3	4	47165.5250	47165.5976	-0.0726
9	4	6	8	3	5	47166.8500	47166.9115	-0.0615
11	4	8	10	3	7	47169.5470	47169.5934	-0.0464
12	4	9	11	3	8	47170.9510	47170.9609	-0.0099
15	4	12	14	3	11	47175.1530	47175.1666	-0.0136
16	4	13	15	3	12	47176.6060	47176.6019	0.0041
17	4	14	16	3	13	47178.1190	47178.0533	0.0657
18	4	15	17	3	14	47179.5730	47179.5204	0.0526
19	4	16	18	3	15	47180.9630	47181.0029	-0.0399
20	4	17	19	3	16	47182.4580	47182.5002	-0.0422
21	4	18	20	3	17	47183.9420	47184.0120	-0.0700
22	4	19	21	3	18	47185.4550	47185.5375	-0.0825
23	4	20	22	3	19	47187.0910	47187.0764	0.0146
24	4	21	23	3	20	47188.6290	47188.6280	0.0010
25	4	22	24	3	21	47190.1260	47190.1916	-0.0656
8	4	4	7	3	5	47165.5250	47165.5976	-0.0726
9	4	5	8	3	6	47166.8500	47166.9116	-0.0616
11	4	7	10	3	8	47169.5470	47169.5937	-0.0467
12	4	8	11	3	9	47170.9510	47170.9615	-0.0105
15	4	11	14	3	12	47175.1530	47175.1688	-0.0158
16	4	12	15	3	13	47176.6060	47176.6052	0.0008
17	4	13	16	3	14	47178.1190	47178.0582	0.0608
18	4	14	17	3	15	47179.5730	47179.5274	0.0456
19	4	15	18	3	16	47180.9630	47181.0127	-0.0497
20	4	16	19	3	17	47182.4580	47182.5138	-0.0558
13	5	9	12	4	8	47179.5730	47179.6803	-0.1073
14	5	10	13	4	9	47180.9630	47181.0796	-0.1166
15	5	11	14	4	10	47182.4580	47182.4958	-0.0378
16	5	12	15	4	11	47183.9420	47183.9285	0.0135
6	6	1	5	5	0	47175.1530	47175.1355	0.0175
8	6	3	7	5	2	47177.6320	47177.7008	-0.0688
9	6	4	8	5	3	47178.9570	47179.0102	-0.0532
10	6	5	9	5	4	47180.3890	47180.3372	0.0518
11	6	6	10	5	5	47181.6750	47181.6816	-0.0066
12	6	7	11	5	6	47183.1230	47183.0432	0.0798
13	6	8	12	5	7	47184.4250	47184.4219	0.0031
14	6	9	13	5	8	47185.6820	47185.8174	-0.1354
15	6	10	14	5	9	47187.0910	47187.2294	-0.1384
16	6	11	15	5	10	47188.6290	47188.6577	-0.0287
17	6	12	16	5	11	47190.1260	47190.1020	0.0240
18	6	13	17	5	12	47191.4860	47191.5620	-0.0760
19	6	14	18	5	13	47192.9040	47193.0374	-0.1334
20	6	15	19	5	14	47194.3580	47194.5279	-0.1699

H2CS

UPPER STATE			LOWER STATE			OBSERVATION	CALCULATION	RESID.
J	KA	KC	J	KA	KC			
21	6	16	20	5	15	47195.8820	47196.0332	-0.1512
22	6	17	21	5	16	47197.4160	47197.5528	-0.1368
23	6	18	22	5	17	47199.0280	47199.0864	-0.0584
24	6	19	23	5	18	47200.5310	47200.6336	-0.1026
25	6	20	24	5	19	47202.0970	47202.1941	-0.0971
26	6	21	25	5	20	47203.6200	47203.7672	-0.1472
27	6	22	26	5	21	47205.2470	47205.3527	-0.1057
18	7	12	17	6	11	47193.5390	47193.6064	-0.0674
19	7	13	18	6	12	47195.0380	47195.0756	-0.0376
20	7	14	19	6	13	47196.5030	47196.5596	-0.0566
21	7	15	20	6	14	47197.9650	47198.0579	-0.0929
9	8	2	8	7	1	47180.3890	47180.4233	-0.0343
10	8	3	9	7	2	47181.6750	47181.7432	-0.0682
11	8	4	10	7	3	47183.1230	47183.0798	0.0432
12	8	5	11	7	4	47184.4250	47184.4330	-0.0080
13	8	6	12	7	5	47185.6820	47185.8025	-0.1205
14	8	7	13	7	6	47187.0910	47187.1881	-0.0971
15	8	8	14	7	7	47188.6290	47188.5896	0.0394
17	8	10	16	7	9	47191.4860	47191.4389	0.0471
18	8	11	17	7	10	47192.9040	47192.8862	0.0178
19	8	12	18	7	11	47194.3580	47194.3483	0.0097
21	8	14	20	7	13	47197.4160	47197.3151	0.1009
3	1	2	3	0	3	47119.0590	47119.0350	0.0240
5	1	4	5	0	5	47119.4910	47119.3968	0.0942
8	1	7	8	0	8	47120.2900	47120.2452	0.0448
9	1	8	9	0	9	47120.5210	47120.6106	-0.0896
10	1	9	10	0	10	47121.1720	47121.0179	0.1541
11	1	10	11	0	11	47121.5190	47121.4674	0.0516
12	1	11	12	0	12	47121.9600	47121.9594	0.0006
13	1	12	13	0	13	47122.5800	47122.4945	0.0855
14	1	13	14	0	14	47123.1220	47123.0729	0.0491
15	1	14	15	0	15	47123.7080	47123.6952	0.0128
16	1	15	16	0	16	47124.2500	47124.3617	-0.1117
17	1	16	17	0	17	47125.1260	47125.0727	0.0533
18	1	17	18	0	18	47125.8270	47125.8288	-0.0018
19	1	18	19	0	19	47126.4760	47126.6300	-0.1540
20	1	19	20	0	20	47127.4780	47127.4768	0.0012
23	1	22	23	0	23	47130.1800	47130.2909	-0.1109
24	1	23	24	0	24	47131.4030	47131.3201	0.0829
4	2	3	4	1	4	47133.8630	47133.9114	-0.0484
7	2	6	7	1	7	47134.6980	47134.5702	0.1278
8	2	7	8	1	8	47134.7630	47134.8623	-0.0993
9	2	8	9	1	9	47135.1610	47135.1904	-0.0294
10	2	9	10	1	10	47135.4800	47135.5544	-0.0744

H2CS

UPPER STATE			LOWER STATE			OBSERVATION	CALCULATION	RESID.
J	KA	KC	J	KA	KC			
11	2	10	11	1	11	47135.9020	47135.9539	-0.0519
14	2	13	14	1	14	47137.3900	47137.3635	0.0265
15	2	14	15	1	15	47137.8120	47137.9028	-0.0908
16	2	15	16	1	16	47138.4390	47138.4763	-0.0373
18	2	17	18	1	18	47139.6940	47139.7241	-0.0301
19	2	18	19	1	19	47140.4990	47140.3977	0.1013
20	2	19	20	1	20	47141.1480	47141.1037	0.0443
21	2	20	21	1	21	47141.8070	47141.8417	-0.0347
24	2	23	24	1	24	47144.0940	47144.2423	-0.1483
10	3	8	10	2	9	47146.9410	47146.9404	0.0006
13	3	11	13	2	12	47147.6430	47147.6445	-0.0015
16	3	14	16	2	15	47148.5310	47148.5342	-0.0032
5	3	2	5	2	3	47146.1320	47146.1635	-0.0315
7	3	4	7	2	5	47146.3790	47146.4049	-0.0259
13	4	10	13	3	11	47157.3760	47157.4522	-0.0762
15	4	12	15	3	13	47157.9340	47157.9834	-0.0494
17	4	14	17	3	15	47158.4940	47158.5822	-0.0882
18	4	15	18	3	16	47158.8370	47158.9063	-0.0693
19	4	16	19	3	17	47159.1660	47159.2465	-0.0805
20	4	17	20	3	18	47159.5490	47159.6025	-0.0535
21	4	18	21	3	19	47159.8890	47159.9742	-0.0852
22	4	19	22	3	20	47160.3140	47160.3611	-0.0471
23	4	20	23	3	21	47160.7190	47160.7631	-0.0441
24	4	21	24	3	22	47161.1070	47161.1798	-0.0728
25	4	22	25	3	23	47161.5330	47161.6109	-0.0779
1	1	1	2	0	2	47116.3940	47116.5014	-0.1074
3	1	3	4	0	4	47114.1830	47114.2041	-0.0211
8	1	8	9	0	9	47108.4590	47108.4554	0.0036
9	1	9	10	0	10	47107.2630	47107.3077	-0.0447
10	1	10	11	0	11	47106.1200	47106.1617	-0.0417
11	1	11	12	0	12	47104.9900	47105.0181	-0.0281
12	1	12	13	0	13	47103.8770	47103.8774	-0.0004
13	1	13	14	0	14	47102.7150	47102.7401	-0.0251
16	1	16	17	0	17	47099.3720	47099.3566	0.0154
17	1	17	18	0	18	47098.1980	47098.2404	-0.0424
18	1	18	19	0	19	47097.1080	47097.1314	-0.0234
19	1	19	20	0	20	47095.9700	47096.0302	-0.0602
7	2	6	8	1	7	47124.2500	47124.2896	-0.0396
8	2	7	9	1	8	47123.1220	47123.1408	-0.0188
9	2	8	10	1	9	47121.9600	47121.9935	-0.0335
10	2	9	11	1	10	47120.8480	47120.8477	0.0003
12	2	11	13	1	12	47118.5670	47118.5599	0.0071
16	2	15	17	1	16	47113.9590	47113.9959	-0.0369
18	2	17	19	1	18	47111.7100	47111.7171	-0.0071

H2CS

UPPER STATE			LOWER STATE			OBSERVATION	CALCULATION	RESID.
J	KA	KC	J	KA	KC			
20	2	19	21	1	20	47109.4660	47109.4385	0.0275
8	4	5	9	3	6	47146.1320	47146.1190	0.0130
11	1	10	11	2	9	47084.7330	47084.7246	0.0084
12	1	11	12	2	10	47085.1720	47085.1648	0.0072
17	1	16	17	2	15	47087.7860	47087.7613	0.0247
4	3	1	4	4	0	47036.3560	47036.3873	-0.0313
2	0	2	1	1	1	47103.8770	47104.0323	-0.1553
3	0	3	2	1	2	47105.2890	47105.2704	0.0186
4	0	4	3	1	3	47106.5710	47106.5443	0.0267
5	0	5	4	1	4	47107.8830	47107.8533	0.0297
6	0	6	5	1	5	47109.1100	47109.1966	-0.0866
7	0	7	6	1	6	47110.5300	47110.5733	-0.0433
8	0	8	7	1	7	47112.1040	47111.9822	0.1218
9	0	9	8	1	8	47113.4380	47113.4220	0.0160
10	0	10	9	1	9	47114.9700	47114.8914	0.0786
11	0	11	10	1	10	47116.3940	47116.3887	0.0053
12	0	12	11	1	11	47117.8520	47117.9124	-0.0604
13	0	13	12	1	12	47119.4910	47119.4606	0.0304
7	1	6	6	2	5	47091.2960	47091.3174	-0.0214
8	1	7	7	2	6	47092.8400	47092.7794	0.0606
11	1	10	10	2	9	47097.3940	47097.3931	0.0009
6	1	6	5	2	3	47089.0040	47089.0209	-0.0169
6	2	4	5	3	3	47067.6430	47067.6451	-0.0021
8	2	6	7	3	5	47070.2920	47070.2411	0.0509
9	2	7	8	3	6	47071.5890	47071.5733	0.0157
10	2	8	9	3	7	47072.8100	47072.9294	-0.1194
11	2	9	10	3	8	47074.1610	47074.3106	-0.1496
12	2	10	11	3	9	47075.6460	47075.7178	-0.0718
13	2	11	12	3	10	47077.1370	47077.1522	-0.0152
12	2	11	11	3	8	47075.6460	47075.5570	0.0890
13	2	12	12	3	9	47076.9310	47076.9332	-0.0022
16	3	13	15	4	12	47057.0020	47057.1297	-0.1277
17	3	14	16	4	13	47058.6080	47058.6004	0.0076
16	3	14	15	4	11	47057.0020	47057.1192	-0.1172
17	3	15	16	4	12	47058.6080	47058.5853	0.0227
6	4	2	5	5	1	47016.9660	47016.9611	0.0049
15	4	11	14	5	10	47029.1580	47029.1304	0.0276
16	4	12	15	5	11	47030.6090	47030.5728	0.0362
17	4	13	16	5	12	47032.0300	47032.0326	-0.0026
18	4	14	17	5	13	47033.5460	47033.5098	0.0362
19	4	15	18	5	14	47035.1090	47035.0040	0.1050
23	4	19	22	5	18	47041.1590	47041.1478	0.0112
25	4	21	24	5	20	47044.2620	47044.3166	-0.0546
26	4	22	25	5	21	47046.0210	47045.9244	0.0966

H2CS

UPPER STATE			LOWER STATE			OBSERVATION	CALCULATION	RESID.
J	KA	KC	J	KA	KC			
32	4	28	31	5	27	47055.9040	47055.8838	0.0202
9	6	3	8	7	2	46960.7060	46960.6915	0.0145
18	6	12	17	7	11	46973.2690	46973.2726	-0.0036
20	6	14	19	7	13	46976.2440	46976.2497	-0.0057
22	6	16	21	7	15	46979.3720	46979.2882	0.0838

D2CS

UPPER STATE			LOWER STATE			OBSERVATION	CALCULATION	RESID.
J	KA	KC	J	KA	KC			
3	0	3	4	1	4	47317.7480	47317.7109	0.0371
4	0	4	5	1	5	47317.0450	47316.9516	0.0934
5	0	5	6	1	6	47316.2240	47316.2300	-0.0060
6	0	6	7	1	7	47315.5400	47315.5435	-0.0035
7	0	7	8	1	8	47314.8910	47314.8894	0.0016
9	0	9	10	1	10	47313.6990	47313.6646	0.0344
10	0	10	11	1	11	47313.0550	47313.0863	-0.0313
11	0	11	12	1	12	47312.4970	47312.5254	-0.0284
12	0	12	13	1	13	47311.9340	47311.9778	-0.0438
5	2	4	6	3	3	47295.9680	47295.9562	0.0118
6	2	5	7	3	4	47295.1150	47295.1153	-0.0003
7	2	6	8	3	5	47294.2890	47294.2896	-0.0006
8	2	7	9	3	6	47293.4300	47293.4777	-0.0477
5	2	3	6	3	4	47295.9680	47295.9769	-0.0089
6	2	4	7	3	5	47295.1150	47295.1566	-0.0416
7	2	5	8	3	6	47294.2890	47294.3640	-0.0750
3	3	1	4	4	0	47286.2230	47286.1789	0.0441
4	3	2	5	4	1	47285.3280	47285.3069	0.0211
5	3	3	6	4	2	47284.4770	47284.4539	0.0231
6	3	4	7	4	3	47283.6210	47283.6200	0.0010
7	3	5	8	4	4	47282.7950	47282.8054	-0.0104
8	3	6	9	4	5	47282.0520	47282.0102	0.0418
9	3	7	10	4	6	47281.2500	47281.2345	0.0155
10	3	8	11	4	7	47280.4930	47280.4785	0.0145
11	3	9	12	4	8	47279.7620	47279.7422	0.0198
12	3	10	13	4	9	47279.0070	47279.0257	-0.0187
13	3	11	14	4	10	47278.3140	47278.3288	-0.0148
14	3	12	15	4	11	47277.6810	47277.6513	0.0297
15	3	13	16	4	12	47277.0180	47276.9931	0.0249
16	3	14	17	4	13	47276.3860	47276.3537	0.0323
17	3	15	18	4	14	47275.7470	47275.7325	0.0145
18	3	16	19	4	15	47275.1960	47275.1289	0.0671
19	3	17	20	4	16	47274.4720	47274.5418	-0.0698
20	3	18	21	4	17	47273.9510	47273.9704	-0.0194
3	3	0	4	4	1	47286.2230	47286.1789	0.0441
4	3	1	5	4	2	47285.3280	47285.3069	0.0211
5	3	2	6	4	3	47284.4770	47284.4540	0.0230
6	3	3	7	4	4	47283.6210	47283.6204	0.0006
7	3	4	8	4	5	47282.7950	47282.8062	-0.0112
8	3	5	9	4	6	47282.0520	47282.0120	0.0400
9	3	6	10	4	7	47281.2500	47281.2382	0.0118
10	3	7	11	4	8	47280.4930	47280.4853	0.0077
11	3	8	12	4	9	47279.7620	47279.7540	0.0080
12	3	9	13	4	10	47279.0070	47279.0453	-0.0383

D2CS

UPPER STATE			LOWER STATE			OBSERVATION	CALCULATION	RESID.
J	KA	KC	J	KA	KC			
13	3	10	14	4	11	47278.3140	47278.3602	-0.0462
14	3	11	15	4	12	47277.6810	47277.6999	-0.0189
15	3	12	16	4	13	47277.0190	47277.0658	-0.0468
16	3	13	17	4	14	47276.3860	47276.4596	-0.0736
19	3	16	20	4	17	47274.7830	47274.8295	-0.0465
4	4	1	5	5	0	47272.7570	47272.7228	0.0342
5	4	2	6	5	1	47271.8660	47271.8693	-0.0033
6	4	3	7	5	2	47271.0600	47271.0345	0.0255
7	4	4	8	5	3	47270.2320	47270.2186	0.0134
8	4	5	9	5	4	47269.4440	47269.4217	0.0223
9	4	6	10	5	5	47268.7020	47268.6438	0.0582
10	4	7	11	5	6	47267.9060	47267.8851	0.0209
11	4	8	12	5	7	47267.1630	47267.1457	0.0173
12	4	9	13	5	8	47266.4520	47266.4258	0.0262
13	4	10	14	5	9	47265.7730	47265.7254	0.0476
14	4	10	15	5	10	47265.0470	47265.0457	0.0013
15	4	12	16	5	11	47264.4530	47264.3841	0.0689
16	4	13	17	5	12	47263.8240	47263.7434	0.0806
17	4	14	18	5	13	47263.1720	47263.1230	0.0490
18	4	15	19	5	14	47262.5230	47262.5229	0.0001
19	4	16	20	5	15	47261.9590	47261.9433	0.0157
20	4	17	21	5	16	47261.3820	47261.3842	-0.0022
21	4	18	22	5	17	47260.8230	47260.8458	-0.0228
22	4	19	23	5	18	47260.3730	47260.3280	0.0450
23	4	20	24	5	19	47259.8460	47259.8307	0.0153
5	5	1	6	6	0	47258.2810	47258.2109	0.0701
6	5	2	7	6	1	47257.4010	47257.3754	0.0256
7	5	3	8	6	2	47256.5690	47256.5585	0.0105
8	5	4	9	6	3	47255.7510	47255.7603	-0.0093
9	5	5	10	6	4	47254.9580	47254.9807	-0.0227
10	5	6	11	6	5	47254.2260	47254.2197	0.0063
11	5	7	12	6	6	47253.5050	47253.4775	0.0275
12	5	8	13	6	7	47252.7350	47252.7541	-0.0191
13	5	9	14	6	8	47252.0190	47252.0495	-0.0305
14	5	10	15	6	9	47251.3330	47251.3638	-0.0308
15	5	11	16	6	10	47250.6790	47250.6970	-0.0180
16	5	12	17	6	11	47250.0550	47250.0493	0.0057
17	5	13	18	6	12	47249.4320	47249.4207	0.0113
18	5	14	19	6	13	47248.8040	47248.8113	-0.0073
19	5	15	20	6	14	47248.2410	47248.2211	0.0199
20	5	16	21	6	15	47247.6490	47247.6503	-0.0013
21	5	17	22	6	16	47247.0730	47247.0990	-0.0260
22	5	18	23	6	17	47246.5570	47246.5673	-0.0103
23	5	19	24	6	18	47246.0510	47246.0551	-0.0041

D2CS

UPPER STATE			LOWER STATE			OBSERVATION	CALCULATION	RESID.
J	KA	KC	J	KA	KC			
24	5	20	25	6	19	47245.5560	47245.5628	-0.0068
25	5	21	26	6	20	47245.0890	47245.0903	-0.0013
6	6	0	7	7	1	47242.6210	47242.6415	-0.0205
7	6	1	8	7	2	47241.7950	47241.8237	-0.0287
8	6	2	9	7	3	47241.0050	47241.0242	-0.0192
9	6	3	10	7	4	47240.2360	47240.2431	-0.0071
10	6	4	11	7	5	47239.4600	47239.4803	-0.0203
11	6	5	12	7	6	47238.8150	47238.7359	0.0791
12	6	6	13	7	7	47238.0510	47238.0099	0.0411
13	6	7	14	7	8	47237.2610	47237.3022	-0.0412
14	6	8	15	7	9	47236.5450	47236.6128	-0.0678
15	6	9	16	7	10	47235.8960	47235.9418	-0.0458
16	6	10	17	7	11	47235.2530	47235.2891	-0.0361
17	6	11	18	7	12	47234.7150	47234.6548	0.0602
18	6	12	19	7	13	47234.0530	47234.0389	0.0141
19	6	13	20	7	14	47233.4450	47233.4414	0.0036
20	6	14	21	7	15	47232.8580	47232.8622	-0.0042
21	6	15	22	7	16	47232.3200	47232.3014	0.0186
22	6	16	23	7	17	47231.7390	47231.7590	-0.0200
23	6	17	24	7	18	47231.2070	47231.2350	-0.0280
24	6	18	25	7	19	47230.7740	47230.7294	0.0446
25	6	19	26	7	20	47230.2720	47230.2423	0.0297
26	6	20	27	7	21	47229.8200	47229.7736	0.0464
7	7	1	8	8	0	47225.9750	47226.0119	-0.0369
8	7	2	9	8	1	47225.1790	47225.2112	-0.0322
9	7	3	10	8	2	47224.4320	47224.4285	0.0035
10	7	4	11	8	3	47223.6410	47223.6639	-0.0229
11	7	5	12	8	4	47222.9370	47222.9174	0.0196
12	7	6	13	8	5	47222.1870	47222.1889	-0.0019
13	7	7	14	8	6	47221.5080	47221.4783	0.0297
14	7	8	15	8	7	47220.7720	47220.7857	-0.0137
15	7	9	16	8	8	47220.1100	47220.1110	-0.0010
16	7	10	17	8	9	47219.4590	47219.4542	0.0048
17	7	11	18	8	10	47218.8660	47218.8153	0.0507
18	7	12	19	8	11	47218.2250	47218.1941	0.0309
19	7	13	20	8	12	47217.6050	47217.5908	0.0142
20	7	14	21	8	13	47217.0190	47217.0051	0.0139
21	7	15	22	8	14	47216.4530	47216.4371	0.0159
22	7	16	23	8	15	47215.8970	47215.8867	0.0103
23	7	17	24	8	16	47215.3610	47215.3540	0.0070
24	7	18	25	8	17	47214.8170	47214.8387	-0.0217
25	7	19	26	8	18	47214.3460	47214.3409	0.0051
8	8	1	9	9	0	47208.3450	47208.3182	0.0268
9	8	2	10	9	1	47207.5120	47207.5339	-0.0219

D2CS

UPPER STATE			LOWER STATE			OBSERVATION	CALCULATION	RESID.
J	KA	KC	J	KA	KC			
10	8	3	11	9	2	47206.7320	47206.7673	-0.0353
11	8	4	12	9	3	47205.9920	47206.0184	-0.0264
12	8	5	13	9	4	47205.3210	47205.2873	0.0337
13	8	6	14	9	5	47204.5500	47204.5739	-0.0239
14	8	7	15	9	6	47203.8580	47203.8780	-0.0200
15	8	8	16	9	7	47203.0770	47203.1997	-0.1227
16	8	9	17	9	8	47202.5940	47202.5389	0.0551
18	8	11	19	9	10	47201.2280	47201.2695	-0.0415
19	8	12	20	9	11	47200.6320	47200.6607	-0.0287
20	8	13	21	9	12	47200.0730	47200.0692	0.0038
21	8	14	22	9	13	47199.5160	47199.4948	0.0212
22	8	15	23	9	14	47199.0080	47198.9375	0.0705
23	8	16	24	9	15	47198.4000	47198.3972	0.0028
24	8	17	25	9	16	47197.8560	47197.8737	-0.0177
25	8	18	26	9	17	47197.3870	47197.3670	0.0200
9	9	1	10	10	0	47189.4990	47189.5550	-0.0560
10	9	2	11	10	1	47188.7670	47188.7862	-0.0192
11	9	3	12	10	2	47188.0330	47188.0349	-0.0019
12	9	4	13	10	3	47187.3170	47187.3009	0.0161
13	9	5	14	10	4	47186.5830	47186.5843	-0.0013
14	9	6	15	10	5	47185.8200	47185.8850	-0.0650
15	9	7	16	10	6	47185.2090	47185.2029	0.0061
16	9	8	17	10	7	47184.4800	47184.5379	-0.0579
17	9	9	18	10	8	47183.9290	47183.8899	0.0391
18	9	10	19	10	9	47183.2970	47183.2590	0.0380
19	9	11	20	10	10	47182.6660	47182.6449	0.0211
20	9	12	21	10	11	47182.0580	47182.0475	0.0105
21	9	13	22	10	12	47181.4930	47181.4669	0.0261
22	9	14	23	10	13	47180.9170	47180.9028	0.0142
23	9	15	24	10	14	47180.3840	47180.3552	0.0288
24	9	16	25	10	15	47179.8400	47179.8240	0.0160
25	9	17	26	10	16	47179.3210	47179.3090	0.0120
10	10	1	11	11	0	47169.6240	47169.7158	-0.0918
12	10	3	13	11	2	47168.2120	47168.2246	-0.0126
13	10	4	14	11	3	47167.5230	47167.5045	0.0185
11	11	1	12	12	0	47148.8040	47148.7926	0.0114
12	11	2	13	12	1	47148.0860	47148.0521	0.0339
13	11	3	14	12	2	47147.3300	47147.3283	0.0017
14	11	4	15	12	3	47146.6510	47146.6211	0.0299
15	11	5	16	12	4	47145.9930	47145.9303	0.0627
16	11	6	17	12	5	47145.2900	47145.2560	0.0340
17	11	7	18	12	6	47144.6270	47144.5979	0.0291
18	11	8	19	12	7	47143.9630	47143.9561	0.0069
19	11	9	20	12	8	47143.3850	47143.3303	0.0547

D2CS

UPPER STATE			LOWER STATE			OBSERVATION	CALCULATION	RESID.
J	KA	KC	J	KA	KC			
20	11	10	21	12	9	47142.7340	47142.7205	0.0135
21	11	11	22	12	10	47142.1450	47142.1265	0.0185
22	11	12	23	12	11	47141.5420	47141.5482	-0.0062
5	1	5	4	0	4	47333.9200	47334.0351	-0.1151
6	1	6	5	0	5	47334.9490	47334.9321	0.0169
7	1	7	6	0	6	47335.8040	47335.8228	-0.0188
8	1	8	7	0	7	47336.7360	47336.7085	0.0275
9	1	9	8	0	8	47337.5620	47337.5906	-0.0286
12	1	12	11	0	11	47340.2260	47340.2337	-0.0077
13	1	13	12	0	12	47341.0740	47341.1205	-0.0465
14	1	14	13	0	13	47341.9730	47342.0138	-0.0408
15	1	15	14	0	14	47342.8700	47342.9158	-0.0458
16	1	16	15	0	15	47343.8490	47343.8287	0.0203
17	1	17	16	0	16	47344.7700	47344.7544	0.0156
19	1	19	18	0	18	47346.6480	47346.6508	-0.0028
20	1	20	19	0	19	47347.5760	47347.6240	-0.0480
21	1	21	20	0	20	47348.5720	47348.6151	-0.0431
22	1	22	21	0	21	47349.6560	47349.6244	0.0316
25	1	25	24	0	24	47352.7940	47352.7611	0.0329
27	1	27	26	0	26	47354.9520	47354.9386	0.0134
28	1	28	27	0	27	47356.0380	47356.0510	-0.0130
2	2	1	1	1	0	47338.5300	47338.5450	-0.0150
5	2	4	4	1	3	47341.4160	47341.3972	0.0188
6	2	5	5	1	4	47342.2910	47342.3372	-0.0462
9	2	8	8	1	7	47345.1920	47345.1227	0.0693
11	2	10	10	1	9	47346.9340	47346.9496	-0.0156
12	2	11	11	1	10	47347.8040	47347.8538	-0.0498
14	2	13	13	1	12	47349.6500	47349.6436	0.0064
17	2	16	16	1	15	47352.3200	47352.2836	0.0364
18	2	17	17	1	16	47353.2000	47353.1529	0.0471
19	2	18	18	1	17	47354.0610	47354.0176	0.0434
20	2	19	19	1	18	47354.9520	47354.8785	0.0735
21	2	20	20	1	19	47355.7000	47355.7365	-0.0365
2	2	0	1	1	1	47338.5300	47338.5926	-0.0626
7	2	5	6	1	6	47344.3210	47344.3315	-0.0105
9	2	7	8	1	8	47346.9340	47347.0044	-0.0704
3	3	1	2	2	0	47345.5650	47345.6675	-0.1025
4	3	2	3	2	1	47346.6480	47346.6881	-0.0401
5	3	3	4	2	2	47347.8040	47347.7258	0.0782
7	3	5	6	2	4	47349.7890	47349.8489	-0.0599
9	3	7	8	2	6	47352.0900	47352.0257	0.0643
10	3	8	9	2	7	47353.2000	47353.1297	0.0703
12	3	10	11	2	9	47355.3670	47355.3577	0.0093
13	3	11	12	2	10	47356.4130	47356.4768	-0.0638

D2CS

UPPER STATE			LOWER STATE			OBSERVATION	CALCULATION	RESID.
J	KA	KC	J	KA	KC			
14	3	12	13	2	11	47357.6490	47357.5957	0.0533
15	3	13	14	2	12	47358.7740	47358.7118	0.0622
16	3	14	15	2	13	47359.8150	47359.8224	-0.0074
17	3	15	16	2	14	47360.9050	47360.9253	-0.0203
19	3	17	18	2	16	47363.1260	47363.0988	0.0272
17	3	14	16	2	15	47362.1190	47362.1633	-0.0443
19	3	16	18	2	17	47364.9660	47365.0592	-0.0932
3	3	0	2	2	1	47345.5650	47345.6679	-0.1029
4	3	1	3	2	2	47346.6480	47346.6900	-0.0420
5	3	2	4	2	3	47347.8040	47347.7316	0.0724
7	3	4	6	2	5	47349.7890	47349.8760	-0.0870
9	3	6	8	2	7	47352.0900	47352.1078	-0.0178
10	3	7	9	2	8	47353.2000	47353.2596	-0.0596
11	3	8	10	2	9	47354.4160	47354.4371	-0.0211
12	3	9	11	2	10	47355.7000	47355.6422	0.0578
13	3	10	12	2	11	47356.8390	47356.8770	-0.0380
15	3	12	14	2	13	47359.3870	47359.4450	-0.0580
4	4	0	3	3	1	47351.6070	47351.6852	-0.0782
5	4	1	4	3	2	47352.7940	47352.7242	0.0698
6	4	2	5	3	3	47353.7660	47353.7814	-0.0154
8	4	4	7	3	5	47356.0380	47355.9506	0.0874
9	4	5	8	3	6	47357.0650	47357.0626	0.0024
11	4	7	10	3	8	47359.3870	47359.3411	0.0459
13	4	9	12	3	10	47361.6320	47361.6926	-0.0606
14	4	10	13	3	11	47362.9540	47362.8960	0.0580
4	4	1	3	3	0	47351.6020	47351.6852	-0.0832
5	4	2	4	3	1	47352.7940	47352.7241	0.0699
6	4	3	5	3	2	47353.7660	47353.7813	-0.0153
8	4	5	7	3	4	47356.0380	47355.9502	0.0878
9	4	6	8	3	5	47357.0650	47357.0617	0.0033
11	4	8	10	3	7	47359.3870	47359.3378	0.0492
13	4	10	12	3	9	47361.6320	47361.6827	-0.0507
14	4	11	13	3	10	47362.9540	47362.8800	0.0740
15	4	12	14	3	11	47364.0870	47364.0931	-0.0061
16	4	13	15	3	12	47365.3360	47365.3214	0.0146
5	5	1	4	4	0	47356.7240	47356.6125	0.1115
6	5	2	5	4	1	47357.6490	47357.6684	-0.0194
7	5	3	6	4	2	47358.7740	47358.7423	0.0317
8	5	4	7	4	3	47359.8150	47359.8342	-0.0192
9	5	5	8	4	4	47360.9050	47360.9441	-0.0391
10	5	6	9	4	5	47362.1190	47362.0720	0.0470
11	5	7	10	4	6	47363.1260	47363.2177	-0.0917
12	5	8	11	4	7	47364.3960	47364.3812	0.0148
13	5	9	12	4	8	47365.6180	47365.5624	0.0556

D2CS

UPPER STATE			LOWER STATE			OBSERVATION	CALCULATION	RESID.
J	KA	KC	J	KA	KC			
14	5	10	13	4	9	47366.7180	47366.7611	-0.0431
15	5	11	14	4	10	47367.9280	47367.9774	-0.0494
17	5	13	16	4	12	47370.4690	47370.4617	0.0073
18	5	14	17	4	13	47371.7830	47371.7295	0.0535
19	5	15	18	4	14	47373.0470	47373.0141	0.0329
20	5	16	19	4	15	47374.3270	47374.3154	0.0116
22	5	18	21	4	17	47377.0710	47376.9667	0.1043
23	5	19	22	4	18	47378.3490	47378.3161	0.0329
24	5	20	23	4	19	47379.6950	47379.6809	0.0141
25	5	21	24	4	20	47380.9720	47381.0607	-0.0887
27	5	23	26	4	22	47383.7900	47383.8628	-0.0728
28	5	24	27	4	23	47385.3110	47385.2839	0.0271
11	6	6	10	5	5	47366.0250	47365.9771	0.0479
12	6	7	11	5	6	47367.1750	47367.1376	0.0374
13	6	8	12	5	7	47368.2930	47368.3155	-0.0225
17	6	12	16	5	11	47373.2620	47373.2006	0.0614
19	6	14	18	5	13	47375.7320	47375.7456	-0.0136
20	6	15	19	5	14	47377.0710	47377.0433	0.0277
21	6	16	20	5	15	47378.3490	47378.3577	-0.0087
22	6	17	21	5	16	47379.6950	47379.6886	0.0064
23	6	18	22	5	17	47380.9720	47381.0358	-0.0638
25	6	20	24	5	19	47383.7900	47383.7787	0.0113
26	6	21	25	5	20	47385.0670	47385.1739	-0.1069
7	7	1	6	6	0	47363.1260	47363.1548	-0.0288
9	7	3	8	6	2	47365.3360	47365.3471	-0.0111
11	7	5	10	6	4	47367.6380	47367.6090	0.0290
12	7	6	11	6	5	47368.7000	47368.7659	-0.0659
13	7	7	12	6	6	47369.9290	47369.9400	-0.0110
14	7	8	13	6	7	47371.1260	47371.1312	-0.0052
15	7	9	14	6	8	47372.3860	47372.3395	0.0465
17	7	11	16	6	10	47374.8490	47374.8067	0.0423
18	7	12	17	6	11	47376.0470	47376.0654	-0.0184
19	7	13	18	6	12	47377.3230	47377.3408	-0.0178
20	7	14	19	6	13	47378.5680	47378.6327	-0.0647
21	7	15	20	6	14	47379.9350	47379.9409	-0.0059
22	7	16	21	6	15	47381.2800	47381.2654	0.0146
23	7	17	22	6	16	47382.5200	47382.6060	-0.0860
24	7	18	23	6	17	47384.0200	47383.9625	0.0575
25	7	19	24	6	18	47385.3110	47385.3348	-0.0238
26	7	20	25	6	19	47386.7730	47386.7227	0.0503
10	8	3	9	7	2	47366.9670	47366.9668	0.0002
13	8	6	12	7	5	47370.4690	47370.4254	0.0436
16	8	9	15	7	8	47373.9570	47374.0350	-0.0780
17	8	10	16	7	9	47375.1980	47375.2714	-0.0734

D2CS

UPPER STATE			LOWER STATE			OBSERVATION	CALCULATION	RESID.
J	KA	KC	J	KA	KC			
18	8	11	17	7	10	47376.5940	47376.5241	0.0699
20	8	13	19	7	12	47379.1440	47379.0783	0.0657
21	8	14	20	7	13	47380.3050	47380.3794	-0.0744
22	8	15	21	7	14	47381.6930	47381.6965	-0.0035
23	8	16	22	7	15	47383.0270	47383.0292	-0.0022
24	8	17	23	7	16	47384.3730	47384.3776	-0.0046
25	8	18	24	7	17	47385.6640	47385.7413	-0.0773
13	9	5	12	8	4	47369.7230	47369.7597	-0.0367
17	9	9	16	8	8	47374.5830	47374.5830	0.0001
19	9	11	18	8	10	47377.0710	47377.0911	-0.0201
20	9	12	19	8	11	47378.3490	47378.3688	-0.0198
21	9	13	20	8	12	47379.6950	47379.6622	0.0328
22	9	14	21	8	13	47380.9720	47380.9710	0.0010
23	9	15	22	8	14	47382.2600	47382.2952	-0.0352
25	9	17	24	8	16	47385.0670	47384.9889	0.0781
31	9	23	30	8	22	47393.4200	47393.4201	-0.0001
11	10	1	10	9	2	47365.6180	47365.6264	-0.0084
12	10	2	11	9	3	47366.7180	47366.7701	-0.0521
13	10	3	12	9	4	47367.9280	47367.9299	-0.0019
18	10	8	17	9	9	47373.9570	47373.9672	-0.0102
19	10	9	18	9	10	47375.1980	47375.2216	-0.0236
20	10	10	19	9	11	47376.5940	47376.4913	0.1027
22	10	12	21	9	13	47379.1440	47379.0762	0.0678
24	10	14	23	9	15	47381.6930	47381.7207	-0.0277
25	10	15	24	9	16	47383.0270	47383.0649	-0.0379
26	10	16	25	9	17	47384.3730	47384.4235	-0.0505
29	10	19	28	9	20	47388.4980	47388.5837	-0.0857
31	10	21	30	9	22	47391.4340	47391.4256	0.0084
12	11	2	11	10	1	47363.8270	47363.7677	0.0593
13	11	3	12	10	2	47364.9660	47364.9218	0.0442
14	11	4	13	10	3	47366.0250	47366.0915	-0.0665
15	11	5	14	10	4	47367.2850	47367.2768	0.0082
17	11	7	16	10	6	47369.7230	47369.6934	0.0296
18	11	8	17	10	7	47370.8510	47370.9245	-0.0735
20	11	10	19	10	9	47373.4370	47373.4317	0.0053
22	11	12	21	10	11	47376.0470	47375.9979	0.0491
23	11	13	22	10	12	47377.3230	47377.3028	0.0202
24	11	14	23	10	13	47378.5680	47378.6219	-0.0539
25	11	15	24	10	14	47379.9350	47379.9551	-0.0201
26	11	16	25	10	15	47381.2800	47381.3023	-0.0223
28	11	18	27	10	17	47384.0200	47384.0377	-0.0177
30	11	20	29	10	19	47386.7730	47386.8265	-0.0535
32	11	22	31	10	21	47389.7250	47389.6669	0.0581
34	11	24	33	10	23	47392.5870	47392.5572	0.0298

D2CS

UPPER STATE			LOWER STATE			OBSERVATION	CALCULATION	RESID.
J	KA	KC	J	KA	KC			
13	13	1	12	12	0	47355.3670	47355.3091	0.0579
14	13	2	13	12	1	47356.4130	47356.4652	-0.0522
15	13	3	14	12	2	47357.6560	47357.6359	0.0201
16	13	4	15	12	3	47358.7770	47358.8210	-0.0440
18	13	6	17	12	5	47361.2550	47361.2342	0.0208
19	13	7	18	12	6	47362.4020	47362.4620	-0.0600
21	13	9	20	12	8	47364.9660	47364.9593	0.0067
2	1	2	3	0	3	47326.6120	47326.5631	0.0489
3	1	3	4	0	4	47325.5870	47325.5926	-0.0056
4	1	4	5	0	5	47324.6270	47324.6163	0.0107
5	1	5	6	0	6	47323.6950	47323.6353	0.0597
6	1	6	7	0	7	47322.6520	47322.6512	0.0008
7	1	7	8	0	8	47321.6540	47321.6656	-0.0116
8	1	8	9	0	9	47320.6550	47320.6804	-0.0254
9	1	9	10	0	10	47319.7130	47319.6977	0.0153
10	1	10	11	0	11	47318.7540	47318.7198	0.0342
11	1	11	12	0	12	47317.7480	47317.7488	-0.0008
12	1	12	13	0	13	47316.8820	47316.7871	0.0949
13	1	13	14	0	14	47315.7910	47315.8370	-0.0460
14	1	14	15	0	15	47314.8910	47314.9006	-0.0096
15	1	15	16	0	16	47314.0490	47313.9798	0.0692
16	1	16	17	0	17	47313.0550	47313.0763	-0.0213
17	1	17	18	0	18	47312.1500	47312.1915	-0.0415
5	2	4	6	1	5	47330.7620	47330.7234	0.0386
6	2	5	7	1	6	47329.6940	47329.7252	-0.0312
7	2	6	8	1	7	47328.7220	47328.7227	-0.0007
11	2	10	12	1	11	47324.6270	47324.6720	-0.0450
12	2	11	13	1	12	47323.6950	47323.6499	0.0451
13	2	12	14	1	13	47322.6520	47322.6247	0.0273
4	3	2	5	2	3	47338.1760	47338.1528	0.0232
5	3	3	6	2	4	47337.2230	47337.2882	-0.0652
9	3	7	10	2	8	47333.9200	47333.9393	-0.0193
12	3	10	13	2	11	47331.5550	47331.4814	0.0736
14	3	12	15	2	13	47329.8960	47329.8317	0.0643
3	1	2	3	0	3	47329.6940	47329.7079	-0.0139
4	1	3	4	0	4	47329.8960	47329.8950	0.0010
5	1	4	5	0	5	47330.1420	47330.1304	0.0116
6	1	5	6	0	6	47330.4070	47330.4153	-0.0083
7	1	6	7	0	7	47330.7620	47330.7508	0.0112
8	1	7	8	0	8	47331.1510	47331.1383	0.0127
9	1	8	9	0	9	47331.5550	47331.5794	-0.0244
10	1	9	10	0	10	47332.0460	47332.0754	-0.0294
11	1	10	11	0	11	47332.6200	47332.6279	-0.0079
12	1	11	12	0	12	47333.2280	47333.2382	-0.0102

D2CS

UPPER STATE			LOWER STATE			OBSERVATION	CALCULATION	RESID.
J	KA	KC	J	KA	KC			
13	1	12	13	0	13	47333.9200	47333.9076	0.0124
14	1	13	14	0	14	47334.6540	47334.6369	0.0171
15	1	14	15	0	15	47335.4030	47335.4266	-0.0236
16	1	15	16	0	16	47336.2450	47336.2765	-0.0315
17	1	16	17	0	17	47337.2230	47337.1859	0.0371
18	1	17	18	0	18	47338.1760	47338.1534	0.0226
20	1	19	20	0	20	47340.2260	47340.2533	-0.0273
21	1	20	21	0	21	47341.4160	47341.3793	0.0367
25	1	24	25	0	25	47346.2630	47346.2858	-0.0228
26	1	25	26	0	26	47347.5760	47347.5873	-0.0113
27	1	26	27	0	27	47348.9310	47348.9081	0.0229
29	1	28	29	0	29	47351.6620	47351.5889	0.0731
2	2	0	2	1	1	47336.6290	47336.6041	0.0249
7	2	5	7	1	6	47336.5380	47336.5547	-0.0167
10	2	8	10	1	9	47336.6290	47336.6329	-0.0039
11	2	9	11	1	10	47336.7360	47336.7023	0.0337
2	2	1	2	1	2	47336.7360	47336.7444	-0.0084
5	2	4	5	1	5	47337.2230	47337.2496	-0.0266
8	2	7	8	1	8	47338.1760	47338.1320	0.0440
9	2	8	9	1	9	47338.5300	47338.5094	0.0206
14	2	13	14	1	14	47341.0740	47341.0094	0.0646
16	2	15	16	1	16	47342.2910	47342.2880	0.0030
20	2	19	20	1	20	47345.2850	47345.2947	-0.0097
23	2	22	23	1	23	47347.9440	47347.9139	0.0301
24	2	23	24	1	24	47348.9310	47348.8502	0.0808
25	2	24	25	1	25	47349.7890	47349.8160	-0.0270
26	2	25	26	1	26	47350.8360	47350.8098	0.0262
28	2	27	28	1	28	47352.7940	47352.8758	-0.0818
4	3	1	4	2	2	47342.8700	47342.8957	-0.0257
11	3	8	11	2	9	47343.8490	47343.7657	0.0833
13	3	10	13	2	11	47344.0330	47344.0851	-0.0521
3	3	1	3	2	2	47342.8700	47342.8262	0.0438
4	3	2	4	2	3	47342.8700	47342.9013	-0.0313
10	3	8	10	2	9	47343.8490	47343.7903	0.0587
11	3	9	11	2	10	47344.0330	47344.0190	0.0140
12	3	10	12	2	11	47344.3210	47344.2733	0.0477
15	3	13	15	2	14	47345.1920	47345.1995	-0.0075
16	3	14	16	2	15	47345.5650	47345.5659	-0.0009
19	3	17	19	2	18	47346.8170	47346.8510	-0.0340
20	3	18	20	2	19	47347.3490	47347.3437	0.0053
24	3	22	24	2	23	47349.6560	47349.6510	0.0050
6	0	6	6	1	5	47321.0120	47321.0188	-0.0068
10	0	10	10	1	9	47320.6550	47320.6482	0.0068
13	0	13	13	1	12	47320.0020	47320.0736	-0.0716

D2CS

UPPER STATE			LOWER STATE			OBSERVATION	CALCULATION	RESID.
J	KA	KC	J	KA	KC			
2	1	1	2	2	0	47311.9340	47311.9370	-0.0030
3	1	2	3	2	1	47312.1500	47312.0737	0.0763
5	1	4	5	2	3	47312.4970	47312.4756	0.0214
6	1	5	6	2	4	47312.7390	47312.7364	0.0026
7	1	6	7	2	5	47313.0550	47313.0335	0.0215
8	1	7	8	2	6	47313.4030	47313.3636	0.0394
9	1	8	9	2	7	47313.6990	47313.7228	-0.0238
10	1	9	10	2	8	47314.0490	47314.1071	-0.0581
11	1	10	11	2	9	47314.5060	47314.5117	-0.0057
12	1	11	12	2	10	47314.8910	47314.9317	-0.0407
9	5	4	9	6	3	47264.4530	47264.4486	0.0044
12	5	7	12	6	6	47265.0470	47265.0638	-0.0168
13	5	8	13	6	7	47265.2740	47265.3067	-0.0327
14	5	9	14	6	8	47265.5430	47265.5686	-0.0256
15	5	10	15	6	9	47265.7730	47265.8496	-0.0766
4	0	4	3	1	3	47325.2150	47325.2635	-0.0485
5	0	5	4	1	4	47326.4330	47326.3872	0.0458
7	0	7	6	1	6	47328.7220	47328.7342	-0.0122
8	0	8	7	1	7	47329.8960	47329.9510	-0.0550
9	0	9	8	1	8	47331.1510	47331.1918	-0.0408
3	1	2	2	2	1	47314.8910	47314.9173	-0.0263
5	1	4	4	2	3	47317.2750	47317.2240	0.0510
7	1	6	6	2	5	47319.7130	47319.7083	0.0047
8	1	7	7	2	6	47321.0120	47321.0153	-0.0033
10	1	9	9	2	8	47323.6950	47323.7539	-0.0589
11	1	10	10	2	9	47325.2150	47325.1831	0.0319
12	1	11	11	2	10	47326.6120	47326.6503	-0.0383
13	1	12	12	2	11	47328.1490	47328.1537	-0.0047
14	1	13	13	2	12	47329.6940	47329.6913	0.0027
15	1	14	14	2	13	47331.1510	47331.2608	-0.1098
16	1	15	15	2	14	47332.8160	47332.8597	-0.0437
8	5	3	7	6	2	47271.8660	47271.8552	0.0108
11	5	6	10	6	5	47275.1960	47275.2550	-0.0590
12	5	7	11	6	6	47276.3860	47276.4262	-0.0402
13	5	8	12	6	7	47277.6810	47277.6164	0.0646
16	5	11	15	6	10	47281.2500	47281.3023	-0.0523

References

1. M. W. Sinclair, J. C. Ribes, N. Fourikis, R. D. Brown and P. D. Godfrey, Int. Astron. Union Circular No. 2362, Nov., 1971.

2. L. H. Doherty, J. M. McLeod and T. Oka, Astrophysics J. 192, L157 (1974).

3. A. Jones and F. P. Lossing, J. Phys. Chem. 71, 4111 (1967).

4. (a) A. B. Callear, J. Connor and D. R. Dickson, Nature 221, 1238 (1969).

   (b) A. B. Callear and D. R. Dickson, Trans. Faraday Soc. 66, 1987 (1970).

5. (a) D. R. Johnson and F. X. Powell, Science 169, 679 (1970).

   (b) D. R. Johnson, F. X. Powell and W. H. Kirchhoff, J. Mol. Spectr. 39, 136 (1971).

   (c) Y. Beers, G. P. Klein, W. H. Kirchhoff and D. R. Johnson, J. Mol. Spectr. 44, 553 (1972).

6. J. W. C. Johns and W. B. Olson, J. Mol. Spectr. 39, 479 (1971).

7. M. E. Jacox and D. E. Milligan, J. Mol. Spectr. 58, 142 (1975).

8. H. W. Kroto and R. J. Suffolk, Chem. Phys. Letters 15, 545 (1972).

9. (a) B. Solouki, P. Rosmus and H. Bock, J. Am. Chem. Soc. 98, 6054 (1976).

   (b) H. Bock, B. Solouki, S. Mohmand, E. Block and L. K. Revelle, J. Chem. Soc. Chem. Comm. 287 (1977).

10. (a) R. H. Judge and G. W. King, Can. J. Phys. 53, 1927 (1975).

    (b) R. H. Judge and G. W. King, J. Mol. Spectr. 74, 175 (1979).

    (c) R. H. Judge and G. W. King, J. Mol. Spectr. 78, 51 (1979).

    (d) R. H. Judge, D. C. Moule and G. W. King, J. Mol. Spectr. in press.

11. R. S. Mulliken, J. Chem. Phys. 23, 1997 (1955).

12. I. N. Levine, "Quantum Chemistry", Volume I, Allyn and Bacon, Boston (1970).

13. G. Herzberg, "Electronic Spectra of Polyatomic Molecules", D. Van Nostrand Reinhold Co., New York (1966).

14. M. D. Harmony, "Introduction to Molecular Energies and Spectra", Holt, Rinehart and Winston, Inc., New York (1972).

15. M. Born and R. Oppenheimer, Ann. Physik. 84, 457 (1927).

16. M. B. Robin, "Higher Excited States of Polyatomic Molecules", Volume I, Academic Press, New York (1974).

17. (a) R. S. Mulliken, J. Am. Chem. Soc. 86, 3183 (1964).

    (b) R. S. Mulliken, J. Am. Chem. Soc. 88, 1849 (1966).

18. A. D. Walsh, J. Chem. Soc. 2260 (1953).

19. P. J. Bruna, S. D. Peyerimhoff and R. J. Buenker, Chem. Phys. 3, 35 (1974).

20. B. S. Ray, Z. Physik 78, 74 (1932).

21. G. W. King, R. M. Hainer and P. C. Cross, J. Chem. Phys. 11, 27 (1943).

22. G. Herzberg, "Infrared and Raman Spectra", D. Van Nostrand Reinhold Co., New York (1945).

23. D. M. Dennison, Rev. Mod. Phys. 3, 280 (1931).

24. D. Kivelson and E. Wilson, Jr., J. Chem. Phys. 20, 1575 (1952).

25. H. H. Nielsen, Encyclop. Phys. 3711, 173 (1959).

26. (a) G. Herzberg and E. Teller, Z. Phys. Chem. B21, 410 (1933).

    (b) H. Sponer and E. Teller, Revs. Mod. Phys. 13, 75 (1941).

27. E. U. Condon, Am. J. Phys. 24, 1104 (1956).

28. (a) C. R. Lessard and D. C. Moule, J. Chem. Phys. 66, 3908 (1977).

    (b) C. R. Lessard, M.Sc. Thesis, Brock University, 1975.

29. S. D. Peyerimhoff, R. J. Buenker, W. E. Kammer and H. Hsu, Chem. Phys. Letters 8, 129 (1971).

30. V. A. Job, V. Sethuraman and K. K. Innes, J. Mol. Spectr. 30, 365 (1969).

31. F. W. Birss, R. Y. Dong and D. A. Ramsay, Chem. Phys. Letters 18, 11 (1973).

32. R. H. Judge and D. C. Moule, private communication.

33. J. C. D. Brand, J. H. Callomon, D. C. Moule, J. Tyrrell and T. H. Goodwin, Trans. Faraday Soc. 61, 2365 (1965).

34. R. H. Judge and D. C. Moule, J. Mol. Spectr., in press.

35. C. C. Costain, J. Chem. Phys. 29, 864 (1958).

36. J. Kraitchman, Am. J. Phys. 21, 17 (1953).

37. C. R. Lessard and D. C. Moule, Spectrochim. Acta 29A, 1085 (1973).

38. E. R. Farnworth and G. W. King, J. Mol. Spectr. 46, 419 (1973).

39. J. E. Parkin, J. Mol. Spectr. 15, 483 (1965).

40. R. Balfour, Ph.D. Thesis, McMaster University, 1973.

41. D. C. Moule and A. D. Walsh, Chem. Rev. 75, 67 (1975).

42. D. A. Condirston and D. C. Moule, Theor. Chim. Acta 29, 133 (1973).

43. D. C. Moule and A. K. Mehra, J. Mol. Spectr. 35, 137 (1970).

44. C. R. Drury, B.Sc. Thesis, Brock University, 1972.

45. D. C. Moule and C. R. Subramaniam, J. Mol. Spectr. 53, 443 (1974).

46. D. J. Clouthier, R. P. Steer, A. R. Knight, R. H. Judge and D. C. Moule, J. Mol. Spectr., in press.

47. R. M. Badger, J. Chem. Phys. 2, 128 (1934).

48. K. Morita and S. Kokayashi, Chem. Pharm. Bull. 15, 988 (1967).

49. Sales catalogue from Oriel Corporation of America.